

Modern Views on Desilicification: Biosilica and Abiotic Silica Dissolution in Natural and Artificial Environments

Hermann Ehrlich,^{*,†} Konstantinos D. Demadis,^{*,‡} Oleg S. Pokrovsky,[§] and Petros G. Koutsoukos^{||}

Institute of Bioanalytical Chemistry, Dresden University of Technology, D-01069 Dresden, Germany, Crystal Engineering, Growth and Design Laboratory, Department of Chemistry, University of Crete, Voutes Campus, GR-71003 Heraklion, Crete, Greece, Laboratory of Mechanisms and Transfer in Geology, Observatory Midi-Pyrenees (OMP), UMR 5563, CNRS, 14 Avenue Edouard Belin, 31400 Toulouse, France, and FORTH-ICEHT and Laboratory of Inorganic and Analytical Chemistry, Department of Chemical Engineering, University of Patras, GR-265 04 Patras, Greece[007f]

Received October 7, 2009

Contents

1. Introduction	4656
2. Biosilica: Diversity in Structure and Composition	4657
2.1. Biosilica at the Microlevel: Protozoa and Diversity of Siliceous Structures	4658
2.2. Biosilica at the Macrolevel: Marine Glass Sponges	4660
2.3. Pathological Silicification: Silica Calculi and Stones	4661
3. Biodegradation and Silica Utilization in Nature	4662
3.1. Silica Bioleaching: Bacteria and Fungi	4663
3.2. Silica Bioleaching: Diatoms	4665
3.3. Silica Bioleaching: Sponges (Porifera)	4665
3.4. Silica Bioleaching: Worms (Annelida)	4666
4. Possible Mechanisms of Biologically Mediated Desilicification	4666
4.1. Interaction between Silica and Cells and Tissues	4666
4.2. Enzymatic Degradation of Silica	4668
5. Mechanism and Kinetics of Silica Dissolution	4669
5.1. Dissolution of Inorganic Silica and Quartz	4669
5.2. Dissolution of Biogenic Silica: Diatoms and Their Frustules	4675
5.3. Dissolution of Biogenic Silica: Plants and Their Phytoliths	4678
6. Desilicification and Isolation of Organic Templates	4681
6.1. Alkali versus Hydrofluoric Acid	4681
6.2. Isolation of Protein-Based Templates	4682
6.3. Isolation of Polysaccharide-Based Templates	4683
7. Epilogue, Conclusions, and Outlook	4684
8. Acknowledgments	4684
9. References	4684

1. Introduction

Of the intriguing topics that are receiving renewed attention nowadays, the study of the “triangle” biomineralization/demineralization/remineralization is among the most fascinating. Biominerals may be deposited within the tissues of biota, as well as within the corresponding immediate surroundings or environment, as a result of the metabolism of the living organism.¹ The variety of biomineralizers

recently reviewed by Ehrlich et al.² can best be demonstrated by the existence of approximately 128 000 species of molluscs, about 800 species of corals, 5000 species of sponges (including 550 species of glass sponges), 700 species of calcareous green, red, and brown algae, more than 300 species of deep-sea benthic foraminifera, and 200 000 diatom species.³

There is no doubt that for the complete and detailed study of the role of organic matrices (frameworks or templates) involved in biomineralization, they must be first isolated (in a “pristine”, undamaged form, ideally) from biocomposites using appropriate demineralization techniques. Therefore, demineralization as a tool is an inevitable step in most modern strategies related to investigations of biomineralization mechanisms. The isolation of an organic component from any naturally biomineralized material, whether mineralized with calcium- or silica-containing compounds, is indispensable. The most efficient and effective technique should be not based upon fast dissolution of the inorganic component; it is a slow and gentle, biomimetically inspired process that enables the preservation of the organic component in the biomineral-based naturally occurring composites without artifacts.^{2,4}

The building of discrete or extended organic architectures in biomineralization often involves hierarchical processing. In these reactions, the molecularly based construction of organic assemblies is used to provide frameworks for the synthesis of organized inorganic materials, which, in turn, are exploited as prefabricated units in the production of higher order complex microstructures.^{5–10} Animal skeletons appear to have been optimized by natural selection to physically support and physiologically maintain diverse tissue types encompassing a variety of functions.^{11,12} Increased understanding of biomineralization has initiated developments in biomimetic synthesis with the production of synthetic biomimetic materials fabricated according to biological principles and processes of self-assembly and self-organization.¹³

Among different biominerals, silicon dioxide (silica) in its different amorphous (and occasionally porous) forms is probably the most intriguing one, for the following reasons: (a) it is definitely the first and the oldest natural bioskeleton; (b) it has unique mechanical properties; (c) it has extremely high specific surface area and, therefore, adsorption properties with respect to dissolved components of external milieu. These properties made silica the most widely distributed biomineral.

Although biomineralization/demineralization/remineralization phenomena are probably among the most widely

* To whom correspondence should be addressed. E-mail addresses: hermann.ehrlich@tu-dresden.de; demadis@chemistry.uoc.gr.

[†] Dresden University of Technology.

[‡] University of Crete.

[§] Observatory Midi-Pyrenees (OMP).

^{||} University of Patras.



Hermann Ehrlich received his Ph.D. degree from the University of Lemberg in 1984. Hermann served as a postdoctoral researcher at Max-Bergmann Centre of Biomaterials and Institute of Materials Science in Dresden, Germany, and currently holds a position as a Staff Scientist at the Institute of Bioanalytical Chemistry at the Dresden University of Technology. His research is focused on the phenomena of biomineralization—demineralization—remineralization, as well as on biological materials of marine origin. Using biochemical, cellular, molecular, and analytical approaches, he and his co-workers have for the first time discovered and characterized chitin and novel hydroxylated collagen in skeletal formations of marine sponges. During last five years, he has published over 30 peer reviewed articles and three book chapters, and he holds three patents.



Kostas Demadis was born in 1967 in Komotini of Thrace in Greece. He received a B.S. Degree from the National University of Athens, Greece, in 1990. He then moved to the University of Michigan, Ann Arbor, where he earned his Ph.D. Degree in 1995, working with Prof. Dimitri Coucouvanis. He then joined Prof. Tom Meyer's research group at the University of North Carolina at Chapel Hill. In 1998, he moved to the Chicagoland area and joined the Research & Development Division of the (then) Nalco Chemical Company as a Senior Chemist. In 2003, he was elected Assistant Professor at the Chemistry Department, University of Crete, Greece, where he is currently Associate Professor. His current research interests extend over a range of scientific areas and include crystal growth and inhibition, bioinspired materials science, metal phosphonate chemistry, materials corrosion control, and technology of polymers and colloids. Kostas is a member of the American Chemical Society, the National Association of Corrosion Engineers, and the Association of Greek Chemists. He has published ~100 peer reviewed papers and 8 book chapters, and he holds 2 patents.

studied topics in modern geochemistry, materials science, biomedicine, and biomimetics, a review relating to modern views on biosilica and abiotic silica *in vivo* as well as *in vitro* with the basic information on principles of desilicification has been lacking up to now.

2. Biosilica: Diversity in Structure and Composition

Biogenic silica exhibits diversity in structure, density, and composition and can exist in several structural forms, including sheet-like, globular, fibrillar, helical, tubular, and folded sheets. Different levels of structural organization of biosilica, from nanogranules in bacteria (Figure 1) or in mitochondria to up to 2 m high and 70 cm wide three-



Oleg S. Pokrovsky was born in 1972 in Moscow, Russia. He studied geology and geochemistry at the Geochemistry Department in Moscow State University where he received his Ph.D. in 1994. After two postdoctoral stays at Florida State University (Laboratory of *f*-elements) and Laboratoire de Géochimie de Toulouse, he entered CNRS in 1999. Since 2004, he has been senior CNRS researcher at the Observatory of Midi-Pyrenees working on mineral dissolution and precipitation, weathering, speciation and migration of trace elements, and metal—microorganism interaction and biomineralization. He has published over 80 peer reviewed articles in international and Russian journals and several book chapters.



Petros Koutsoukos is a Professor of the Department of Chemical Engineering of the University of Patras, Director of the Laboratory of Inorganic and Analytical chemistry. He received the Pichion of chemistry from the University of Patras (1972), Diploma of Specialization in Business Administration (1974) from the Athens School of Economics, and Ph.D from the State University of New York at Buffalo (1980) under the supervision of Prof. G. H. Nancollas. During 1980–1981, he was a postdoctoral fellow in the Physical and Colloid Chemistry Laboratory at the Agricultural State University of Wageningen (The Netherlands), under the guidance of Prof. J. Lyklema. In 1981, he joined the Department of Chemistry of the University of Patras (chair of physical chemistry) where he was awarded the title of Ifigeia (D.Sc.) and was gradually promoted to the rank of the Associate Professor. In 1989, he joined the Department of Chemical Engineering as a full professor. Research interests include the crystallization of inorganic salts from aqueous solutions, physico-chemical phenomena at interfaces between solids and water, and metal corrosion. Over 160 publications in refereed international journals, more than 10 book chapters, and six patents have resulted from this work. Between the years 1994 and 2004, he served as a president and CEO of the board of the Patras Science Park S.A. and during 2006–2007 served as Deputy Director of the Institute of Chemical Engineering and High Temperature Chemical Processes (ICEHT) of the Foundation of Research and Technology Hellas (FORTH).

dimensional siliceous skeletons of marine glass sponges (Figure 2), are observed. Based on thorough analysis of the literature, numerous examples of siliceous structures described in plants, bacteria, yeast, fungi, protists, sponges, molluscs, ascidians, crustaceans, brachiopods, fishes, mammals, and humans are summarized in Table 1. Also examples of pathological biosilicification observed in animal and human organisms are included and discussed below.

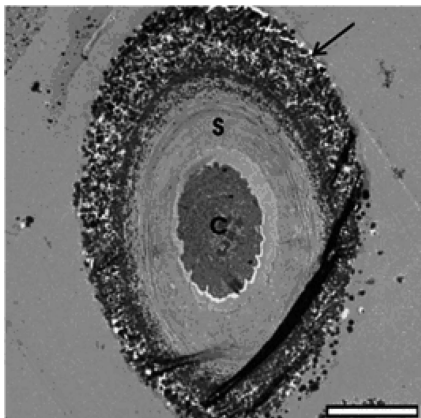


Figure 1. TEM micrograph of a cyanobacterial cell encrusted in silica colloids. C = cell; S = polysaccharide sheath; arrow = layer of colloidal amorphous silica. Scale bar = 5 μm . Reproduced with permission from ref 14, copyright 2006, Wiley.

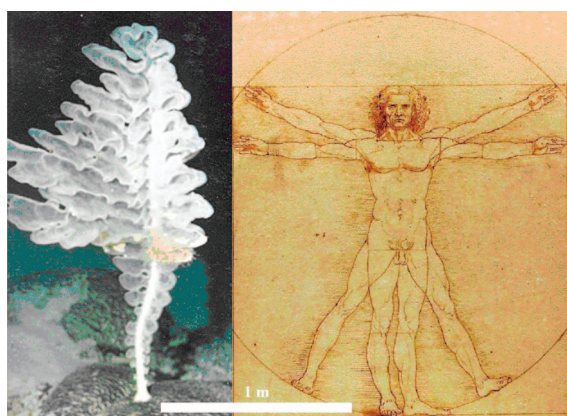


Figure 2. Unique hierarchically structured skeletons of up to 2 m high and 70 cm wide of *Aspidoscopulia* sp. (Hexactinellida, Porifera) deep-sea glass sponges have not been investigated. Image courtesy of K.R. Tabachnick, copyright 2010.

2.1. Biosilica at the Microlevel: Protozoa and Diversity of Siliceous Structures

Siliceous products deposited at the cell surface of amoeboid protists include a wide variety of species-specific structures: spicules, scales, solid plates, granules, meshwork frustules, and other elaborate geometric forms (Table 1). The siliceous nature of certain protozoan plates was first noted by Dujardin in 1841.⁷⁷ Siliceous protist scales can persist in marine and fresh water sediments once the organism has perished, leaving a record of their presence. The siliceous scales can be preserved over time as microfossils or as microfossils in sediments of freshwater and marine habitats, providing a window into modern and, potentially, ancient protist communities.^{78,79} The role of these unicellular organisms in the silica cycle and distribution in the world oceans is very significant. For example, radiolarians are the second (after diatoms) major producers of suspended (dispersed) amorphous silica in waters. They occur from the Arctic to the Antarctic, being most abundant in the equatorial zone. In waters of the equatorial Pacific, there are about 16 000 specimens per cubic meter.⁸⁰ Because the diversity of structural forms observed in diatoms is well documented in the literature,^{40,41,81–85} we took the initiative to present in this review silica-based representatives of unicellular Protozoa, other than diatoms.

A common secretory mechanism has been reported in testate amoebae, heliozoa and heliozoon-like amoebae, and radiolarians as follows.⁸⁶ Silica deposition vesicles (SDVs), either situated in the cell cytoplasm (as in testate amoebae and heliozoans and relatives) or within an expanded portion of the peripheral cytoplasm known as a cytolymma (in radiolaria), are the site of silicification. Moreover, in some testate amoebae Golgi-derived vesicles fuse with the membrane surrounding silica deposition sites. These vesicles possibly contribute to additional incorporation of silica-secreting membrane into the surface of the SDV while increasing the membrane surface area. Silica products of testate amoebae and heliozoa are deposited on the cell surface by exocytosis. The cytolymma of radiolaria, while containing a silica-secreting vacuolar space, is decidedly different in form and activity from the intracellular secretory spaces of testate amoebae and heliozoa. The cytolymma is a dynamic structure exhibiting cytoplasmic flowing activity and in a mold-like manner determines the remarkable species-specific shape of the skeleton. Consequently, the deposited silicate product of the radiolarian is an endoskeleton and is not released on the surface by exocytosis. Further research is needed to determine whether Golgi-derived vesicles, designated Golgi-fibrillar vesicles (GFV) in some testate amoebae, are also the source of SDV membranes in other silicate-secreting sarcodines. To date, none of the various SDVs have been isolated.

Normal *Raphidiophrys ambigua* cells have a rounded body form that extends a small number of stiff radiating axopodia that are used in food capture. Around the cell body lies a periplast of loosely adhering boat-shaped scales (Figure 3). The scales (1.5 $\mu\text{m} \times 4 \mu\text{m}$) are constructed as a thin, flat mesh of siliceous material, with the edges curved over to form a rim.

Testate amoebae (or testaceans), which occur abundantly and ubiquitously from the tropics to polar soils, contribute considerably to the terrestrial silica cycle as silica accumulators. Siliceous tests are formed in one of two ways: they are composed either of ingested and subsequently agglutinated siliceous material such as sand grains and diatom frustules or from ingested dissolved silica that is internally metabolized into uniformly shaped plates and held together by organic cement.^{87,88}

Testate amoebae are classified into two types by their test morphology, idiosomes and xenosomes. The test of idiosomes is composed of self-secreted siliceous scales, and that of xenosomes is composed of exogenous materials. Idiosomes, in particular, absorb dissolved silica from the environment to produce their siliceous scales. The scales are very small (ca. 10 μm) and thin (ca. 1 μm) and probably dissolve readily in the soil solutions. Siliceous plate-bearing genera include *Euglypha*, *Assulina*, *Placocista*, *Sphenoderia*, *Tracheleuglypha*, *Cyphoderia*, *Campascus*, *Heleopera*, *Lesqueruesia*, *Nebela*, *Quadrullela*, *Paulinella*, *Trinema*, and *Corythion*.⁸⁷

Recently, Aoki et al.,⁸⁹ found that testate amoebae *Euglypha rotunda* and *Trinema enchelys* consumed 55% of silica absorbed by microbes in the incubation experiments. Although biosilica preserved by living testate amoebae was as small as 0.45–1.57 kg of $\text{SiO}_2 \text{ ha}^{-1} \text{ month}^{-1}$ perhaps due to the fast turnover of amoebean silica in the terrestrial silica cycle, in various forest soils it was estimated to range from 10 to 227 kg $\text{SiO}_2 \text{ ha}^{-1} \text{ year}^{-1}$. These authors concluded that testate amoebae have a high potential as silica consumers

Table 1. Structural Diversity of Biosilica

organism	structure and form of biosilica	ref
	Bacteria	
cyanobacteria	siliceous "geyser eggs"	15
filamentous microorganisms	siliceous shrubs	16
hyperthermophilic microorganisms	siliceous sinters	17
	siliceous oncoids	18, 19
<i>Nostoc</i> -type cyanobacteria	"biospeleotherms" and shrubs	20
biofilm community	siliceous microstromatolite laminae	21
<i>Thermus thermophilus</i> TMY	silica scale from geothermal power plant	22
<i>Thermus</i> spp., <i>Hydrogenobacter</i> spp.		23, 24
<i>Phormidium</i> , <i>Fischerella</i>	lilypad stromatolites (up to 3 m long and 1.5 m wide)	25
<i>Cyanidium</i> , <i>Alicyclobacillus</i>	siliceous spicules (up to 3 cm high and up to 5 mm in diameter)	26
<i>Cyanidium caldarium</i>	granular silica spherules	27
	Yeast	
	silicified cell walls	28, 29
	Fungi	
	siliceous coated grains	30
	desert varnish	31
	Protozoa	
sarcodines		32
Gymnamoebae	siliceous boat-shaped scales	33
testate amoebae	siliceous curved rods	34
	siliceous body plates	
	siliceous particles	
heliozoa	siliceous needles, spines	
radiolaria	siliceous spicules	
	siliceous porous shells	
	siliceous spongiöse shells	
flagellates	stomatocysts, scales, spines, bristles	35
chrysophytes, synurophytes		36
choanoflagellates	siliceous loricae	
dinoflagellates	siliceous skeletons, cysts, granules, external skeleton, scales	
ebridians	statosphores (siliceous resting cysts)	37
silicoflagellates	silicified cell walls (quartz-cellulose-calcite composite)	38
thaumatomastigids	silicified cell walls	
chlorophytes		
xanthophytes		
	Foraminifera	
<i>Silicosigmoilina futabaensis</i>	siliceous cement	39
	Diatoms	
	frustule	40
	spines	41
	heavily silicified resting spores	42
	nanogranules in mitochondria	43
	Sponges	
Hexactinellida	skeletal frameworks and	44
Demospongiae	spicule (macrosclerae) microsclerae	45, 46
	Mollusca	
<i>Patellacea</i> spp. (Gastropoda)	silica in radula teeth	47
<i>Onchidiella celtica</i>	siliceous spicules and penial spines	48–51
	Ascidians	
<i>Styela clava</i>	intracellular granules	52
	Crustaceans	
(Copepoda)	opal and willemite-based teeth	53, 54
<i>Acartia tonsa</i>		55, 56
<i>Neocalanus</i> spp.		
<i>Calanus pacificus</i>		
	Brachiopods	
<i>Discinisca tenuis</i>	siliceous tablets	57
	Fishes	
<i>Psammobatis extenta</i> (Rajidae)	chalcedony in electrocytes and cholinergic nerves	58–60
	Mammals	
dog	silica calculi and stones	61
cattle	silica calculi and stones	62
monkey (<i>Macaca fuscata</i>)	dental calculi	63
rat liver mitochondria	silica nanogranules	64
		65
	Human	
cerebral cortex	chalcedony	59, 66
urinary bladder and urethra	silica calculi and stones (urolithiasis)	67
kidney	renal silica calculi	68
human glial malignant tumors	chalcedony	69
	Plants	
<i>Chaetoceros gracilis</i> (Bacillariophyceae)	siliceous setae	70
canary grass (<i>Phalaris canariensis</i>)	silica fiber	71
foxtail millet (<i>Setaria italica</i>)	inflorescence bristles	72
<i>Pleioblastus chino</i> (Poaceae, Bambusoidea)	silica cells	73
heath grass (<i>Sieglingia decumbens</i>)	silica bodies (phytoliths)	74
Bambusoideae	tabasheer	75
higher plants	siliceous nodular deposits	76

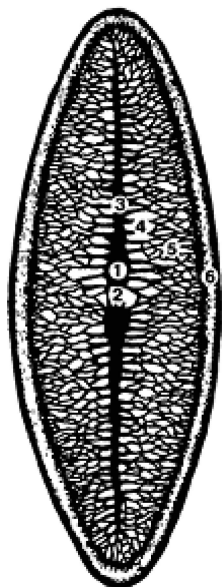


Figure 3. Siliceous scale of the *R. ambigua* (Protista, Centroheliozoa). Pattern center (1), isthmus (2), sternum (3), ribs (4), mesh (5), rim (6). Figure reproduced with permission from ref 33, copyright 1988, The Company of Biologists Ltd.

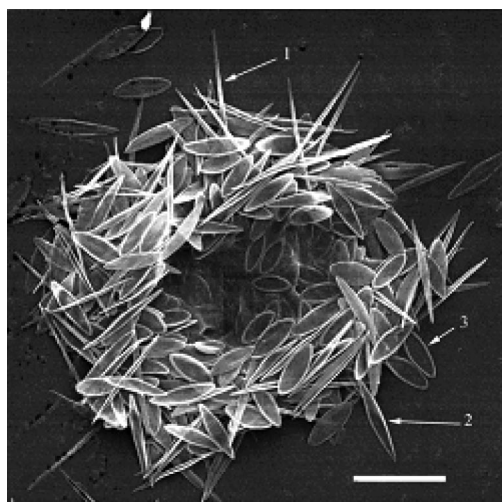


Figure 4. Periplast of *Polyplacocystis ambigua*: (1) fusiform scales; (2) naviculoid scales; (3) oval scales. Scale bar 10 μm .

and suppliers and play a role comparable to that of higher plants in the terrestrial silica cycle.

Heliozoa are ubiquitous unicellular phagotrophs with slender radiating axopodia for trapping prey.⁹⁰ In most centrohelids, the axopodia (bearing numerous kinetocysts used for prey capture) project through a thick coat, often double, of silica scales, which are well characterized by electron microscopy. Recently, Gaponova and Dovga⁹¹ reported about diversity of the siliceous scale morphologies within one species, *Polyplacocystis ambigua* (Protista, Centrohelida). A scanning electron microscopy image (Figure 4) showed strong evidence of the presence of the fusiform, naviculoid, and oval forms of the *P. ambigua* periplast scales.

The basic structure of the choanoflagellate lorica comprises a pattern of siliceous costae arranged in longitudinal and transverse (or helical) arrays (Figure 5).

The abundance of loricate choanoflagellates in the oceans today can be directly related to the enormous scope for variation as is illustrated from the basic structure of the siliceous lorica.⁹² For example, one group of choanoflagel-

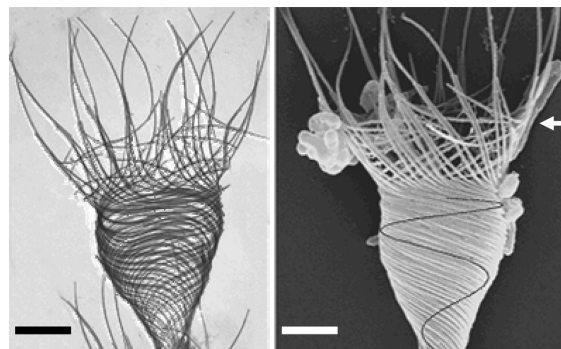


Figure 5. TEM image (left) of *Acanthoeca spectabilis* siliceous lorica showing the left-handed orientation of costae comprising the lorica chamber and the continuity of individual helical costae with the costal strips subtending the spines (bar = 2 μm). SEM image (right) of a lorica showing the arrangement of helical costae forming the chamber in continuity with bases of the spines (bar = 2 μm). The inner layer of costal strips within the lantern of spines is also apparent (arrow). Figure reproduced with permission from ref 92, copyright 2008, Elsevier.

lates, the *Acanthoecidae norris*, are exclusive to marine and brackishwater environments and are distinguished by the possession of a basket-like lorica comprising an arrangement of siliceous costae. The lorica typically contains an outer arrangement of longitudinal costae with an inner arrangement of helical or transverse costae; the combined positioning of these structures gives the lorica its overall mechanical stability. Individual costae are made up of rod-shaped costal strips attached to each other end-to-end.

Each costal strip is deposited within the cell in a membrane-bound vesicle and, when complete, is exocytosed to the exterior.^{93–95} Costal strips are accumulated outside the cell until a sufficient number has been produced to form a lorica. Assembly of the lorica occurs as a single, discrete movement that lasts 2–5 min after which no further adjustments can be made. While all loricate species adhere to these basic principles, there are, nevertheless, two distinctive types.⁹⁶ In one variant, the nudiform condition, a lorica-bearing cell divides to produce a “juvenile” flagellated cell, which swims away from the parent lorica, settles onto a substratum, accumulates costal strips on its surface, and, when a complete set have been produced, assembles a lorica.⁹⁷ In the second variant, the tectiform condition, a lorica-bearing cell produces a complete set of costal strips prior to cell division and stores them at the top of the collar. When a complete set of strips have been produced, the cell divides and the resulting “juvenile” is inverted and pushed out backward from the parent lorica taking with it the accumulated strips. Within minutes of the “juvenile” being liberated from the parent a new lorica is assembled.^{94,97}

2.2. Biosilica at the Macrolevel: Marine Glass Sponges

Sponges (Porifera) are the simplest and oldest multicellular animals on earth and live attached to the seabed or another substratum. Sponges diverged from other animals earlier in evolutionary history than any other known animal group, extant or extinct, with the first sponge-related record in earth history found in 1.8 billion year old sediments.⁹⁸ The huge diversity with respect to their natural habitat is probably the reason for the estimated number of approximately 15 000 different sponge species.⁹⁹ The phylum Porifera is divided into three classes, Hexactinellida and Demospongiae that

comprise a siliceous skeleton and the Calcareia with a calcareous skeletal network.¹⁰⁰ In contrast to the high diversity of spicules, there are relatively few basic types of skeletal frameworks in demosponges. Six elemental types of skeletons with intermediate forms can be differentiated: hymedesmoid, plumose, axial, radiate, reticulate, and arranged in strength confusion.⁴⁴ Hexactinellida Schmidt (Porifera) are mainly deep-water marine sponges defined by their production of siliceous spicules of hexactinic, triaxonic (cubic) symmetry or shapes clearly derived from such forms by reduction of primary rays or terminal branches added to the ends of primary rays. Hexactinellids include about 600 described species, 7% of all Porifera, distributed in 5 orders, about 17 families, and about 118 genera (as reviewed by Ehrlich⁴). The spicules of most hexactinellids are larger (see Figure 2) and more luxuriously architected than those in demosponges.¹⁰¹ For example, Antarctic giant hexactinellids, such as *Rossella nuda* and *Scolymastra joubini*, which may be up to 2 m tall, 1.4 m in diameter, and up to 600 kg wet weight, contain up to 50 kg biogenic silica each.¹⁰² They are extremely slow-growing and seemingly reproduce only at long time intervals¹⁰³ and become old, probably more than 1500 years.^{104,105} While their living tissues represent only a modest biomass, the silicious spicules of hexactinellids become an important ecological factor. After the death of the sponges, the megascleres do not dissolve but accumulate on the bottom and over large areas to form spicule mats commonly about 50 cm thick but occasionally exceeding 2 m.^{104,106}

Sponges seem to be important players in numerous geobiological processes including the silica demineralization—biomineralization—remineralization cycle.¹⁰⁷ For example, siliceous sponge reefs had a wide distribution in prehistoric times and once constructed the largest reefs known on earth, reaching an acme in the Upper Jurassic when a deep-water reef belt on the northern Thetis shelf existed that was 7000 km long.¹⁰⁸ In present times, hexactinellid sponges of the order Hexactinosida have constructed reefs at several localities off the coast of British Columbia, Canada. The reefs occur on relict glaciated seafloor areas with a low sedimentation rate and a high dissolved silica concentration in the Queen Charlotte Basin and in Georgia Basin,^{109,110} and the reefs represent stable communities that have been growing for up to 9000 years. The main builders of the reef frame include the hexactinosidan species *Aphrocallistes vastus*, *Farrea occa*, and *Heterochone calyx* in Queen Charlotte Basin and *A. vastus* and *H. calyx* in Georgia Basin.¹⁰⁹ The framework of these reefs is constructed through several processes of framebuilding, and the reef matrix is derived from trapping of suspended sediments.¹⁰⁸ Similar framebuilding processes are thought to have contributed to the formation of the ancient reefs.¹¹¹ Upwelling and downwelling oceanographic processes in a biologically productive coastal sea have contributed to the development of large reef complexes. The reefs form as bioherms (mounds) and biostromes (beds or sheets) that may rise up to 21 m above the seafloor, and they cover around 1000 km² on the continental shelf. Individual reef complexes may cover areas of more than 300 km² and occur in the 90–240 m depth range.^{110,112,113} Trapping fine-grained siliciclastic sediments in suspension in near-bottom currents is an important part of the mound-forming process, because it prevents the reef framework from collapsing under its own increasing weight.

2.3. Pathological Silicification: Silica Calculi and Stones

Silica has been recognized as an essential trace element in the metabolism of mammals.¹¹⁴ Silicon deficiency gives rise to disorders of bone, cartilage formation, and connective tissue metabolism. Silicon, as silicate, is present in vegetables and the husks of whole grains. The blood-plasma level is approximately 1 mg per 100 mL and usually does not rise since any excess is rapidly excreted in the urine.¹¹⁵ In humans, silica is also a normal metabolite, absorbed from the gastrointestinal tract into the blood, and present in the urine in concentrations of about 10 mg/day¹¹⁶ in normal subjects. It is present in urine in amounts proportional to that in a silica-rich diet such as vegetables, whole grains, and seafood.

According to Keeler,¹¹⁷ urinary pH, urinary silicate concentration, and the concentration of matrix constituents have an influence on the formation mechanism of silica urinary stones. Many patients have received silicate in the form of antacids without resulting stone formation in the urinary tract. No significant difference in the urinary silicate concentration and the daily urinary excretion of silicate is found between silicate stone formers and controls. Although urinary silicate levels were within the normal range in described cases, a siliceous fragment and other matrices existed simultaneously. These facts suggest that the urinary concentration of matrix constituents has the greatest influence.

The silica stone was first described by Herman and Goldberg¹¹⁸ in the USA and was attributed to the ingestion of magnesium trisilicate for treatment of esophagitis. Silica occurs in calculi in the opaline state, which is noncrystalline, but on heating, it can be transformed into various crystalline forms depending on the temperature of ignition.⁶⁸ However, silica calculi in humans are known to be extremely rare.^{119–121} In a series of electron microscopic studies of human urinary stones, discrete siliceous deposits were encountered in 3 out of 180 stones. The deposits differed in their morphology from any other components of urinary stones.¹²² Three urinary bladder stones composed of pure silicon dioxide were found in a patient who had been taking magnesium trisilicate compound three times a day for 40 years.⁶⁷

Long-term oral intake of silica-containing antacids (e.g., magnesium trisilicate) is thought to be a causative factor inducing silicate urolithiasis.^{122,123} Briefly, when a silicate reacts with acid in the alimentary tube, especially in the stomach, part of the silica is precipitated as a gel and part remains as a solution in the form of a colloid. The breakdown products can be readily absorbed across the intestinal wall and excreted rapidly in the urine. Alkalinization by the gut fluid changes a silica colloid into a more soluble and absorbable compound. Part of the silica can be reabsorbed and eliminated in the urine. Urinary excretion rises dramatically in proportion with the increase in silicate intake. Synthetic magnesium trisilicate ($2\text{MgO} \cdot 3\text{SiO}_2 \cdot n\text{H}_2\text{O}$), which is a white insoluble powder, was shown not to be absorbed from the intestine and to have absorbent and antacid properties of particular value in the treatment of gastric acidity and chronic peptic ulceration.^{124,125} The value of magnesium trisilicate and the silica resulting from the reaction with gastric hydrochloric acid apparently depends on the fact that both are active hydrated colloids. Although the chemical reaction can be represented as



the conditions of interaction are complex and are not completely understood. Page et al.¹²⁶ suggested that more complex end-products than silicon dioxide (or silica) were produced, namely, various combinations with water to form different silicic acids and silicates. They considered that these products could include soluble orthosilicic acid (H_4SiO_4 , that is, $\text{SiO}_2 + 2\text{H}_2\text{O}$), partially soluble metasilicic acid (H_2SiO_3 , that is, $\text{SiO}_2 + \text{H}_2\text{O}$), partially soluble trisilicic acid ($\text{H}_4\text{Si}_3\text{O}_8$, that is, $3\text{SiO}_2 + 2\text{H}_2\text{O}$), and nearly insoluble disilicic acid ($\text{H}_2\text{Si}_2\text{O}_5$, that is, $2\text{SiO}_2 + \text{H}_2\text{O}$). The variation in the hydration of the SiO_2 molecule thus induces changes in solubility. This factor, as well as the physicochemical state of the silica (which may remain in solution as a colloidal sol or may partially separate as a gel) probably determine its absorption from the intestine.

Literature dealing with silica urolithiasis without the intake of silica-containing antacid is scant. Only two cases of silica calculi without oral intake of magnesium trisilicate were reported.¹²⁵

Siliceous urinary calculi are common among herbivorous animals such as cattle and sheep.^{117,127} Silica calculi are reported also in dogs.^{61,128} As many as 4% of range steers wintered in the northwestern plains of North America develop silica calculi with urethral obstruction. The high incidence of silica in these animals has been attributed to the consumption of forage with a high content of SiO_2 . The grass in certain areas may contain up to 8% of silica on dry weight basis and a large number of steers in these areas develop silica calculi.⁶² Precipitation of silica in the urine of these animals tends to occur when their urine level of silicon exceeds 70–80 ppm. However, following an experimental increase of silicon in steer urine, silica calculi failed to develop, and therefore, it has been postulated that proteinaceous matrix plays a role in silica calculi formation.¹¹⁷

Localized silicon distribution was also found in both fracture and oral surfaces of the dental calculi in *Macaca fuscata* monkeys.⁶³ These authors have suggested that silicon-rich areas containing opal as well as clay minerals may regulate the formation also of human dental calculi.

To the best of our knowledge, there are no works related to demineralization of silica stones and calculi with respect to isolation of organic matrix. However, the presence of organic macromolecules (including fibrin) as nucleators of these biomineral formations was suggested. For example, Lagergren¹²² considered that the structure of the calculi in his cases and the finely crystalline form of the silica supported the view that the silica was precipitated in the gel form apparently mixed with fibrin. Also Bailey¹²⁹ reported results that suggested that urine protein contributes to the formation of siliceous urinary calculi, by affecting the solubility of polymerized silicic acid. He suggested that the reaction involves the silanol groups of the silicic acid polymers and the secondary amide groups of the protein.

3. Biodegradation and Silica Utilization in Nature

Minerals are naturally occurring inorganic solids of definite chemical composition and possessing an ordered internal structure; rocks can be considered to be any solid mass of mineral or mineral-like material and may therefore often

contain several kinds of minerals.¹³⁰ Rocks and minerals represent a vast reservoir of elements, many of which are essential to life and which must be released from their inanimate prison into forms that may be assimilated by the biota. Silicate is widely distributed in nature: in addition to the 28% of the Earth's land surface formed by quartz, an estimated 49% of surface is occupied by other minerals with a silicate structure.¹³¹ The following forms of solid silica are encountered in nature.¹³²

- α -quartz, the most abundant single mineral in sediments
- opal, or opaline silica, a disordered hydrated form of silica
- amorphous silica, a term used to describe materials whose composition is relatively pure SiO_2 that are in the mesomorphous state.

Under the classification of amorphous silica, the various kinds of hydrated and dehydrated silica gels, silica glass, siliceous sinters, powders from the condensation of vapor phases, and skeletal materials of numerous silica-secreting organisms are included. All forms of solid silica listed above and represented in Figure 6 are involved into the silica cycle on the Earth.

Through the weathering process, silicate minerals contribute to the dissolved silica in surface waters and may be concomitantly altered to colloidal aluminosilicates (clays). In the ocean, via the biochemical precipitation by siliceous organisms, silica is precipitated as amorphous silica or opaline silica. During diagenesis, amorphous silica deposited in the oceans recrystallizes to quartz and the silica in solution in formation waters gradually comes to equilibrium with quartz by precipitation of secondary overgrowths, authigenic crystals, etc. Hot springs waters precipitate silica as they cool at the surface and become supersaturated, forming opaline or siliceous sinters through intermediate stages of gel formation.

From a biological perspective, silicon can be accumulated by diatoms and other living organisms such as silicoflagellates, some xanthophytes, radiolarians, actinopods, plants such as grasses, ferns, horseradish, some trees, and flowers, some sponges, ascidians, molluscs, and bacteria and fungi.¹³⁴

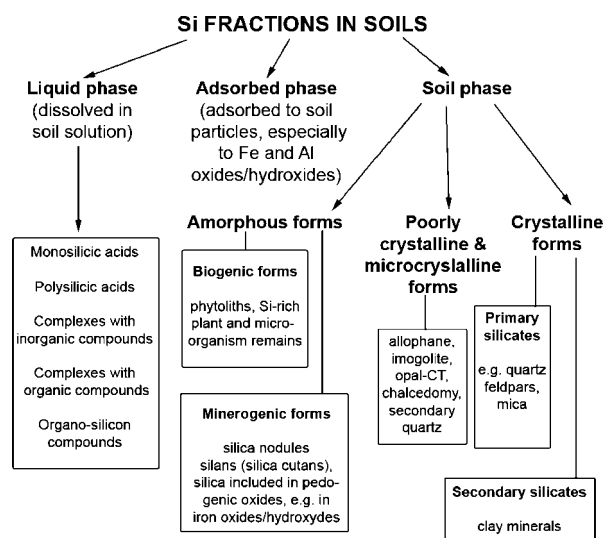


Figure 6. Classification of silicon compounds in the soil. Figure reproduced with permission from ref 133, copyright 2006, Springer.

Given these roles in living organisms, it is reasonable to analyze here the peculiarities of silica biodegradation in Nature.

3.1. Silica Bioleaching: Bacteria and Fungi

Microorganisms are intimately associated with global phenomena such as bioweathering, soil formation, and the biodegradation of rocks and minerals. The biologically mediated destruction of silicate minerals to liberate limiting inorganic nutrients is a fundamental observation of subsurface microbial ecology.^{135,136} Interactions between microbiota and silicates may be classified into the following reactions:¹³⁷

- (1) Dissolution and destruction of the silicate crystal lattice
- (2) Uptake and utilization of silicon
- (3) Release of silicon and sedimentation in the environment.

The cycle of biological degradation (Figure 7) of polymeric silicates is completed by an abiotic polymerization and separation. There are numerous ways of interaction between the biosphere and silicon in its various forms and maintaining this cycle is of vital importance for a plethora of lower and higher organisms.¹³⁸ Because of its greater chemical mobility than crystalline silica phases, biogenic opal plays a major role in the cycling of silica in soils as well as in aquatic environments.¹³⁹

Plants contribute significantly to the biogeochemical cycle of silicon.¹⁴⁰ Alexandre et al.,¹⁴¹ reported that 92% of the biogenic silica in the soil is recycled by plants and is the main source of this nutrient. They take up silicon from soil water in the form of water-soluble silicic acid, which is polymerized and precipitated as amorphous silica, frequently in close proximity to the transpiration conduit. After plant death, silica returns to the soil, and plant decay generates humic acid, which increases weathering activity in soils. Biocycling of silica in soil also occurs through microbial

activities that involve fungi, bacteria, and actinomycetes. Thus, plants and microbes, through their intricate interplay with soil minerals, contribute appreciably to the global silicon cycle.¹⁴²

Bacteria (and possibly archaea) accelerate silica dissolution in the sea by colonizing and enzymatically degrading the organic matrix of diatom frustules.¹⁴³ The resolubilization and internal recycling of the silica in diatom frustules can provide the soluble silica that is essential for further growth of diatoms.¹⁴⁴ Empirical evidence from a number of oceanic systems has revealed that Si regeneration in the upper mixed layer, via dissolution of biogenic silica, is a critical Si supply mechanism to diatoms. These regions, where diatom silica is recycled more rapidly, possess a regenerating source of the required Si in addition to the exchange with new, nutrient-rich subsurface water. It has been estimated that an atom of Si is cycled 39 times before burial to the seabed,¹⁴⁵ which illustrates that silicon regeneration is robust and efficient. Moreover, the extent of Si regeneration within the upper water column is quite substantial and sustains significant diatom production.¹⁴³

Why do bacteria utilize silicon and silica? It was shown that silicic acid increased numbers of both aerobic and facultative anaerobic bacteria in ultrapure water incubated under strict oligotrophic conditions.¹⁴⁶ Soil extracts acted as the bacterial inoculum. These authors speculated that silicic acid, produced by the hydrolysis of silicates on the early Earth, could have stimulated the growth of the first bacterium, thereby allowing it to become established in the then prevailing conditions (presumed to be oligotrophic). It was reported that addition of Si in culture media showed a remarkable growth accelerating effect on *Staphylococcus aureus*¹⁴⁷ and in Nocardioform microorganisms.¹⁴⁸ Silicon is also known to enhance the growth and pathogenicity of *Mycobacterium tuberculosis*.¹⁴⁹

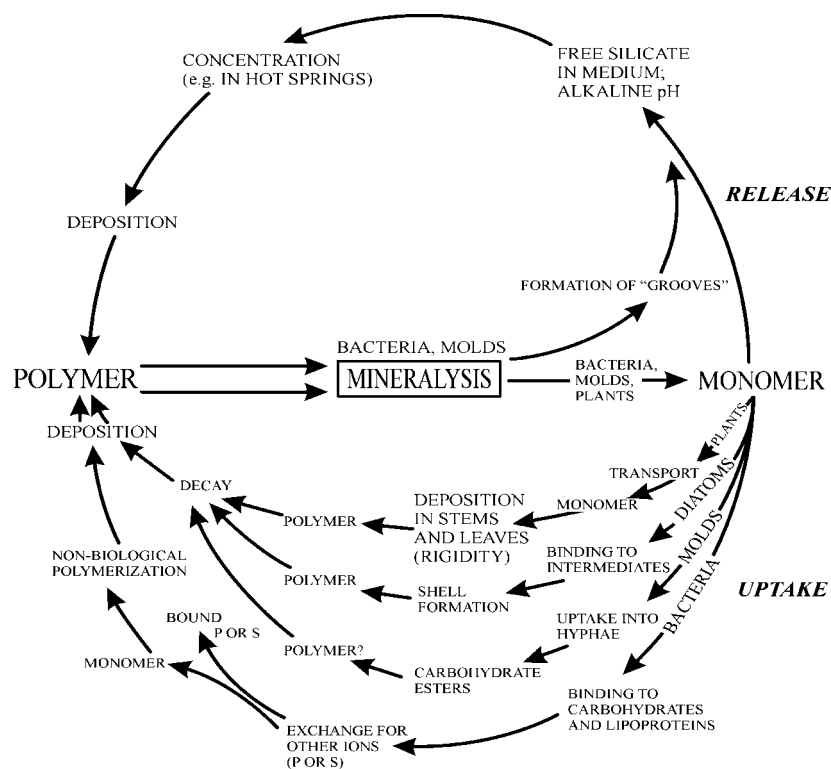


Figure 7. Biodegradation of polymer silica, and the release, uptake, and repolymerization of monomer silica by various organisms, leading to a cycling between the polymer and monomer forms of silica.

The action of bacteria on silicate-based minerals has been characterized as nonenzymatic.¹⁵⁰ Microorganisms capable of growing on the silicates in the absence of organic substances may have developed autotrophically and have been proposed to be categorized as “silicate microorganisms”.¹⁵¹ The existence of “silicate bacteria”, defined as chemolitho-autotrophic bacteria that gain their energy breaking Si–O bonds in silicates, has been suggested by Vernadsky.¹⁵² Brussoff¹⁵³ has isolated a thermophilic *Bacillus siliceus*, which abundantly deposited silica in its cells. *B. siliceus* is capable of breaking down the insoluble potassium aluminosilicates in the soil and may even be cultured in a granite bowl or in a medium of powdered glass.¹⁵⁴ Furthermore, a plate method for studying the breakdown of synthetic and natural silicates by soil bacteria was established.¹⁵⁵ Also, silicates that contain sulfide minerals can be present during heap bioleaching for metal extraction. Weathering of silicates is catalyzed by heterotrophic bacteria and fungi via the production of acidic metabolites, as well as by the action of acidophilic microorganisms.^{156,157} Acidophilic microorganisms preferentially attach to sulfide over silicate minerals, and their attachment is attributed to their ability to grow on the Fe²⁺ released from oxidation of the mineral sulfide bond. However, these microorganisms do not cleave the Si–O–Si bond.

Heinen¹⁵⁸ was able to show that silicon is actively metabolized by certain bacteria. The same author reported that incubation of *Proteus mirabilis* in media containing silicate instead of phosphate, lead to the formation of carbohydrate–silicate esters.¹⁵⁹ It was shown that these bacteria possess an energy-dependent silicon uptake from quartz in its natural environment.¹³⁸ Oberlies and Pohlmann¹⁶⁰ also proved that bacteria that had attached to feldspar or glass produced etchings in the surface structures that corresponded in size, shape, and depth to the dimensions of these bacterial cells. The mechanisms by which they act may involve production of metabolic products such as organic acids that can act as acidulants or ligands, base in the form of NH₃, and specific capsular slime from bacteria. Among the acids, 2-ketogluconic acid formed by some bacteria has been shown very effective in the dissolution of silicates.^{155,161} They furnish protons that help in breaking Si–O bonds through protonation and catalysis. At the same time, some of the acids may also act as ligands that pull cations from the framework of the crystal lattice, facilitating subsequent breakage of framework bonds or mechanical framework collapse. Bacterial acid polysaccharide-based slimes have been reported to form complexes with silicate that lead to silicate solubilization.¹⁶² Recently, Brehm et al.¹⁶³ reported on the role of microorganisms and biofilms in the breakdown and dissolution of quartz. They described microenvironmental photosynthesis-induced alkaline leaching of quartz by cyanobacteria-containing biofilms. Due to their photosynthesis, microorganisms can create a local shift in the pH from 3.4 to evidently higher than 9 (necessary for quartz dissolution). The quartz covered with a biofilm is partially perforated to a depth of more than 4 mm.

Different strains of “silicate” bacteria were used to leach silicon from low-grade bauxite ores in which the silica connected with alumina in the form of aluminosilicates was the main impurity.¹⁶⁴ The strains were isolated from soil and rock samples and were taxonomically related to the species *Bacillus circulans* and *B. mucilaginosus*. The leaching of silicon by these bacteria greatly depended on the method of

treatment. The bacterial action was connected with the formation of mucilaginous capsules consisting of exopolysaccharides. Chemoorganoheterotrophic bacteria *Bacillus circulans* Jordan and *B. circulans* CHBC-1 were used in order to eliminate silicates from oil shale organic matter.¹⁶⁵ This process was expected to substitute the drastic HF-treatment in the kerogen concentrate preparation procedure. The desilicification efficiency of the zymogenous strain *B. circulans* CHBC-1 was about 70%. These experiments indicated that siliceous bacteria may have potential as an alternative, biochemical agent for the isolation of native kerogen from the silicified oil shales. Tests showed that bacteria were not using the shale organic matter as a source of carbon.¹⁶⁶

In most of the previous studies concerned with the effect of bacteria on silicate dissolution, the action of media acidification and organic acid excretion due to bacterial metabolism was the main factor responsible for element release from the solid via metal–O–Si bond breakage. In addition, it was very difficult to separate the effect of live bacteria and their exometabolites from that of the chemical components of nutrient solution. Thus, experiments on live and dead cultures of rhizospheric soil bacteria *Pseudomonas aureofaciens* interaction with calcium silicate (wollastonite, CaSiO₃) revealed that the release rates of both Ca and Si were only weakly affected by the presence of live or dead bacterial cells in inert electrolyte solution and in nutrient media: there is only ~20% increase of dissolution rate in experiments with live cultures compared with dead cultures. Therefore, the effect of extracellular organic products on the weathering rate of Ca-bearing minerals is expected to be weak, and the acceleration of “basic” silicate rock dissolution in natural settings in the presence of soil bacteria is most likely due to the pH decrease alone.¹⁶⁷

In contrast to aluminosilicates and other multiple oxides requiring for dissolution the breaking of Al–O–Si or Mg–, Ca–, or Fe–O–Si bonds, promoted by both pH change and ligand attack on positively charged metal sites, the ≡Si–O–Si≡ bonds in quartz or amorphous silica can be polarized mostly by protons (≡SiOH^o → ≡SiOH₂⁺) or hydroxyl ions (≡SiOH^o → ≡SiO⁻). Indeed, Heinen et al.¹⁶⁸ reported on leaching of silica in a thermal hot spring. The formation of siliceous gels facilitated settling of microorganisms and was accompanied by leaching of silica from the underlying rock, resulting in destruction of rock material to a fine-grained dust beneath microbial mats. The mean silicon concentration was 34.6 μg of Si/mL in the thermal spring water as opposed to a mean value of 2.9 μg of Si/mL in the cold waters. Silica-leaching bacteria are highly tolerant with respect to dissolved silica. For example, *Bacillus licheniformis*, an indigenous strain from high silica-containing magnesite ore was found to tolerate 250 μg of Si/mL in the medium. During growth the bacterium was capable of accumulating about 21 μg of Si/mL within 8 h.¹⁶⁹ The application of *Thiobacillus thiooxydans*, which formed as a result of microbial sulfur oxidation sulfuric acid and strongly acidified leaching medium, brought 131 mg of Si/L into solution after 45 days. In the absence of the microorganism and with addition of sulfuric acid, 65.7 mg of Si/L were leached.¹³⁷

Bacteria are also involved in the transformation between the different forms of silicon. Singh et al.¹⁷⁰ recently reported on the formation of silicon/silica nanocomposites using *Actinobacter* sp. bacterium that was exposed to K₂SiF₆ precursor under ambient conditions. The authors hypoth-

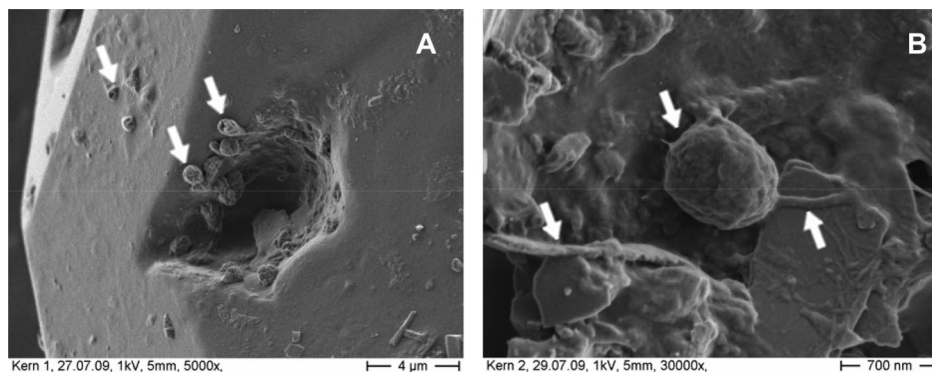


Figure 8. SEM images of unidentified fungi (arrows) that dissolve zirconium silicate collected at the sea bottom.

esized that this bacterium secretes reductases and oxidizing enzymes, which lead to the Si/SiO₂ nanocomposite synthesis. The synthesis of silica nanoparticles by bacteria demonstrates the versatility of the organism.

Endolithic and epilithic microbial communities produce polyols as osmotic protectants in response to desiccation. Low molecular weight polyols and polysaccharides bind to the siloxane layers within layered siliceous minerals, such as micas and soapstone, by hydrogen bonding.¹⁷¹ These interlaminar complexes cause expansion of the crystalline layer, weakening the structure, and may allow entry of chelating agents that mobilize the ions stabilizing the crystal structure. During periods of desiccation, the polyols become concentrated, forming nonaqueous systems. Basic catalysis in such water-deficient ecosystems favors the formation of water-soluble organosilicon compounds, principally organic siloxanes. Polyols and complex organic acids can also attack siliceous minerals under alkaline conditions. Extracellular carbohydrate polymers released by fungi and bacteria can react with organic siloxanes to form water-soluble organic siloxanes.¹⁷¹

Biocorrosion of historical and optical glasses is often linked to the growth of fungi.¹⁷² Fungi provoked remarkable etching rates due to their ability to synthesize ligands (siderophores) specific for ferric and other metal ions. Initial symptoms of glass biodeterioration comprise of etching, pit corrosion, and leaching.¹⁷³

Recently, Bansal et al.¹⁷⁴ have shown a *Fusarium oxysporum* fungus-based bioleaching approach for the synthesis of hollow silica nanospheres from sand. The formation of the silica nanoparticles is believed to proceed by a two-step process. The first step involved leaching of silica from the sand grains in the form of silicic acid by proteins present in fungal biomass, while in the second step the silicate complex is hydrolyzed by other specific proteins in the fungus to silica. The silica is in the form of nanoparticles capped by stabilizing proteins from 2 to 5 nm in size and is released into solution by the fungus. An approach was also reported¹⁴² that involves the use of the same plant pathogenic fungus in the biotransformation of naturally occurring amorphous plant biosilica into quasi-spherical crystalline silica nanoparticles and its extracellular leaching in the aqueous environment at room temperature. The silica biotransformation is fairly rapid and occurs within 1 day of reaction of the fungal biomass with the rice husk.

Bioerosion of very hard silica-based minerals also takes place in natural environments. Recently, bioleaching trails made by fungi that are responsible for dissolution of zirconium silicate in marine environment (Figure 8A,B) were

observed. It seems that bioerosion of this very ancient mineral is also of correspondingly ancient origin.

Therefore, microorganisms have been shown to accelerate the dissolution of silicate-based minerals by the production of excess proton and organic ligands and in some cases by the production of hydroxyl anion, extracellular polysaccharides, enzymes, and proteins^{135,142,174} or, in the special case of nitrogen-rich systems, from the creation of alkaline environments.¹⁷⁵

3.2. Silica Bioleaching: Diatoms

The marine biogeochemical cycle of silicon largely depends upon the balance between biological precipitation of amorphous silica by siliceous organisms (mainly diatoms) and postmortem dissolution of their skeletons.¹⁷⁶ Prior to the diatom appearance, biogenic silica burial was probably equitably divided between radiolarians and siliceous sponges as more ancient organisms.¹⁷⁷ Dissolution begins in the water column when the silica skeleton is exposed to undersaturated seawater and can continue after deposition at the seafloor.

Recently, Penna et al.¹⁷⁸ reported *in vitro* investigations of the influence of particulate silica sources on growth and silicon uptake of different diatom species. Each diatom strain was incubated in controlled conditions with mineral (quartz sand and two pure quartz dusts with variable degree of hydrophilicity/hydrophobicity) and biogenic (diatomaceous earth and sponge spicules) silica substrates. It was shown that investigated species grew much better with crystalline than amorphous substrates, free from their solubility in artificial seawater. Furthermore, diatom biomass increased when the pure hydrophilic quartz was converted into the hydrophobic one; this may be due to an enhancement of diatom adhesion onto the silica particles, probably mediated by protein–surface adsorption. The authors suggested a hypothetical surface driven uptake mechanism as follows. Marine diatoms might be able to make bioavailable dissolved silicon from particulate silica by excretion of some compounds, which facilitate silicon release in the form of silicic acid, either by cell–particle contact for benthic diatoms or by diffusion into the medium for pelagic species.

3.3. Silica Bioleaching: Sponges (Porifera)

According to Maldonado and co-workers,¹⁰² our current understanding of the silicon cycle in the ocean is based on the presumption that diatoms dominate not only the uptake of silicic acid but also the production and recycling of biogenic silica and also that other organisms with siliceous skeletons, including sponges, radiolarians, and silicoflagel-

lates, play a negligible role. These authors showed that the retention of Si by siliceous sponges in some sublittoral and bathyal environments is substantial and that sponge populations function as Si sinks. Therefore, sponges may affect Si cycling dynamics and Si availability for diatoms, particularly in Si-depleted environments. It was demonstrated that the role of sponges in the benthopelagic coupling of the Si cycle is significant.¹⁰²

Although the soluble form of silicon is generally considered the only available source of silicon for aquatic biota, there is some evidence that silica sponges may dissolve and use quartz or other insoluble silicates as available Si source.¹⁷⁸ For example, gemmules of *Spongilla lacustris* reared in silicon-free freshwater may produce a complete spicular complement, using different kinds of silicates, such as quartz sand on the aquarium bottom.¹⁷⁹

Sponges as benthic species react differently in the presence of different mineral forms of silica, suggesting the existence of complex mechanisms to recognize and select, at the cellular level, the different surface properties of the silicate mineral.¹⁸⁰ The common Atlanto-Mediterranean demosponge *Chondrosia reniformis* incorporates mineral grains such as quartz, plagioclase, sanidine, and muscovite, as well as opaline spicules. The quartz selection is performed on the sponge surface (pinacoderm), which also variantly reacts to different form of silica. When the quartz grains settle on the sponge, the pinacoderm breaks and the pinacocytes contract themselves to form a rim around them, while the presence of opaline spicules elicits a motile response of pinacocytes that quickly recover them. In the sponge body, these two forms of silica have different fates: the quartz grains are strongly etched, rounded, made uniform in size and expelled as pellets, while the amorphous silica (chalcedony and opal) are stored.¹⁸¹ The dissolution process of quartz in *C. reniformis* is due to the ascorbic acid activity, which reaches in sponges levels from 1 to 10 $\mu\text{g/g}$ wet weight of tissue. The quartz dissolution mechanism by ascorbic acid has been partially clarified: it is supposed to change the quartz surface area "roughness", leading to an increased radical production.¹⁸²

The exact mechanism of how a sponge selects and engulfs particles to dissolve them remains a mystery. A possible explanation was suggested by the evidence that the expression of the gene for collagen was found to be dependent on the silicate concentration. In this way, the induction of collagen production by quartz dissolution may be hypothesized.¹⁸³

A possible relationship between silica turnover and symbiotic organisms in sponges is postulated.¹⁸⁰ The sponge *Chondrilla nucula* presenting a remarkable population of autotrophic symbiots increases its biomass during the summer months and its spicules show impressive signs of corrosion.¹⁸⁴ This phenomenon suggests a drastic increase of the ascorbic acid levels to protect against the increasing levels of free radicals due to the increased photosynthetic activity. It was speculated¹⁸⁰ that in such conditions, the levels of ascorbic acid in the sponge tissues become sufficiently high to determine the partial dissolution of the sponge spicules.

3.4. Silica Bioleaching: Worms (Annelida)

Recently, the production and characterization of silica nanoparticles by Californian red worms (*Eisenia foetida*) through a biodigestion process of rice husk were reported; the rice husk contains, naturally, high concentrations of silica

(22%).¹⁸⁵ The worms were fed gradually with rice husk and water during 5 months to clean the worm's digestive system from other types of food. The efficiency in the production of the particles was 88%. These results were compared with those obtained using other agro-industrial wastes that contain silica: coffee (12%) and cane (8%) husk.

Californian red worms were selected to produce silica nanoparticles because they possess many important characteristics that make them unique for this purpose: their daily food intake is equal to their own weight and they excrete 60% of the ingest as humus, are very prolific, live up to 16 years, can live at temperatures from 14 to 27 °C, require a relative humidity between 70% and 80%, support pH from 5 to 8.5, and resist aggressive environments. In addition to the aforementioned attributes their main characteristic is that they can eat and process agro-industrial wastes containing high concentrations of silica.¹⁸⁵

The high silica content of the rice husk makes it very suitable as raw material for the production of silica particles: the worm's digestive process together with the calcination produce silica nanoparticles of narrow size distribution and spherical shape. The worm digestive process can be briefly described as follows. The food is wetted and predigested by the worm using an enzymatic liquid (containing lipases, amylases, trypsinogen, etc.). The faring (located at ring 6) smashes and sucks the food sending it to the esophagus where the pH is neutralized using CaCO_3 . At ring 20, the intestine initiates the digestion and absorption processes.

During the digestion, the strong action of the muscles at the intestinal wall smashes the food, while endocrine and calciferous glands provide the enzymes (amylases, proteases) producing the degradation of the organic matter. Because silica has a chemically resistant structure, enzymes during the digestion process do not attack it, but the mechanical work produced by the muscular movements in the worm intestine is capable of grounding silica to 55–250 nm size nanoparticles.¹⁸⁵

4. Possible Mechanisms of Biologically Mediated Desilicification

4.1. Interaction between Silica and Cells and Tissues

Very little is known of biological silicate interactions in higher animals, and despite many efforts, a biological process or silicate binding site has not been identified so far.²⁹ The mechanism by which the silica particles become bound to the surface of the cells or partially dissolved by them is not clear. Silica is believed to play a critical role in bioactivity. For example, bioactive glass is an ideal biocompatible material.¹⁸⁶ However, inhalation of the crystalline form of silica is associated with a variety of pathologies, from acute lung inflammation to silicosis, in addition to autoimmune disorders and cancer.^{187–191} The International Agency for Research on Cancer (IARC) recently concluded that there is sufficient evidence that inhaled crystalline silica is a human lung carcinogen.¹⁹²

Although much experimental work remains to be done, a comprehensive view of the biological reactions of vertebrates to silica particles and the pathogenesis of silicosis in humans is emerging.¹⁹³ This is an entirely immunological process that begins with the stimulation of the innate immune system (IIS), which senses the surface of the silica particles as if it

were the surface of bacteria or fungi. This happens because somehow the chemical properties of this surface mimic those pathogen-associated molecular patterns (PAMP) that can react with one, or many, of the receptors of the IIS. Subsequently, the activation of the IIS is followed by a polyclonal hyperactivity of the lymphoid cells (adaptive immune system).¹⁸⁷ The whole process reflects the effort of the vertebrate immunity to eliminate what is sensed as a potentially threatening pathogen, but of course, the silica particles are indestructible during a short period of time,¹⁹⁴ and the only viable solution is to bury them inside collagenous tissue. The immunological pathogenesis of silicosis has much in common with that of the so-called “collagen” diseases,¹⁹³ and it is not surprising that these are detected with increased frequency in humans exposed to silica. The “pathological” oversynthesis of collagen *in vivo* by exposure to silica could be explained because of the following effect. Recently, Reffitt et al.¹⁹⁵ reported that human osteoblast-like cells treated with physiological levels of bioavailable Si have been shown to stimulate collagen type I production *in vitro*. From this point of view, it could be hypothesized that some amounts of silica are nevertheless dissolved during the contact of silica-based material with animal or human.

Basic science investigators looking at the mechanisms involved with the earliest initiators of disease are focused on how the alveolar macrophage interacts with the inhaled silica particle and the consequences of silica-induced toxicity at the cellular level.¹⁹⁶ Based on experimental results, several rationales have been developed for exactly how crystalline silica particles are toxic to the macrophage cell that is functionally responsible for clearance of the foreign particle.¹⁹⁶ For example, silica is capable of producing reactive oxygen species (ROS) either directly (on the particle surface) or indirectly (produced by the cell as a response to silica), triggering cell-signaling pathways initiating cytokine release and apoptosis. With murine macrophages, reactive nitrogen species are produced in the initial respiratory burst in addition to ROS.

In all silica polymorphs, SiO_4 tetrahedra share corners forming a three-dimensional network of Si–O–Si bonds that have mainly a covalent character. When these bonds are broken as a result of mechanical fracture two different situations can occur, as depicted in Figure 9.

Homolytic cleavage gives rise to free radical $\cdot\text{Si}$ and $\text{Si}\cdot\text{O}$ species, often referred to as dangling bonds. Heterolytic cleavage generates electrically charged surface species (Si^+ and $\text{Si}\cdot\text{O}^-$). Both types of surface states are highly reactive, and they are likely to be the main cause of the pathogenic effects induced by inhaled silica dust. Another factor to consider is that charge separation at the silica surface results in increased hydrophilicity of the mineral. This hydrophilicity can affect interaction with biological molecules.¹⁹⁷

The formation of oxygen free radicals at the quartz surface is a key mechanism for silica toxicity and carcinogenicity.¹⁹⁸ It was demonstrated that crystalline silica can induce oxygen-dependent DNA strand breakage and that silanol groups on the silica surface bind strongly to the phosphate–sugar backbone of DNA at physiologic pH. Hydroxyl radicals, responsible for DNA damage, have an extremely short half-life and are active only over distances of approximately 15 Å or one-half the diameter of a DNA helix. The authors suggested that the binding of DNA to the silica surface provides an anchoring mechanism whereby the hydroxyl

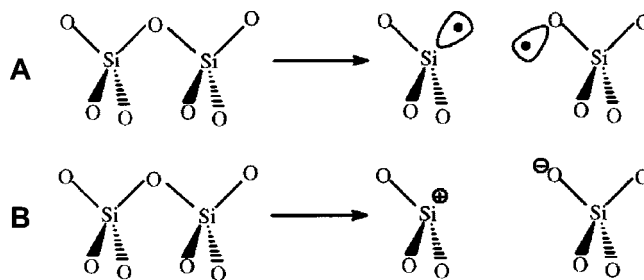


Figure 9. Homolytic (A) and heterolytic (B) cleavage of Si–O–Si bonds in silica. Figure reproduced with permission from ref 197. copyright 1999, Royal Society of Chemistry.

radicals are generated close enough to the target DNA to generate strand breaks.^{189,199}

An alternative explanation for silica toxicity includes lysosomal permeability, by which silica disrupts the normal internalization process leading to cytokine release and cell death. Still, other research efforts have focused on the cell surface receptors (collectively known as scavenger receptors) involved in silica binding and internalization. The silica-induced cytokine release and apoptosis are described as the function of receptor-mediated signaling rather than free radical damage. Current research ideas on silica toxicity and binding in the alveolar macrophage are reviewed and discussed by Hamilton et al.¹⁹⁶

Probably silicate could play a role in organisms by its chemical interactions with metal ions.^{28,29} Silicate–metal complexes could influence the availability of metals that are important for the organism (e.g., as an enzymatic cofactor). The effects on several biological processes could then be ascribed to the availability of important metal ions.²⁹ In order to investigate this hypothesis, the single cell organism Baker’s yeast was used. Yeast is the most common model for eukaryotic cells, it is easy to handle and culture, and it lacks the many additional complicating experimental parameters of a higher organism. The study on Baker’s yeast²⁹ revealed that silicate affects metal concentrations and metal uptake rates in the cell and that under certain conditions, the growth rate was affected. It was proposed that silicate adsorbed on the cell wall and influenced the metal availability for the cell by the formation of silicate–metal complexes.²⁸

Literature reports consistently emphasize that crystalline forms of silica have greater toxic effects on living organisms¹⁸⁸ than similarly sized amorphous forms.²⁰⁰ In the past, amorphous silica sized several hundred nanometers and greater was generally deemed nontoxic in chemical terms and relatively inert in biological systems, the well-known exception being its toxicity toward macrophages.¹⁹¹ However, Bhatt et al.⁷¹ reported on the isolation of hydrated amorphous silica fibres from canary grass that were carcinogenic. Mean length is 150 μm and mean width is 15 μm ; there are 10.9×10^6 of these fibres in each gram (Figure 10). No particles smaller than 5 μm in any dimension were seen. The length distribution of the fibres is sharply peaked at a mode close to 200 μm . Experiments reported indicate that the silica fiber present on the grain of *Phalaris canariensis* promotes the occurrence of tumors on the skin of mice. The majority of these tumors were papillomas, but a small proportion went on to form invasive carcinomas.

Silicotic nodules are a characteristic response to the more fibrogenic dusts, of which silica is the best known. Nodules are rounded or stellate in appearance, range in size from a few millimeters to one centimeter across, are firm to palpation, and have a predilection for the upper lung zones.¹⁹⁰

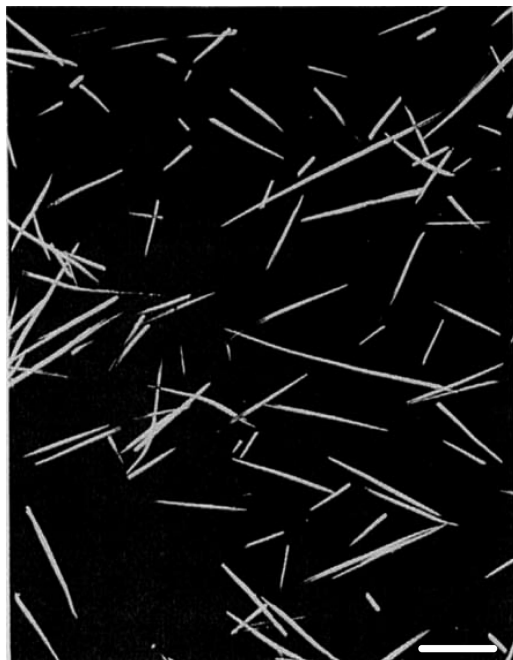


Figure 10. Biogenic silica fibers isolated from canary grass *Phalaris canariensis* are the promoters of carcinogenesis in the skin of mice. This differential interference micrograph shows the birefringence of these fibers (bar = 200 μm). Figure reproduced with permission from ref 71, copyright 1984, Wiley.

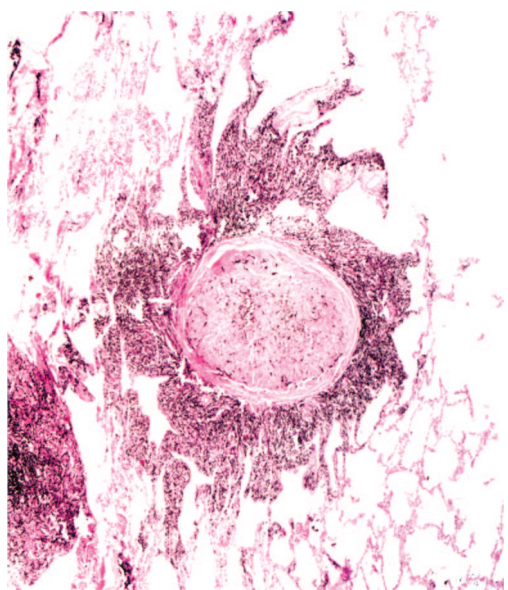


Figure 11. Classic silicotic nodule in a human. The nodule has rounded borders and is composed of whorled hyalinized collagen. Black pigment is seen within and around the nodule and by polarized light. Birefringent particles of silica were seen in the central and peripheral portions. Note the absence of epithelial hyperplasia or acute inflammation. Figure reproduced with permission from ref 190, copyright 2007, Society of Toxicologic Pathology.

Crystalline silica of the proper size (i.e., powdered tridymite, quartz, or cristobalite) in contact with living tissues is responsible for the silicotic nodule. The silicotic nodule is the classic nodule (Figure 11). This nodule is sharply circumscribed from the surrounding tissues and the collagen has a whorled “onion skin” appearance in which varying amounts of dust are embedded. Polarizing microscopy usually shows crystalline particles consistent with silica in the centers and periphery of these lesions.

It was suggested previously¹⁹⁴ that particles of silica deposited in the lungs of human beings were gradually dissolved under the influence of the weak alkali of the body fluids. Siliceous spicules of the fresh-water sponge *Spongilla fragilis*, when introduced into the tissues of animals, are slowly but definitely dissolved. For example, marked alteration in the structure of spicules occurred in the lung of dog after 472 days. Definite fibrosis of the lung of a dog into which the spicules had been introduced suggests that there is a concomitant injury attributable to the disappearance by dissolution of the siliceous elements of the sponge spicules.¹⁹⁴

Besides quartz and silica forms discussed above, also chalcedony has recently been identified in animal and human tissues. Chalcedony of a biogenic origin has been reported previously in electric organs from living *Psammobatis extenta* during oxidative stress.^{58,66}

Chalcedony is a microcrystalline fibrous form of silica that can occur in optically length-fast or length-slow forms but actually consists of nanoscale intergrowths of quartz and the optically length-slow fibrous silica polymorph moganite.²⁰¹ A slight oversaturation of silicon is necessary for allowing chalcedony precipitation from solution. Chalcedony was identified at the molecular layer, in the Purkinje neurons layer, and in granular cells layer of the human cerebellum from aged patients when observed under a mineralogical microscope.

It was also identified in the human cerebral cortex and brain hippocampus.⁶⁶ The large amount and size of chalcedony identified in the human hippocampus is very surprising. The hippocampus receives a large cholinergic innervation. The memory loss we all begin to experience with age may result from an impairment of the cholinergic system, which may also be altered in Alzheimer’s disease.²⁰² Synchronous neural activity causes rapid changes of extracellular pH in the nervous system. Chalcedony precipitation occurs at a specific pH (7–8) and oxidation potential (E_h 0.0 to -0.2) in geological environments. This observation supports the important role played by pH and E_h conditions in silica precipitation in elderly brains, as has also been reported in peripheral cholinergic nerves in electric organ from living electric fish.²⁰³

Siliceous dusts of abiotic and biotic origins surround all animal organisms, and indeed, such materials are continually inhaled and ingested. It is not surprising that in the evolution of the animal organism quite efficient methods have developed to handle these undesired substances.¹⁵⁴

Further studies are needed to settle the debate over the link between dissolution and biochemically mediated desilicification of crystalline and amorphous silica in animal and human organisms and different kinds of pathologies and diseases.

4.2. Enzymatic Degradation of Silica

Dissociation of solid silica in spicular formations of marine sponges was observed and visualized using SEM (Figure 12). Therefore, studies on identification and isolation of enzymes responsible for this phenomenon are recently in progress.

Besides the silica-anabolic enzymes, the silicateins, another enzyme, termed silicase (silase), has been identified in the marine sponge *S. domuncula*. Silicase is able to depolymerize amorphous silica.²⁰⁴ The expression of the gene encoding this silica-catabolic enzyme is strongly upregulated in

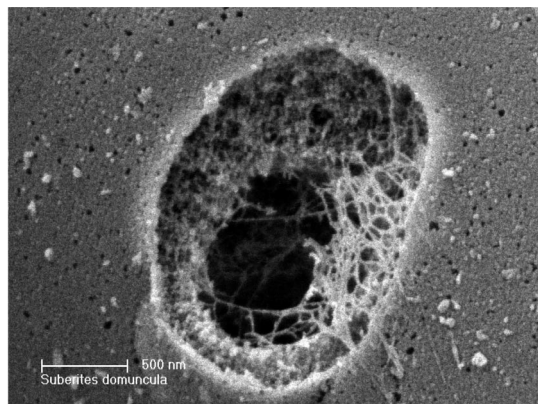


Figure 12. SEM image of the biologically mediated dissolution of silica layers observed on the surface of *Suberites domuncula* demosponge spicule. Image courtesy C. Eckert, copyright 2010.

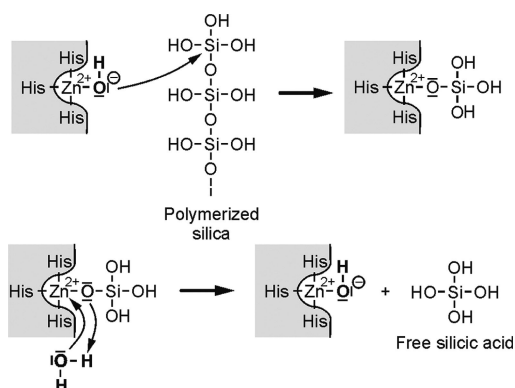


Figure 13. Proposed mechanism of action of silicase enzyme active site. Silicase binds with its three histidine residues to one zinc ion. The zinc ion is a Lewis acid that interacts with water, a Lewis base. The zinc-bound hydroxide ion formed by splitting of the water molecule undertakes a nucleophilic attack at one of the silicon atoms linked by oxygen bond(s). This results in hydrolysis of the polymerized amorphous silica, which remains, with one of the product halves, bound first to the enzyme. Through consumption of H_2O , the silicic acid product is released, and the zinc-bound hydroxide is regenerated allowing the start of the catalytic cycle.²⁰⁴

response to higher concentrations of silicon, like the expression of silicatein²⁰⁵ and collagen.^{205,206} The silicase cDNA has been identified in primmorphs from *S. domuncula*, applying the technique of differential display of transcripts. The deduced polypeptide is closely related to the carbonic anhydrases. Most of the amino acids that are characteristic for the eukaryotic-type carbonic anhydrase signature are also present in the sponge silicase.²⁰³ Carbonic anhydrases (CAs) are a family of zinc-containing enzymes. The three conserved histidine residues that are characteristic for these enzymes are also found in the deduced sponge protein at aa181, aa183, and aa206. These histidine residues bind a zinc ion. The proposed mode of action of the silicase (depolymerization of amorphous silica) is shown in Figure 13. It is assumed that the reaction mechanism of the sponge enzyme is analogous to that of other zinc-dependent enzymes involved in ester hydrolysis. The Zn^{2+} ion (Lewis acid) interacts with water (Lewis base). The hydroxide ion formed by splitting of the water molecule is bound to the zinc ion. This hydroxide ion then performs a nucleophilic attack at one of the silicon atoms of the polymeric silicate. In the next step, the zinc complex binds to the silicon under cleavage of the Si–O bond in the polymeric silicate. The transiently formed zinc-bound silicate is then hydrolyzed by water, resulting in

the release of the silicic acid product and regeneration of the zinc-bound hydroxide.

Based on its ability to dissolve or to etch silica substrates, the silicase is of interest for a wide range of applications in nanobiotechnology. Isolation, purification, and cloning of the gene encoding this enzyme has been reported.²⁰⁷

There are no additional data regarding distribution of silicases in other organisms. It was suggested that silica degradation in electric organs of fishes may be mediated by the CAs (silicase).⁶⁶ However, no convincing evidence has been found that ferredoxin–NADP reductase from diatom *Thalassiosira pseudonana* is involved in silica restructuring or maintenance.²⁰⁸

Thus far in this review desilicification phenomena have been described in living systems (*in vivo*). However, this description would be incomplete without envisioning silica as a pure inorganic material. Hence, in the following paragraphs a concise look will be presented into the fundamental mechanisms of silica dissolution in chemically pure systems. Often studies of these *in vitro* systems can reveal useful information, which can be used in a biomimetic approach to gain further understanding of living, more complex systems.

5. Mechanism and Kinetics of Silica Dissolution

5.1. Dissolution of Inorganic Silica and Quartz

Colloidal silica dissolution has been studied by numerous researchers from diverse technical fields. There are numerous reviews in the literature. Herein, we present a brief survey of the most significant recent results.

The general equation for the rate of dissolution of quartz and amorphous silica in aqueous solutions is fairly well established and can be written as a function of the concentration of three surface species, a protonated, a neutral, and a deprotonated surface species ($>\text{SiOH}_2^+$, $>\text{SiOH}$, and $>\text{SiO}^-$).^{211–215}

$$R_{\text{diss}} = k_{\text{H}^+}\{>\text{SiOH}_2^+\}^m + k_{\text{H}_2\text{O}}\{>\text{SiOH}\} + k_{\text{OH}^-}\{>\text{SiO}^-\}^p \quad (2)$$

where m and p stand for reaction orders and k_{H^+} , $k_{\text{H}_2\text{O}}$, and k_{OH^-} refer to rate constants. This concept is consistent with general macroscopic equation

$$R_{\text{diss}} = k_{\text{H}^+}a_{\text{H}^+} + k_{\text{H}_2\text{O}}a_{\text{H}_2\text{O}} + k_{\text{OH}^-}(a_{\text{OH}^-})^{0.33} \quad (3)$$

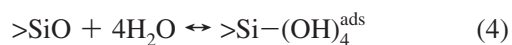
Note that this mechanistic approach provides a simplified view of the actual species present at the quartz surface; *ab initio* calculations of the hydrolysis of protonated, neutral, and deprotonated silica dimers^{209,210} showed that protonation of bridging oxygens is thermodynamically more favorable than that of a terminal OH group.

Quartz and vitreous silica dissolution in acidic solutions ($\text{pH} < 4$) has been studied in a number of works.^{211–216} In order to probe the surface speciation of quartz in strongly acidic solutions ($\text{pH} = 0–3$), where surface titration and electrophoresis are extremely difficult to perform, dissolution rates of this mineral were measured at 25 °C and constant ionic strength (1.0 M) using mixed-flow and batch reactors.²¹³ Dissolution rates increased with proton activity in the range $0 \leq \text{pH} \leq 3$ suggesting the adsorption of H^+ ions on the mineral surface leading to polarization of Si–O bonds and

detachment of the silicon atom from the structure. This scheme is consistent with the presence of significant amounts (i.e., up to 30–50% at pH close to 0) of protonated $>\text{SiOH}_2^+$ species on the surface, as was demonstrated using X-ray photoelectron spectroscopy (XPS) analysis of a quartz sample,²¹⁷ and is in agreement with molecular modeling predictions.²¹⁸

A two-pK, electric double layer (EDL) constant capacitance surface speciation model has been used to model kinetic data.²¹³ The set of surface stability constants consistent with previous spectroscopic XPS measurements ($\text{p}K_1 = -1.0$ and $\text{p}K_2 = 4.0$) and EDL capacitance of 1.5 F/m^2 provide adequate description of the dissolution rate with reaction order with respect to $[\text{>SiOH}_2^+]$ close to 1.

Water itself is a strong promoter of quartz dissolution. New insights on the quartz hydrolysis mechanism may be obtained also from the dependence of quartz dissolution rate on water activity. Schott et al.²¹⁵ reported on the rates of quartz dissolution in binary mixtures of water with methanol, formamide, or dioxane) at $25 \text{ }^\circ\text{C}$ and pH of 3–4. Normalization of the quartz dissolution rates with the rates obtained in pure water and plotting as a function of water activity produced a straight line with a slope of 4 by linear regression. The dependence of quartz dissolution rates on water activity could be explained by a simple reaction mechanism involving the fast reversible adsorption of four water molecules on the silica surface



followed by a slow hydrolysis step



Finally, hydroxyl ions are the most active chemical agents capable of polarizing and breaking Si–O bonds at the silica and quartz surface, supported by high solubility and dissolution rates of silica in alkaline solutions. The kinetics of silica aerogel dissolution in 0.05–0.79 M NaOH aqueous solutions at temperatures 15–56 $^\circ\text{C}$ was studied.²¹⁹ The aerogel samples are prepared via common one- and two-step procedures and differ considerably in the primary particle size. Kinetic peculiarities of the process are studied under both reaction and diffusion controlled modes, and kinetic parameters are established by experimental curve fitting. The dissolution activation energy is found to be equal to $82 \pm 6 \text{ kJ/mol}$ for all the aerogels. The dissolution kinetic curves appear to be S-shaped, so that the process rate passes through a maximum. The coincidence of small-angle X-ray scattering (SAXS) and Brunauer–Emmett–Teller (BET) specific surface areas indicates that the aerogels have no closed porosity so the initial rate increase cannot be explained by the opening of closed pores. A new modification of the Iler dissolution kinetic model has been developed to describe the experimentally observed kinetic curves.

Structural deformations of three types of silica aerogels due to their dissolution in aqueous solution of NaOH at pH = 13.6–13.9 have been explicitly studied *in situ* using small-angle X-ray scattering of synchrotron radiation.²²⁰ For all aerogels studied, the scattered intensity, I , increased rapidly in the scattering vector range $h = 0.15\text{--}0.6 \text{ nm}^{-1}$ suggesting aerogel threshold disintegration. When the scattering at $h = 0.15 \text{ nm}^{-1}$ reaches the maximum, the dependence of $\ln I$ on $\ln h$ gave a straight line with the slope critically dependent

on the solution pH and, to a lesser extent, on the nature of the aerogel. The observed phenomena are discussed in terms of the percolation theory.²²¹

Dissolution rates of amorphous silica in 0.1 M NaOH, pH 13 have also been investigated.²²² The observed dissolution rates were interpreted by a model that assumed particle size decrease with dissolution. Commercial colloidal silicas and a geothermal silica scale were used for the study. The activation energy of dissolution was determined to be $\sim 77 \text{ kJ/mol}$. Another significant conclusion was that the dissolution rate constants were on the order of 10^{-8} to $10^{-7} \text{ mol}^{-1} \text{ m}^{-2} \text{ s}^{-1}$ at $\sim 37 \text{ }^\circ\text{C}$ and were higher than those reported for crystalline silica (quartz). Finally, the BET specific surface area (SSA) was found to be an important factor in dissolution. The higher the SSA, the higher the dissolution rates of silica.

Rapid dissolution of crystalline silica in NaOH solutions ($\text{SiO}_2/\text{Na}_2\text{O}$ ratio was 2) in a pressure vessel at $220 \text{ }^\circ\text{C}$ and 2.7 MPa has been reported.²⁴¹ It was shown that the variation of the degree of conversion can be described quite accurately by the empirical expression $\alpha = A[1 - \exp(-Bt)]$, where A and B are constants depending on the hydroxyl concentration, $[\text{OH}^-]$. Values for A ranged from 0.95 to 0.98 and for B from 0.03 to 0.14 for $[\text{OH}^-]$ in the range 0.5 to 12.5 M. The kinetic order with respect to $[\text{OH}^-]$ was 0.470 ± 0.013 , and the kinetic constant at $220 \text{ }^\circ\text{C}$ was $3.933 \times 10^{-6} \text{ g/m}^2$. In a follow-up paper, the same authors studied the dependence of the dissolution of crystalline silica in NaOH solutions on temperature and particle size.²²² The activation energy of dissolution was found to be 74.4 kJ/mol .

The influence of $\text{Al}(\text{OH})_4^-$ on the dissolution rate of quartz at pH 10–13 and 59–89 $^\circ\text{C}$ was determined from batch experiments.²²³ $\text{Al}(\text{OH})_4^-$ at concentrations below gibbsite solubility depressed the dissolution rate by as much as 85%, and this effect was more pronounced at lower pH values and at higher $\text{Al}(\text{OH})_4^-$ concentration. Dissolution rates increased with increasing temperature; however, the percent decrease in rate due to the presence of $\text{Al}(\text{OH})_4^-$ was invariant with temperature for given $[\text{H}^+]$ and $[\text{Al}(\text{OH})_4^-]$ concentrations. These data, along with what is known about Al–Si interactions at high pH, are consistent with $\text{Al}(\text{OH})_4^-$ adsorbing on silanol sites and passivating the surrounding quartz surface. The observed pH dependence and lack of temperature dependence of inferred $\text{Al}(\text{OH})_4^-$ sorption is also in concert with the assumption that the acid–base behavior of the surface silanol groups has only a small temperature dependence in this range. A Langmuir-type adsorption model was used to express the degree of rate depression for a given *in situ* pH and $\text{Al}(\text{OH})_4^-$ concentration. Incorporation of the rate data in the absence of aluminate into models that assume a first-order dependence of the rate on the fraction of deprotonated silanol sites was unsuccessful. However, the data are consistent with the hypothesis proposed in the literature that two dissolution mechanisms may be operative in alkaline solutions: nucleophilic attack of water on siloxane bonds catalyzed by the presence of a deprotonated silanol group and OH^- attack catalyzed by the presence of a neutral silanol group. The data support the dominance of the second mechanism at higher pH and temperature.

The kinetics of amorphous silica dissolution in deionized water and NaCl solutions were quantified by Icenhower and Dove.²²⁴ Using two sources of pure SiO_2 glass (fused purified quartz and pyrolyzed SiCl_4), they measured rates at 40–250 $^\circ\text{C}$ by applying three types of reactor systems to assess kinetic behavior over the entire temperature range investi-

gated. Dissolution rates of the two materials were similar within experimental error. Absolute rates of amorphous silica dissolution in deionized water exhibited an experimental activation energy, $E_{a,\text{exp}}$ of 81.9 ± 3.0 and 76.4 ± 6.6 kJ/mol for the fused quartz and pyrolyzed silica, respectively. These values were similar to estimates for quartz within experimental errors. Absolute dissolution rates of amorphous SiO_2 in deionized water were ~ 10 times faster compared with quartz. Amorphous silica dissolution rates were significantly enhanced with the introduction of NaCl to near-neutral pH solutions such that 0.05 M NaCl enhanced rates by 21 times compared with deionized water.

Dove et al.²²⁵ examined the dissolution rates for two amorphous silica glasses and compared them to those for crystalline quartz. They discovered a paradox. In electrolyte solutions, the amorphous silicas showed the same exponential dependence on driving force as their crystalline counterpart, quartz. Previous studies showed that the dissolution rates of both quartz and the amorphous silicas increased by 50–100 times when alkaline or alkaline earth cations are introduced to otherwise pure solutions.^{224–227} This enigma was analyzed considering that amorphous silicas present two predominant types of surface-coordinated silica tetrahedra to solution. Electrolytes overcome the energy barrier to nucleated detachment of higher coordinated species to create a periphery of reactive, lesser coordinated groups that increase surface energy. This approach resulted in a plausible mechanism-based model that is formally identical with the classical polynuclear theory developed for crystal growth. This model also accounts for reported demineralization rates of natural biogenic and synthetic colloidal silicas. It is very interesting that these insights could be applicable to materials with a wide variety of compositions and structural order when the reacting units are defined by the energies of their constituent species. For amorphous silica, the physical result is that, with increasing chemical driving force, silica production from the surface should increase as well.^{228,229} That was exactly measured for amorphous silica dissolution in salt-free solutions. In electrolytes, the kinetics of amorphous silica dissolution exhibited a strong exponential dependence on driving force. The data were best explained by a crystal-based theory for a nucleated process even though a high degree of structural order and periodicity are absent.

Structural deformations of three types of silica aerogels due to their dissolution in aqueous solution of NaOH at pH 13.6–13.9 (NaOH solutions) have been explicitly studied in situ using small-angle X-ray scattering of synchrotron radiation.²²⁰ For all aerogels studied, the scattered intensity was found to increase rapidly in the scattering vector range $h = 0.15\text{--}0.6\text{ nm}^{-1}$, which indicates the aerogel threshold disintegration. The dissolution was found to critically depend on the pH of solution and, to a lesser extent, on the nature of the aerogel. This study allowed the investigation of space heterogeneities over 2–30 nm size. The observed phenomena were discussed in terms of the percolation theory.

Blesa et al.²³⁰ reviewed the interaction of various metal oxide surfaces with various organic molecules. They reported that in the case of silica, totally dehydroxylated surfaces are highly hydrophobic, and hydroxylation may be achieved only under strong conditions. They also reported a scheme that included interaction of oxalic acid with the oxide surface (Figure 14).

Small-angle X-ray scattering (SAXS) and microcalorimetry were used to study the dissolution of silica nanoparticles

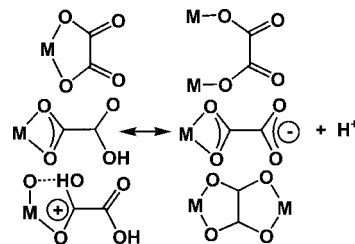


Figure 14. Some possible oxalate–surface complexes. M is the metal.

that serve as precursors in the synthesis of the pure-silica zeolite, silicalite-1.²³¹ Temporal changes in nanoparticle size were monitored by SAXS to obtain radial dissolution rates on the order of 1×10^{-2} nm/min, 10 times greater than those of silicalite-1. Nanoparticle dissolution rates were independent of solution alkalinity (above pH 11) and particle surface area, although contributions from the latter accounted for more than 60% of the nanoparticle enthalpy of dissolution (13.5 ± 0.1 kJ/mol SiO_2 relative to silicalite-1). Dissolution enthalpies and rates correlated to the molecular structure of silicates. Comparisons among amorphous silica, silicalite-1, and silica nanoparticles suggested that the latter are amorphous and therefore not simply small fragments of a crystalline zeolite. Nevertheless, they do possess a degree of ordering greater than that in dense amorphous silica. Dissolution experiments were also performed on heat-treated nanoparticles grown via Ostwald ripening. With increasing time of heat treatment, the nanoparticle dissolution rates and enthalpies decrease in magnitude toward those of silicalite-1, suggesting a structural reorganization of silica within the particles. The results offer insight on silicalite-1 nucleation as well as relevant time scales and rate-determining steps involved in zeolite crystallization. Crystalline silicates had activation energies ~ 90 kJ/mol, whereas amorphous silica was ~ 20 kJ/mol lower. A clear trend emerged from these studies. Specifically, the magnitudes of dissolution rates increase in the order: quartz < TPA–silicalite-1 < amorphous silica. Dissolution rate, unlike activation energy, varied with silica structure, such that differences among crystalline materials, that is, quartz and silicalite-1, are easily discernible.

The modification of the porosity of commercial silica gels in sodium silicate solutions was investigated.²³² The influence of the presence of preadsorbed substances on the effect of modifications was tested. The pore size distributions, total pore volumes, and specific surface areas were determined by the nitrogen method. The same silica samples were investigated also using the SAXS technique. Concerning the effect of dissolved organic substances on silica dissolution, quantitative data for the reaction $3\text{LH} + \text{Si}(\text{OH})_4 + \text{H}^+ \rightarrow [\text{SiL}_3]^+ + 4\text{H}_2\text{O}$ in aqueous solution have been obtained by ^1H NMR spectroscopy, where LH = tropolone, 4-methyl-tropolone, 3-hydroxy-2-methylpyridin-4-one, 1,2-dimethyl-3-hydroxypyridine-4-one, and 1-ethyl-3-hydroxy-2-methylpyridin-4-one.²³³ Equilibrium studies were carried out in D_2O solutions for both types of complex. 3-Hydroxypyridin-4-one is the first air-stable organic substrate capable of etching glass at a significant rate in nonfluorinated acidic solution. The dissolution of silica was confirmed by the detection of the ^{29}Si NMR resonance characteristic of the six-coordinate Si(IV) complex formed. Information has been obtained on the rate of dissolution of glass by 1-ethyl-3-hydroxy-2-methylpyridin-4-one in acid solution.

Using laser Raman and Fourier transform infrared spectroscopic methods, Marley et al. have examined mixed

solutions of oxalic and silicic acids at near neutral pH in the tenth molar concentration ranges in an attempt to directly observe the proposed organo-silicate complexes that might be produced upon silica dissolution by oxalic acid.²³⁴ In both laser Raman and infrared spectra, product bands were observed that indicate an oxalate/silicic acid ester is being formed in the reaction. The oxalate–silica ester was formed quite rapidly (on the order of seconds). At neutral pH and ambient pressure and temperature, the oxalate/silica complex was observed to be quite stable and remained in solution for hours. Silicic acid samples that were brought to near neutral pH with HCl were observed to form gels in tens of minutes. The nucleophilic attack on silicate surfaces by organic acids may also occur in an analogous fashion to increase the rate of dissolution of quartz. These data support the observation that organic diacids can lead to enhanced solubility of quartz in hydrogeological systems.

The rates of silica dissolution in alkaline water containing pyrocatechol were measured.²³⁵ At pH 10 and 25 °C, 0.3 g of SiO₂ are dissolved in the presence of 0.04 mol of pyrocatechol in 15 mL of water. The rates of silica dissolution increased with increasing pyrocatechol concentration. One mole of SiO₂ requires 4 mol of pyrocatechol. The rate of silica dissolution is first order with respect to SiO₂ concentration. Langmuir-type adsorption of pyrocatechol to the silica surface was assumed to explain the rate dependence on the pyrocatechol concentration. Along the same lines with the previous work, the pH dependence of silica dissolution in the presence of pyrocatechol derivatives was studied.²³⁵ The dissolution rates increased with pH. Also, the effect of dissolved catechol on the dissolution of amorphous silica in seawater was studied.²³⁶

Dissolution of silica has been at the epicenter of interest of researchers working in the water treatment field. Formation and deposition of tenacious colloidal silica deposits is one of the most difficult problems of water treatment and has been named as “water treatment’s Gordian Knot”.²³⁷ Such undesirable deposition problems can be avoided after application of chemical water treatment techniques that commonly involve use of additives as inhibitors.

Prevention of scale formation is greatly preferred to chemical cleaning of the adhered scale.²³⁸ Classic examples of scales that require laborious (mechanical) and potentially dangerous (hydrofluoric acid) cleaning are silica and silicate salts. Prevention of the scale deposits can also benefit the water operator by eliminating (or at least by minimizing) unexpected production shut-downs and by offering substantial savings through water conservation (especially in arid areas with high water costs). Scale control additives are fed into the water in “ppm” quantities and increase saturation limits of sparingly soluble salts.²³⁹ There is active research that embraces design, discovery, and application of such additives that are nontoxic and readily biodegradable.

Unfortunately, prevention of scale formation is not always possible. At times, system operators are faced with the difficult task of removing hard and tenacious scale deposits from critical heat exchange surfaces.²⁴⁰ Silica deposits can be cleaned mechanically by “sandblasting” or chemically with NH₄F·HF, a process that is not hazard-free. Therefore, an integrated chemical water treatment approach must contain contingencies that relate to chemical cleaning of a potentially scaled system.

Dissolution of silica is hydrolysis driven.²⁴¹ Addition of OH[−] ions can enhance silica dissolution at high pH regions.

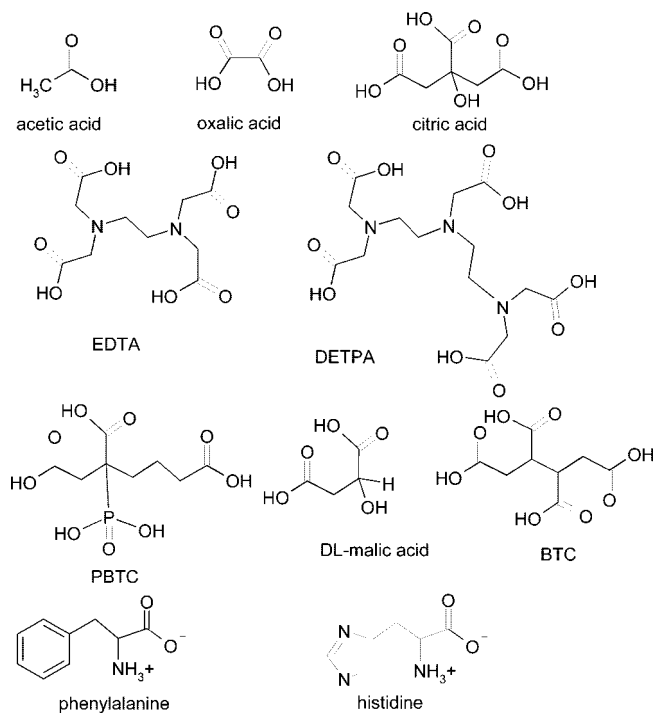


Figure 15. Schematic structures of colloidal silica dissolvers.

However, metallic corrosion of critical system components (heat exchanger tube bundles, piping, etc.) becomes an issue when silica deposit cleaning requires prolonged times and high concentration of OH[−] ions. The acceptable “industry standard” for removing silica deposits is ammonium bifluoride, NH₄F·HF. Although the precise mechanism of action is not known, formation of soluble fluorine-containing “Si compounds” has been invoked (H₂SiF₆ has been proposed as the dissolution product). This approach is not free of problems such as hazard potential and acid-driven metallic corrosion (since cleanings must be done at low pH). It is widely recognized that safer, more environmentally friendly ways to dissolve silica are desirable. This is particularly significant for biological samples, because the integrity of the organic component must not be compromised.

Recently, researchers have turned their attention in the use of environmentally friendly, nontoxic compounds that enhance dissolution of colloidal silica. Some concise comments are given below.^{242,243} Schematic structures of the compounds are given in Figure 15.

Stirred suspensions containing colloidal silica and the dissolution additive at various concentrations are vigorously stirred at a fixed pH of 10 and then tested for soluble silica by the silicomolybdate spectrophotometric method after 24, 48, and 72 h of dissolution time. Results are presented in Table 2 and include performance characteristics of NH₄F·HF₂. This measurement methodology allows for determination of “soluble” or “reactive” silica after dissolution experiments are performed for at least 24 h at appropriate pH’s, relevant to industrial water systems and applications.²⁴⁴ Colloidal silica is completely unreactive to the test.

After 24 h, in control solutions (no additive present) dissolution proceeds until ~120 ppm silica is solubilized (24%). Silica dissolution continues after 48 and 72 h allowing soluble silica levels to increase to 150 ppm (30%) and 190 ppm (38%), respectively. The presence of 2500 ppm of any additive listed in Table 2 enhances silica dissolution within the first 24 h in a wide range, from 139 ppm (BTC) to 206

Table 2. Effect of Various Additives on the Dissolution of Colloidal Silica

dissolution additive ^a	pH	dosage (ppm)	soluble SiO ₂ (ppm)		
			24 h	48 h	72 h
control	10	0	120	150	190
acetate	10	2500	151	219	254
		5000	154	216	199
		7500	175	245	243
		10000	286	367	360
oxalate	10	2500	164	220	241
		5000	165	217	205
		7500	198	246	193
		10000	155	219	239
citrate	10	2500	142	226	267
		5000	186	228	271
		7500	166	216	253
		10000	380	370	407
BTC ^b	10	2500	139	202	246
		5000	140	226	228
		7500	146	198	219
		10000	147	210	202
EDTA ^c	10	2500	305	301	308
		5000	340	345	348
		7500	347	363	391
		10000	341	371	381
DETPA ^d	10	2500	191	281	275
		5000	237	279	289
		7500	322	340	333
		10000	257	206	271
PBTC ^e	10	2500	198	267	292
		5000	242	289	309
		7500	274	316	341
		10000	245	314	330
L-histidine	10	2500	206	259	268
		5000	241	283	282
		7500	249	298	304
		10000	245	283	298
DL-malate	10	2500	135	235	249
		5000	146	210	205
		7500	147	227	213
		10000	142	191	199
ammonium bifluoride	4	0	17	51	10
		2500	506	409	501
		5000	403	455	443
		7500	198	312	400
ammonium fluoride	10	10000	87	110	67
		2500	276	281	285
		5000	289	305	309
		7500	219	265	279
L-phenylalanine	10	10000	109	116	131
		2500	202	248	253
		5000	187	246	245
		7500	230	301	282
10000	231	264	264		

^a The structures of all dissolver additives are given in Figure 15.

^b BTC = 1,2,3,4-butanetetracarboxylate. ^c EDTA = ethylenediaminetetracarboxylate. ^d DETPA = diethylenetriaminepentaacetate. ^e PBTC = 2-phosphonobutane-1,2,4-tricarboxylate.

ppm (L-histidine). This enhancement is more pronounced after 48 and 72 h of dissolution time. Figure 16 shows the dissolution enhancement in the presence of various additives. The fact that silica dissolution is enhanced in the presence of the additives described herein points to the hypothesis that the dissolution effect is not solely due to hydrolysis by OH⁻ ions.

Additive concentration appears to have an effect in only some cases. For example, in the case of acetic acid, concentration increase to 10 000 ppm results into silica dissolution enhancement that reaches 286 ppm (57%) in 24 h compared with 151 ppm (30%) for the 2500 ppm concentration (an increase of 27%). Similar observations can be made for citric acid, which solubilizes 380 ppm silica (76%) in

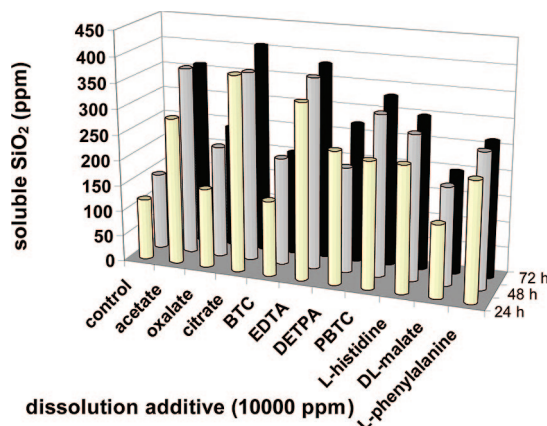


Figure 16. Dissolution enhancement of colloidal SiO₂ in the presence of various additives. Figure reproduced with permission from ref 242, copyright 2005, Springer.

24 h. In the cases of oxalic acid, BTC, and DL-malate, concentration increase has only a marginal effect on dissolution. Higher dosages of ammonium fluoride have actually a detrimental effect on silica dissolution, which is evident particularly in the 10 000 ppm case, allowing only 109 ppm silica to dissolve after 24 h. Similar observations are noted for a concentration increase in NH₄F·HF.

Silica dissolution is also a factor of time. It is enhanced as dissolution time proceeds. The most dramatic demonstration of this effect is in the case of 10 000 ppm of DETPA, which gives 206 ppm soluble silica after 48 h and 271 ppm SiO₂ after 72 h, an enhancement of 13%.

The effect of the number of -COOH groups present in the chemical structure of the cleaner molecule can be seen by examining Table 2. Increase in the number of -COOH groups does not have an obvious effect in dissolution efficiency. For example, acetate (one -COOH group) at 10 000 ppm concentration is more active than oxalate (two -COOH groups). EDTA (four -COOH groups) is more efficient than DETPA (five -COOH groups).

The nature of additional groups in the dissolver molecule also appears to be important. When one -COOH group is replaced with a -PO₃H₂ group in the molecule of BTC, the resulting structure, PBTC, appears to exhibit higher dissolution efficiency. L-Histidine and L-phenylalanine (one -NH₂ group at α -position to a -COOH group) are more active particularly in lower concentrations than acetate, which does not possess such structural features. Both PBTC and citrate possess three -COOH groups but differ in that PBTC has an additional -PO₃H₂ group, whereas citrate has a -OH group. This difference allows PBTC to exhibit higher dissolution efficiency than citrate at concentrations <7500 ppm. However, at 10 000 ppm levels citrate appears more effective.

It is known that colloidal silica dissolution is catalyzed by hydroxyl ions, although H₃O⁺ attack and H₂O attack on Si-O-Si bonds can be also understood from a quantum mechanical point of view.²⁴⁵ It is reasonable to assume that OH⁻ ions attack the surface tetrahedral Si centers belonging to deprotonated silanol groups ($\equiv\text{Si}-\text{O}^-$). Inner Si centers are unreactive because they are well embedded within the silica particle core. Once OH⁻ forms a Si-OH bond with surface Si, the "Si-O" network that connects surface Si with internal Si centers starts to collapse, thus exposing additional Si sites that become susceptible to attack. Additives containing chemical groups that are strongly anionic, such as

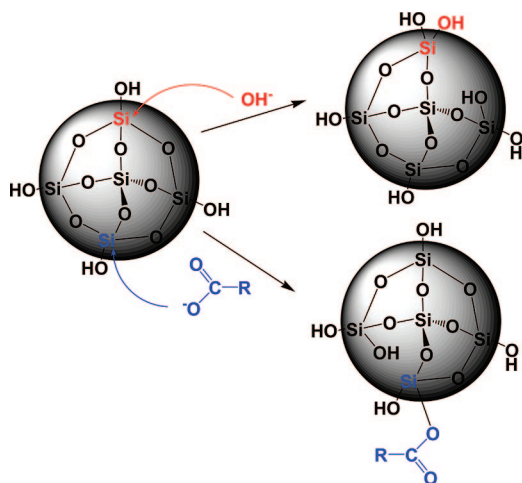


Figure 17. Possible attachment by hydroxide or carboxylate on a silica particle.

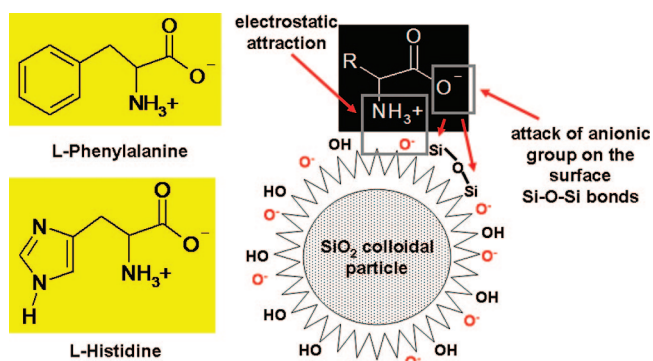


Figure 18. Possible mechanism of dissolution enhancement of colloidal SiO₂ in the presence of amino acid additives.

$-\text{COO}^-$ and $-\text{PO}_3^{2-}$, may react with Si centers in the amorphous network of SiO₂ in a similar fashion as OH⁻. Formation of silicate esters, R-C(O)O-SiO_x, may be a possibility and such dissolution pathways are currently being investigated. This is depicted in Figure 17. Based on the results obtained with the two amino acids and also their chemical structure, a possible mechanism for the dissolution of colloidal silica by such zwitterions may be proposed.

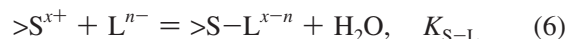
This pathway is shown in Figure 18. One can envision that the first silica–amino acid interaction is an electrostatic association between the negatively charged silica particle and the cationic “ammonium” moiety of the amino acid. The positioning of the amino acid is such that the deprotonated and negatively charged carboxylate group can “swing” and attach a surface Si center, thus enhancing the cleavage of a surface Si–O bond. This function is in a way “mimicking” the action of HO⁻ anions in the hydrolysis of the Si–O–Si network.

In order to verify that the initial stage of silica dissolution is surface “complexation” by the dissolution additive onto the amorphous silica surface, an inhibition experiment was devised. Colloidal silica was first reacted with a cationic polymer, polyethyleneimine, PEI (MW 10,000 Da, containing primary, secondary, and tertiary amine groups in approximately 25/50/25 ratio). Attachment of cationic polymers onto silica surfaces is well established.^{246,247} Coverage of the silica surface by the cationic polymer would be expected to block and inhibit surface complexation by the additive. Indeed, silica dissolution (no dissolvers present) dropped to 16% efficiency in 24 h, in the presence of 500 ppm PEI,

compared with 24% with no PEI present. Even in the presence of 2500 ppm 2-phosphonobutane-1,2,4-tricarboxylate (PBTC), dissolution only reached 69 ppm silica within 24 h (14% efficiency), compared with 198 ppm (40%) for uninhibited silica. Higher PBTC dosages did not show any beneficial effect in increasing soluble silica levels. It appears that blockage of the silica surface by cationic polymers is an irreversible process and is not alleviated by dosage increase of the dissolution additive (in this case PBTC).

In an effort to design agents that could solubilize silica in water under ambient conditions and pH, novel zwitterionic, penta-oxo-coordinated silicon compounds with siliconate cores have been prepared from 4-substituted pyridine *N*-oxides (H, OMe, morpholino, NO₂) as donor ligands, their structures established by ¹H, ¹³C, and MS, and the coordination number of silicon by ²⁹Si NMR²⁴⁸ The formation of complexes from pyridine *N*-oxides is noteworthy since they arise from interaction with a weakly nucleophilic oxygen center. The ability of the pyridine *N*-oxides to enhance the solubilization of silica in water has been experimentally demonstrated. Possible rationalization of this observation on the basis of O → Si coordination via the oxygen atom of pyridine *N*-oxide was suggested. It is likely that the O → Si coordination from pyridine *N*-oxides partly transfers the negative charge to make the silica end charged.

A surface complexation (surface coordination) approach can be used to rationalize the ligand-controlled silica dissolution. Following the framework developed for silicate minerals (smectite, diopside, wollastonite) dissolution^{249,250} and assuming that Si release requires the breaking of the Si–O–Si(Al, Mg, Ca, Fe) bond, one can suggest that the rate of ligand-controlled dissolution is proportional to the concentration of the surface center–ligand complex $>\text{S}-\text{L}^{x-n}$ (S = Si, Al), which can be deduced from the reaction stability constant:



In the presence of a ligand at given pH, the silica forward dissolution rate is thus the sum of H₂O- (or OH⁻) ($k_{\text{H}_2\text{O}}^*$) and ligand-controlled dissolution, similar to that of brucite²⁵¹ and dolomite,²⁵² smectite,²⁴⁹ diopside,²⁵⁰ and wollastonite CaSiO₃.¹⁶⁷

$$R = k_{\text{H}_2\text{O}}^* + k_{\text{L}}(>\text{S}-\text{L}^{x-n}) \quad (7)$$

where k_{L} is the empirical kinetic constant pertinent to each ligand. Upon the adsorption of a ligand on the initial rate-controlling sites, their concentration decreases such that $k_{\text{H}_2\text{O}}^*$ (eq 7) is less than $k_{\text{H}_2\text{O}}^*$ (eq 3). Assuming that at constant pH of our experiments, the ligand sorption on mineral surface follows a Langmuir adsorption isotherm with mass law conservation for the surface sites:

$$\text{S}_{\text{T}} = \{>\text{S}^{x+}\}^* + \{>\text{S}-\text{L}^{x-n}\} \quad (8)$$

where $\{>\text{S}^{x+}\}^*$ designates the rate-controlling surface sites, unoccupied by the ligand ($>\text{SiOH}^{\circ}$). Therefore, the concentration of adsorbed ligand is given by

$$\{>\text{S}-\text{L}^{x-n}\} = \frac{\text{S}_{\text{T}}K_{\text{S-L}}[\text{L}^{n-}]}{1 + K_{\text{S-L}}[\text{L}^{n-}]} \quad (9)$$

and eq 7 transforms into

$$R_+ = k_{\text{Si}} \left(1 - \frac{K_{\text{S-L}}[\text{L}^{n-}]}{1 + K_{\text{S-L}}[\text{L}^{n-}]} \right) + k_{\text{L}} \frac{K_{\text{S-L}}[\text{L}^{n-}]}{1 + K_{\text{S-L}}[\text{L}^{n-}]} \quad (10)$$

In this formula, the dissolution of silica is controlled by water attack (hydrolysis) and ligand attack on a Si–O–Si bond, which can be described by Langmuir adsorption of ligand on rate-controlling surface sites. Generally, the higher the adsorption constant of a ligand on the surface, the higher is the kinetic constant and the accelerating effect of a ligand. For example, among different ligands studied at pH 3–10 (citrate, salicylate, tartrate, glucose, humate, phenol), only catechol is capable of significantly increasing the solubility of silica,²⁵³ and thus, this ligand is expected to profoundly accelerate the dissolution rate.

5.2. Dissolution of Biogenic Silica: Diatoms and Their Frustules

Intracellular silicification occurs in diatoms, chrysophytes, choanoflagellates, radiolarians, and testaceous amoebae.²⁵⁴ Diatoms are unicellular photosynthetic algae enclosed in an external siliceous skeleton called frustules (Figure 19). They are largely widespread in marine and freshwater environments. They constitute an important organic carbon reservoir providing more than a quarter of the primary production on the earth and contribute to about 40% of the annual fixation of CO₂ in the ocean.²⁵⁵ Siliceous plankton have been an important component of the oceanic silica cycle since the evolution of Radiolaria during late Precambrian or early Paleozoic time. Diatoms did not enter the cycle until Jurassic time but now account for as much as 90% of the suspended silica in the oceans. It was postulated²⁵⁶ that the tremendous evolutionary success of the diatoms is responsible for evolutionary trends observable in the Cenozoic fossil record of the Radiolaria. Such trends include decrease in test weight, as well as structural changes such as increased pore size, decreased bar width, reduction or loss of test processes, and

more regular alignment of pores, all changes that result in less silica uptake per test. Natural selection, mediated by the role of the diatoms in the silica cycle, apparently favors radiolarian phenotypes that use less silica in test construction.²⁵⁶

Diatoms originated close to the Permian–Triassic boundary 250 millions of years ago.²⁵⁷ This suggests that silicification evolved late in the evolutionary history of diatoms. It is possible that any earlier silicified diatoms have failed to be preserved for some environmental or taphonomic reasons; however, silicified organisms (sponges) have been found in phosphoritic marine sediments 1.8 billion years old,⁹⁸ and both radiolarians and sponges were common from the Cambrian onward.¹⁷⁷ Furthermore, the past ocean has most commonly been at a lower pH value than the present value, at least in the Tertiary, so that fossilization of diatom frustules would be favored relative to today. The diatoms, radiolarians, and sponges all deposit amorphous silica.^{258,259} There should therefore be similar diagenetic and taphonomic constraints on the preservation of the silica from these three groups. There are also uncertainties about extrapolations of the molecular clock to times before the earliest fossil calibration. However, overall the data suggest that diatoms were unsilicified for half the time for which they have existed.²⁵⁷

The frustule of diatoms is composed of amorphous and porous silica (biogenic opal). Besides its obvious structural role, biogenic silica is an effective buffer, enabling the enzymatic conversion of bicarbonate to CO₂, an important step in inorganic carbon acquisition by these organisms.²⁶⁰ Silicification in diatoms is not only a constitutive mechanical protection for the cell but also a phenotypically plastic trait modulated by grazing.²⁶¹

The organic matrix of the cell wall plays a crucial role in biosilicification of diatoms.^{262,263} On the basis of analysis of amino acid and sugar composition of six diatom species, Hecky et al.²⁶⁴ were the first to propose a mechanism of silicon deposition in diatoms, characterized by “condensation

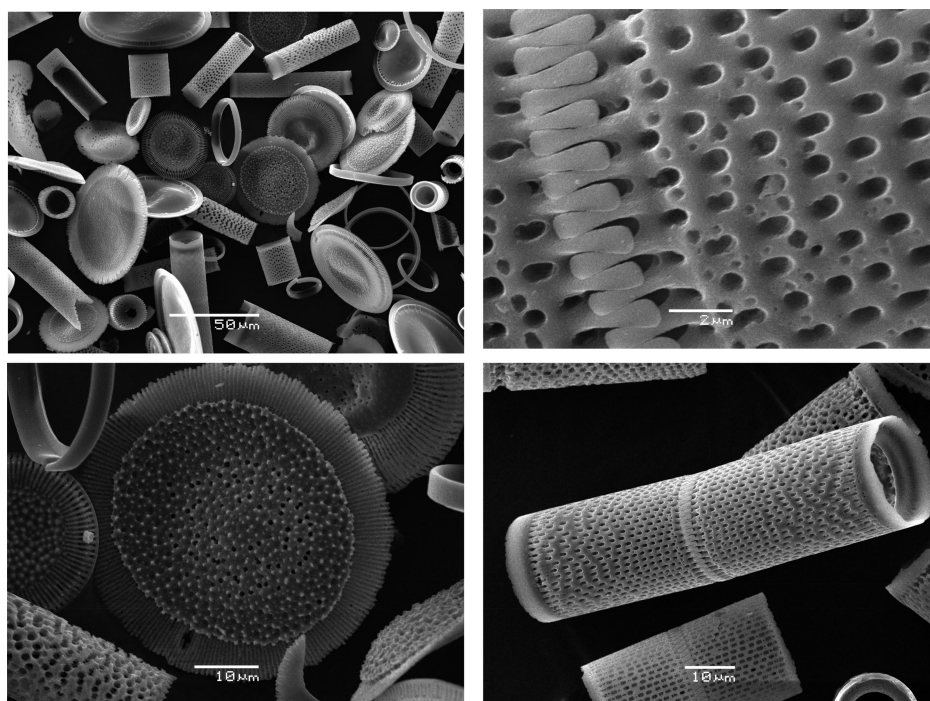


Figure 19. Perfectly preserved diatom frustules from the Baikal Lake sediment (800 m depth), 8–10 thousand years old.

of silicic acid, in epitaxial order, on a protein template enriched in serine and threonine". The present state of knowledge generally supports this mechanism: it has been demonstrated that polycondensation reactions between silicic acid molecules and a hydroxyl-rich β -sheet protein results in stereochemically compatible chemisorbed tetrasiloxane rings.²⁶⁵ Overall silica structure is formed by expansion and molding of the membrane-bound SDV.²⁶⁶ It has been demonstrated that the intercompartmental pH of the SDV controls the silica polymerization process²⁶⁷ while the salinity determines the silicification grade of the frustules.²⁶⁸ The biomineralization in diatoms is mediated through peptide- and polyamine-assisted condensation of silica.^{269–271} Strongly basic proteins (silaffins) and long-chain polyamines of the oligo(*N*-methyl-propylene amine)-type have been characterized as main components of diatom biosilica⁴⁰ whose zwitterionic structure (polyamine moieties and phosphate groups) regulates a self-assembly process via electrostatic interactions.⁸² Recently, a simple model for nanopatterning of diatom biosilica was developed, in which repeated phase separation events during wall biogenesis are assumed to produce self-similar silica patterns in smaller and smaller scales.²⁷²

Both the amount and structure of each type of molecule that can precipitate silica in artificial systems differ between diatom species, consistent with species-specific patterns of cell-wall nanostructures.²⁷³ There is clearly a great need for the development of biochemical, molecular, and genetic tools to better understand various features of diatom frustule biogenesis such as SDV formation, targeting to the SDV, bioinorganic pattern formation, and exocytosis.²⁷⁴

A solid-state ²⁹Si cross-polarization (CP) MAS NMR study demonstrated that the degree of condensation of SiOH units in diatom cell wall ($Q^2/Q^3/Q^4$ ratio) is virtually identical for various diatom species ($Q^4/Q^3 = 2.5–2.8$) suggesting that molecular architecture of the SiOSi/SiOH units in cell walls is the same throughout the diatom phylum.²⁷⁵ Complete (intact) cells showed significantly smaller Q^4/Q^3 ratios (1.8–1.9) than separated cell walls indicating the existence of an intracellular pool of less condensed silica that lacks three-dimensional organization.²⁷⁵ Such an intracellular pool can be also presented by monomeric silica.²⁷⁶ Attribution of Q^0 species CP NMR peak at $\delta = -65$ ppm to silicon-bound organic groups (Si–O•••R or Si–C or Si–N bonds) is not excluded²⁷⁶ because a similar observation (a peak at -26 ppm) was reported in rice hulls and babassu coconut studied via ²⁹Si direct polarization (DP) MAS NMR demonstrating the presence of organically bound silicon species.²⁷⁷ Hyper- (five- and six-) coordinated silicate–polyalcohol and silicate–sugar acid complexes have been proposed to play a role in biologic silicon transport and uptake, based on unexpected ²⁹Si NMR resonances observed at -101 and -141 ppm in aqueous solution.^{278,279} Kinrade et al.²⁸⁰ reported a transient hexacoordinate organosilicon complex in the freshwater diatom *Navicula pellucida* using *in vivo* ²⁹Si NMR spectroscopy. Further support for hypercoordinate organosilicon species in the uptake and transport by biological systems is provided by molecular orbital modeling.²⁸¹ Although only five-membered rings complexes containing penta- and hexacoordinated Si can explain obtained NMR results, it follows from *ab initio* calculations that there is no thermodynamic advantage in transporting and storing silicon as hypercoordinated complex at the conditions of the silica deposition vesicle and quad-

racoordinated complexes may also be involved in silicon transport.²⁸² As for physical characterization of the diatom shell, the specific surface area of cultured diatoms varies from 10 to 200 m²/g²⁶⁸ with periphytic species having 5–10 times more silica per cell and several times smaller specific surface area compared with planktonic species.^{283,284} The granular nanostructure of diatom biosilica is composed of 100–200 nm spherically shaped particles.²⁸⁵ In comparison to chemically derived silicas, diatom opal has a porous structure rather than fractal aggregates as revealed by the small-angle X-ray scattering (SAXS) technique.²⁶⁸ The wideangle X-ray scattering (WAXS) technique did not reveal crystalline phases in the domain 0.07–0.5 nm in this biogenic silica, and the SAXS spectra indicate the pore size to be between 3 and 65 nm.²⁸⁶

Because the dissolution of the silica shell (desilicification) also requires removal of the surrounding organic matrix, below we will describe the chemical composition of diatom cell walls. The diatom frustule is covered by an organic coat, composed of organic molecules such as polysaccharides, amino acids, and glycoproteins, tightly associated with silica.^{264,287–289} Numerous functional groups present on the surface of cell walls can be proton active within the acidity range of natural waters and their protonation/deprotonation is responsible for the amphoteric properties of diatom surfaces in aqueous solution.

Organic coating and mineral parts of four representative diatom species, two marine planktonic and two freshwater periphytic diatom cell surfaces, were studied using high-resolution *in situ* ATR-FT-IR (attenuated total reflection FT-IR spectroscopy) and *ex situ* X-ray photoelectron spectroscopy.²⁸⁴ ATR-IR spectra exhibit the most important differences for absorbance bands at about 1072 cm⁻¹ assigned to the stretching vibration of the Si–O group of diatom frustules. For marine planktonic *Skeletonema costatum* (SC), a very low intensity of this band was observed even when using the ZnSe reflection element that has a penetration depth of 1.3 μ m. This indicates that SC has a very thick outermost organic layer that precludes interaction of the evanescent wave with the silica skeleton. In contrast, the outermost organic layer of freshwater periphytic *Achnantheidium minutissimum* (AMIN) and *Navicula minima* (NMIN) is very thin, and the reflected radiation interacts very strongly with the silica skeleton even when using the germanium reflection element. For estuarine planktonic species *Tallassiosira weissflogii* (TW), the outermost organic layer has an intermediate thickness, which results in the most significant differences in the intensities of the absorbance bands recorded with germanium and ZnSe reflection elements. Taking into account the spectral observations obtained with both reflection elements and the calculated values of penetration depths, it could be estimated that the thickness of the TW organic layer is $\sim 400 \pm 200$ nm, which is consistent with TEM observations.²⁸⁴ The outermost organic layer of *S. costatum* has a thickness >1500 nm, whereas that for AMIN and NMIN is around 150 ± 50 nm.

Another powerful technique to assess the chemical composition of undisturbed (freeze-dried) diatom cell wall is X-ray photoelectron spectroscopy (XPS), which probes the first 10–100 Å of the solid surface in vacuum. The principal constituents of the diatom cell walls are polysaccharides, (lipo)polysaccharides, lipids, and proteins.²⁶⁴ The surface composition of diatom cell walls can therefore be modeled in terms of three classes of basic constituents:

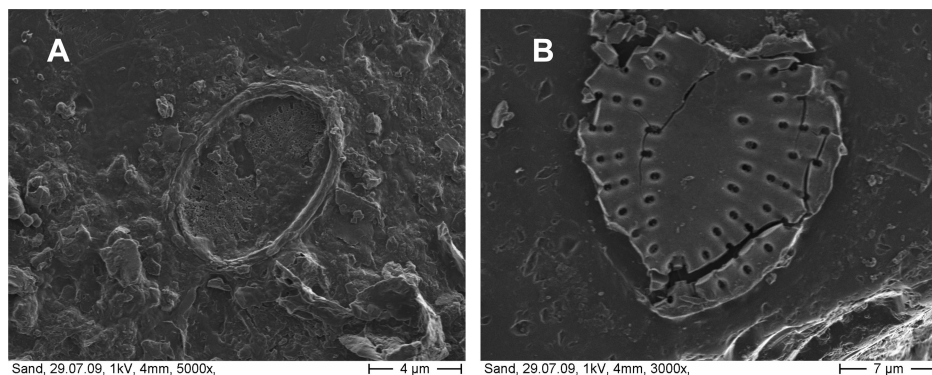


Figure 20. SEM images of partially dissolved diatoms residues observed in the sea bottom sediment.

proteins, polysaccharides, and hydrocarbon-like compounds. Cell wall molecular composition was computed from elemental concentration ratios using the method developed for bacteria surfaces by Dufrière and Rouxhet²⁹⁰ and Dufrière et al.²⁹¹ The resolution of XPS analyses allows quantification of the proportion of these organic molecules for each diatom species.²⁸⁴ The Si/C atomic ratios measured by XPS and the relative intensity of Si–O–Si bands estimated from the ATR spectra of studied diatoms are in good agreement with frustule/whole cell mass ratios measured by Gélalbert et al.²⁸⁴ and reported in literature.²⁸³ In particular, cell walls of planktonic diatoms contain ~5 times less silica than those of periphytic species. Moreover, there is a quantitative agreement between surface group concentration (>SiOH, –COOH, and –NH₂) determined by spectroscopic techniques and modeling of surface charge data.²⁸⁴

An interesting feature of diatom cell walls is the difference between the pH of isoelectric point (pH_{IIEP}) measured by electrophoresis and the pH of the point of zero charge (pH_{PZC}) determined by acid–base surface titration (1–2 vs 6–9, Gélalbert et al.²⁸⁴). This difference can be understood in view of the diatom cell wall structure proposed by Hecky et al.²⁶⁴ based on their chemical analysis. According to this model, the amino groups attached to silica templates are covered by a polysaccharide layer bearing negatively charged carboxylic groups. Reversible protonation/deprotonation of more deeply located amine groups is responsible for the high concentration of surface proton excess measured during titration experiments. These groups are situated far from the shear plane and thus cannot contribute to the ζ potential development. The weak proportion of dissociated –COO[–] groups on the surface (pK = 4) even at pH 2 is enough to provide a negative ζ potential. The carboxylic groups dominating the outermost surface layer are fully deprotonated at pH > 4–5 thus yielding constant surface potential and pH-independent ζ potential.

Over the past decades, intense efforts have been devoted to quantifying the rates of diatom dissolution in aqueous solutions, mostly in relation to the flux of Si in the ocean controlled by diatom shells (i.e., Ragueneau et al.²⁹²). Diatom dissolution rates vary from one species to another, spanning over an order of magnitude.^{293–296} These variations reflect variability in specific surface area values, morphology, and structure of frustules and organic and inorganic coating (see Ragueneau et al.²⁹² for discussion, Figure 20).

The limiting step of diatom dissolution in the water column is removal of external organic matter that exposes

opal surface directly to solution. Bacterial degradation is known to accelerate dissolution rates.¹⁴³ Removal of organic and inorganic coatings enhance diatom reactivity by at least an order of magnitude.²⁹⁷ During the last century, numerous extraction methods were developed to isolate diatoms from water and other tissues. A number of procedures have also been elaborated to separate, clean, and dissolve diatom from marine sediments.^{133,298,299} Nitric acid digestion is a worldwide known method for the extraction of diatoms, and other techniques include ultrasonic radiation, enzymatic digestion, and physical methods such as simple and gradient centrifugation.³⁰⁰ Successive cleaning of diatom shells from sediments for analysis of chemical composition includes reductive treatment, etching of the frustule surface to remove surface contaminants, hot acid digestion to leach any remaining or reabsorbed contaminants, and dissolution of clean biogenic opal using a Na₂CO₃ solution.²⁹⁹

Among various compounds that can modify the reactivity of biogenic silica, sodium chloride is notoriously known to accelerate the dissolution rate of silica.^{301,302} Trace metals (Al, Be, Fe, Ga, Sc, Ti, Y) retard the dissolution of diatom shells.³⁰¹ The role of aluminum on solubility, surface chemistry, and dissolution kinetics of silica frustules has been widely discussed.^{303–305} Aluminum can be structurally associated with silica, it is incorporated in the solid and not surface-adsorbed, being on 4-fold coordination as proven by X-ray absorption near-edge structure (XANES) observations.³⁰⁶ While the solubility of biogenic silica is decreased significantly by only minor amounts of Al (~0.1%, Van Bennekom et al.^{307,308}), the dissolution rate of diatom frustules at pH 8 and within the range of dissolved aluminum in the pore waters (10–200 nM) is not affected by the presence of Al in solution.³⁰³ The authors suggested that the lack of specific kinetic effect of Al may be related to the higher acidity of ≡Si–OH surface groups, relative to ≡Al–OH groups. At the same time, the diatom cultures show a clear inverse relationship between the dissolution rate constant and the Al/Si ratio of the frustules.³⁰⁹

In situ measurements of diatom shell dissolution in the water column yield rates ranging from 0.1 to 0.7 mmol m^{–2} day^{–1} or (1–8) × 10^{–13} mol cm^{–2} s^{–1}.³¹⁰ These values are 1–2 orders of magnitude higher than the rates of plant phytolith dissolution in neutral solutions and comparable to or slightly higher than those for vitreous silica. The dissolution rates of diatom biogenic silica were also measured in stirred flow-through reactors at 25 °C and pH 6–9.²²⁶ The range of 0.2–1 nmol s^{–1} g^{–1} was reported to correspond to (1.8–8.6) × 10^{–5} mol g^{–1} day^{–1}, at least an order of

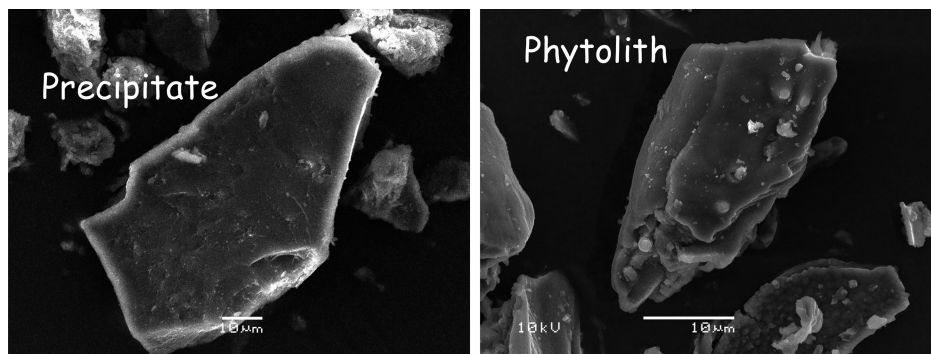


Figure 21. Amorphous silica precipitate (left) formed after 6 months aging of saturated sap solution extracted from horsetail (*E. arvense*) biomass and phytolith obtained from the same species via ashing and acid leaching (right).

magnitude higher than the rates of phytolith dissolution. Overall, specific dissolution rates of diatom shells in water column and sediments differ by several orders of magnitude.³⁰⁹ It has been demonstrated that the surface charge density of aged biogenic silica is significantly lower than that of the cultured diatoms. A decrease in the abundance of ionizable surface silanols explains the observed decrease in reactivity, or aging, of biogenic silica during settling through the water column and subsequent burial in sediments.³⁰⁵

Dissolution kinetics of uncleaned and chemically cleaned planktonic biogenic silica (BSi) was investigated using stirred flow-through reactors.²⁹⁷ The reactivity decrease correlates well with an increase in the integrated peak intensity ratios of Si–O–Si/Si–OH measured by FT-IR spectroscopy. Removal of organic or inorganic coatings enhances the reactivity by at least an order of magnitude. The FT-IR results suggest that internal condensation reactions reduce the amount of surface reaction sites and are partly responsible for the reactivity decrease with depth. One order of magnitude different rate constants measured in Norwegian Sea and Southern Ocean sediment trap material support the so-called opal paradox, that is, high biogenic silica accumulation rates in sediments despite low BSi production rates in surface waters of the Southern Ocean.

5.3. Dissolution of Biogenic Silica: Plants and Their Phytoliths

Silica is found in the walls and lumen of the cells of many plants, especially grasses, sedges, rushes, and horsetails. Silicified cells of the epidermis are the most common, but other cells also may be involved. All parts of the plant, except probably the roots, may have silicified cells. Plants take up different amounts and proportions of silicon from soil or from culture solution, depending on the species and the concentration of dissolved silicic acid present.³¹¹ Phytoliths are present in most plants, ranging in content from 0.5% or less in most dicotyledons, 1–3% in dryland grasses, and up to 10–15% in some wetland plant species.³¹² Examples of plants that produce phytoliths include dicots (e.g., Myrtaceae, Casuarinaceae, Proteaceae, Xanthorrhoeaceae, Mimosaceae), monocots (e.g., Cyperaceae, Gramineae, Palmae), conifers (e.g., Pinaceae, Taxodiaceae), and sphenophytes/scouring rushes (e.g., Equisetaceae).¹⁴² In upper soil horizons, phytoliths are released during organic matter degradation in the litter horizon and finally can be transferred to deeper horizons or

evacuated by aerial or hydrographical methods.^{313,314} A recent review on the potential of phytoliths in nanotechnology presents a through overview of phytolith functions and structure.³¹⁵

The size of Si precipitates in plants ranges from 100 nm to 200 μm, that is, 6 orders of magnitude.¹⁴⁰ Different modes of silicon uptake, active, passive and rejective, have recently been discussed in the review by Richmond and Sussman.³¹⁶ A tabulation of the ranges of the tissue levels of mineral elements found in plants gives the range for Si as 0.1–10% on a dry weight basis.³¹⁷

The biogenic silica in plants often confers a structural advantage, for example, as a supporting element or as a mineral barrier (considered as inorganic precursor to lignin) to both the translocation of water and salts and the invasion of pathogens.³¹⁸ Additionally various functions have been proposed for silica accumulation, such as mechanical stability of tissues, protection against fungi, insects, and herbivores, resistance to drought, facilitation of light interception, and alleviation of problems caused by nutrient deficiency and excess (reviewed by Motomura et al.³¹⁹).

Phytoliths, also called plant opals or opaline silica, are solid deposits of amorphous silica ($\text{SiO}_2 \cdot n\text{H}_2\text{O}$) that are produced in living plants and precipitated in and among their cells in organs such as stems, leaves, and inflorescences.³²⁰ The exact pathway of phytolith formation in plants is still poorly understood. It is certain that sap solution transporting Si in plant tissues contains high concentration of silicic acid, sufficient to precipitate amorphous silica upon drying and deposition in cells. Sap solutions of horsetail (*Equisetum arvense*) were sampled near Garonne river (SW France) and were allowed to precipitate amorphous silica upon aging in the refrigerator. The sterile sap solution, initially close to equilibrium with amorphous silica at room temperature (100 mg/L of SiO_2), produced precipitates of amorphous silica after 6 months of exposure (Figure 21). These amorphous precipitates were surprisingly similar in shape to phytoliths extracted from the same plant via ashing and acid leaching. It follows that, unlike for diatoms precipitating their frustules from initially undersaturated solution, formation of phytoliths is more thermodynamically favorable and may be driven by simple precipitation from supersaturated solutions upon drying in plant cells.

Phytoliths can be preserved over long time scales, and they have been recovered from sediments spanning the Quaternary and even found in late Eocene and early Miocene records.³²¹ Phytoliths are generally resistant to

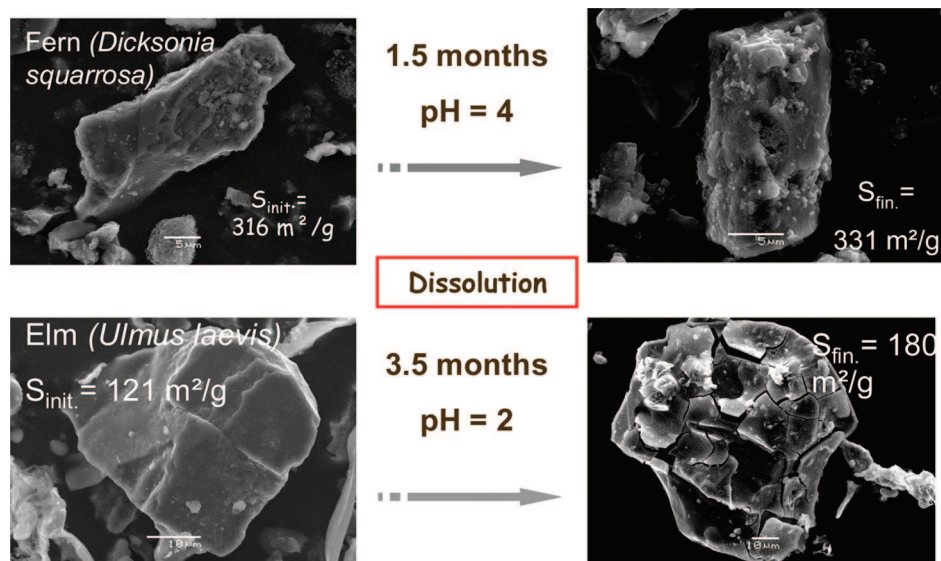


Figure 22. Photophytoliths. SEM images of phytoliths before and after dissolution reaction in mixed-flow experiment.

dissolution in natural environments except under strongly alkaline burial conditions where pH is greater than 9.³²² Today, the exact molecular mechanism controlling Si uptake and transport through cell walls and membranes is not fully understood. It is anticipated that with the increasing use of genetic tools it will be possible to identify those genes involved in the plant silicification process, as it is proceeding in diatoms. An interesting issue is the ultrastructure of plant phytoliths recently assessed via high-resolution confocal Raman microscopy and atomic force microscopy (AFM).³¹⁵ It was demonstrated that the nanostructured phytolith granular surface consists of spherical silica nanoparticles. However, contrary to diatoms, except for the presence of sintered spheres of 50 nm diameter, no hierarchical structures have been observed in phytoliths.³¹⁵

The use of stirred flow-through experiments under controlled laboratory conditions allowed rigorous evaluation of plant and grass phytolith dissolution rate. Examples of phytolith dissolution in acidic solutions during several months of reaction are illustrated in Figure 22.

Phytolith dissolution rates, measured in mixed-flow reactors at far from equilibrium conditions at $1 \leq \text{pH} \leq 10$, are illustrated in Figure 23. It can be seen from Figure 23 that the rate data of all studied phytoliths are quite similar to those of bamboo phytoliths³²³ in neutral solutions. Rates increase with a_{H^+} for pH values < 2 , at $2 \leq \text{pH} \leq 3-4$, the rates for all types of phytoliths are independent of pH, and for pHs from 4 to 9, phytolith dissolution rates increase with pH with a slope of 0.33, close to that measured for quartz and amorphous silica. The rates can be approximated by a three-term equation, similar to that used for quartz and aluminosilicate dissolution description:

$$R \text{ (mol/(cm}^2 \cdot \text{s))} = (6 \pm 3) \times 10^{-16} \times a_{\text{H}^+} + (3 \pm 2) \times 10^{-18} + (3.5 \pm 0.5) \times 10^{-13} \times a_{\text{OH}^-}^{0.33} \quad (11)$$

Similar to amorphous silica and quartz, phytolith dissolution rates can be also modeled within the framework of the surface complexation approach³²⁴ assuming the rate is

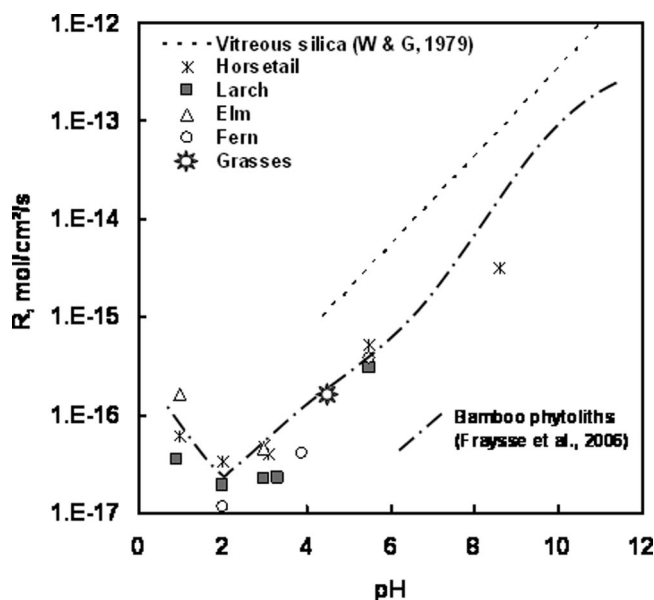


Figure 23. Dissolution rates of horsetail, larch, elm, fern, and grass (*Calamagrostis epigeios*) phytoliths as a function of pH measured in a mixed flow reactor at 25 °C: (— · —) bamboo phytolith dissolution rates;³²³ (---) rates of vitreous silica.³²⁹ Uncertainties of rate measurements are within the size of symbols.

controlled by the protonation, deprotonation, and hydrolysis of surface $>\text{Si}-\text{OH}$ groups:^{211,215,216,325-328}

$$R = k_1 \{>\text{SiOH}_2^+\}^n + k_2 \{>\text{SiOH}^0\} + k_3 \{>\text{SiO}^-\}^m \quad (12)$$

where $\{>\text{SiOH}_2^+\}$, $\{>\text{SiOH}^0\}$, and $\{>\text{SiO}^-\}$ stand for the concentration of the corresponding surface species present at the $\text{SiO}_2/\text{H}_2\text{O}$ interface, k_i are the corresponding rate constants of the three parallel reactions, and n and m represent the order of the proton- and hydroxyl-promoted dissolution reaction, respectively. Assuming the order of the protonation reaction is unity ($n = 1$),²¹⁷ eq 12 can be also used to fit phytolith rate data in the full pH range. It is important to note the similarity of the surface-normalized dissolution rate measured for different phytoliths. This is a

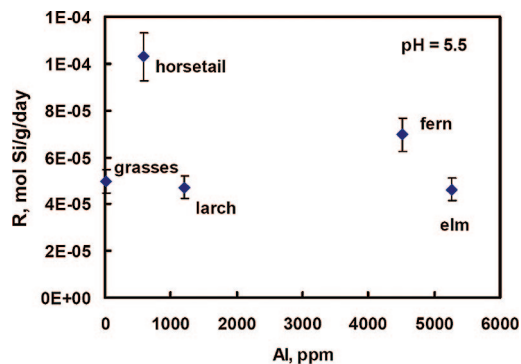


Figure 24. Effect of Al content in solid on dissolution rate of various phytoliths. Figure reproduced with permission from ref 331, copyright 2009, Elsevier.

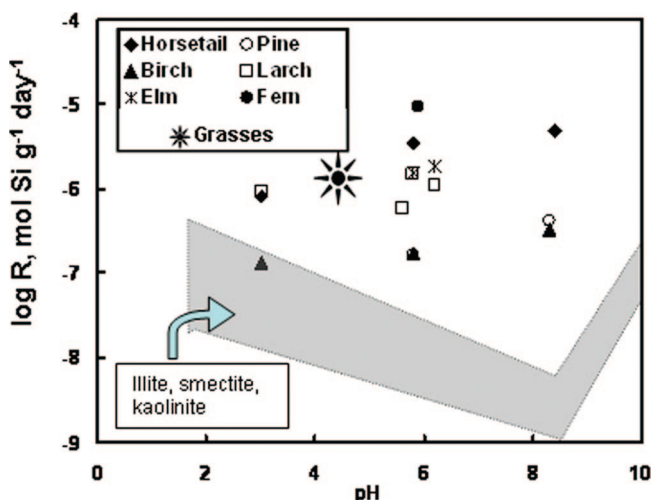


Figure 25. Desilicification of whole plant biomass. Si release rates ($\text{mol Si}/(\text{g}_{\text{DW}} \cdot \text{day})$) for typical soil clay mineral (shaded area) and plant biomass (symbols) dissolution as a function of pH at 25 °C. Uncertainties on rates are within the symbol size.

quite remarkable result, given the extremely large variety of phytolith size, shape, and specific surface areas and huge physiological diversity of plant species that produce them.

It has been widely argued that the presence of Al in phytoliths is able to greatly affect their solubility and dissolution kinetics.^{313,330} Recently, a number of phytoliths extracted from various plants and having Al content from 200 ppm (*Calamagrostis epigeios*) to 5000 ppm (*Ulmus laevis*) were examined.³³¹ At near neutral pH values, the dissolution rates are virtually the same within $\pm 30\%$ and exhibit no trend with Al concentration increase (see Figure 24).

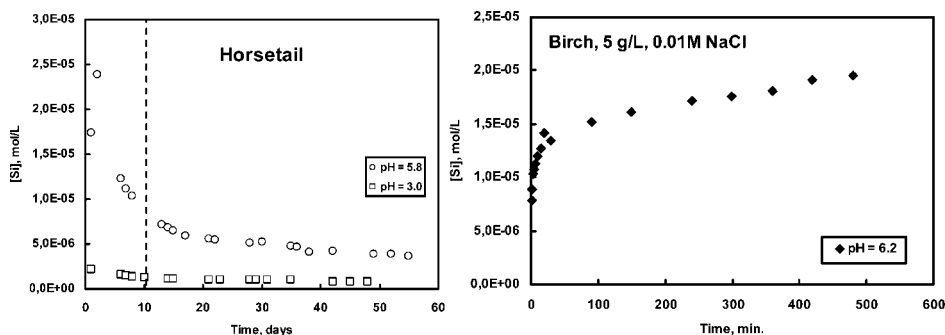


Figure 26. (A) Si concentration as a function of time in mixed-flow reactor equipped with a 1 kDa dialysis bag, dissolution of horsetail biomass at pH = 3.0–5.8. (B) Two stages of Si release from birch biomass in batch (closed) reactor suggesting the presence of two pools of Si in solid phase. All solutions are highly undersaturated with respect to amorphous silica.

Although Si is generally precipitated in phytoliths, many plants do not have distinct phytoliths yet contain relatively large amount of amorphous silica. Inanaga and Okasaka³³² suggested, using spectroscopic techniques, that silicon in rice may be bound with lignin–carbohydrate complexes or phenol–carbohydrate complexes in a similar way to calcium. Watteau et al.³³³ studying the release of Si from decomposing beech leaves, observed that Si associated with polyphenolic substances is more labile than Si associated with the pectocellulosic membranes. Ultrastructural observations of fine beech roots using in situ microanalysis like HR-TEM and EELS (electron energy loss spectroscopy) demonstrated the presence of two forms of Si, either diffused inside the polyphenolic substance or as a pure silica layer.³³⁴ These authors also were able to identify some specific bacterial activity related to the degradation of siliceous cell walls.³³³ Recent results corroborate the existence of two pools of reactive Si in the plant litter, whose aqueous reactivities may be different.^{322,331} In order to achieve further insights in the reactivity of plant silica, a laboratory approach has been applied for determining Si release rates from litter of typical temperate and boreal plants, pine (*Pinus laricio*), birch (*Betula pubescens*), larch (*Larix gmelinii*), elm (*Ulmus laevis* Pall.), tree fern (*Dicksonia squarrosa*), and horsetail (*Equisetum arvense*), in 0.01 M NaCl solutions, pH = 2–10, and $T = 5, 25,$ and 40 °C.^{336,337} Mixed-flow reactors equipped with a dialysis compartment and closed (batch) reactors were used. The values of Si flux due to dissolution of plant litter (moles of Si per gram dry weight (g_{DW}) per day) are illustrated as a function of pH in Figure 25. It can be seen that Si release rates for pine and birch biomass are the lowest, while the rates of elm, horsetail, fern, and larch biomass are 1–2 orders of magnitude higher. The measured order of Si release rate is comparable to Si content in the plant biomass, horsetail > elm \gg birch \geq pine, which indicates the governing role of plant phytoliths in Si release from plant material. Comparison of Si release rates from phytoliths^{323,331} and plant biomass^{336,337} suggests that the reactivity of biogenic amorphous silica within the organic matrix is close to that of the pure solid, and neither organic matter–silica bonding nor the diffusion through the organic template limit the Si release from the solid to the solution.

Analysis of Si behavior in the course of dissolution in short-term batch reactor and in long-term mixed-flow reactors equipped with a dialysis compartment unequivocally demonstrates two dissolution regimes: very fast initial Si release during the first minutes or hours (batch reactor) or 1–10 days (mixed-flow reactor) followed by a slower, long-term silica release (Figure 26). Therefore, one can suggest the

presence of two pools of silica in plant tissues: a “concentrated” pool of phytoliths (amorphous silica aggregates of 1–100 μm size) and individual molecules (H_4SiO_4) or small polymers dispersed in the organic matrix or complexed with pectin or proteins in the cell wall. Although peptide and amino acid interactions with silicic acid via hydrogen bonds and electrostatic force are well documented³³⁵ and known to produce a $\text{SiO}_2 \cdot n\text{H}_2\text{O}$ –protein matrix in the diatom cell walls,^{264,284} complexation of silica with pectin constituents has not been demonstrated. At the same time, ^{29}Si high-resolution solid-state NMR evidenced two pools of Si in biomass of rice hulls and endocarp of babassu coconut: hydrated amorphous silica and organically bound Si species.²⁷⁷

The degradation of plant litter and, therefore, liberation of Si in solution is often enzymatically controlled. In order to quantify the role of heterotrophic bacteria that consume the dissolved organic carbon, we followed the evolution of Si concentration during microbially controlled plant litter demineralization.³³⁶ For larch biomass, the Si release rate was found to be almost an order of magnitude higher than that in a sterile experiment, whereas for fern, the presence of bacteria did not significantly modify the Si release rate compared with that in abiotic experiments.

6. Desilicification and Isolation of Organic Templates

Demineralization is a crucial step for structural investigations as well as the exploration of the biomimetic potential of biocomposites since the analysis of the organic matrix embedded into the materials usually requires dissolution of silica. Isolation of organic matrices from different invertebrates that possess siliceous skeletons is mainly based on two chemical approaches. The first one, most popular and quick, is etching with respect to silica dissolution using hydrofluoric acid (HF) and related compounds. The second, alkali based method is very slow but more “gentle” from a biological point of view. In both cases, only those kinds of biomolecules that are resistant to the corresponding etchant can be isolated.

6.1. Alkali versus Hydrofluoric Acid

Wet chemical etching of silicate glasses in aqueous HF solutions is a subject that has been studied over many years. The first report originates from the discovery of HF by Scheele in 1771.³³⁸ The specific property of HF-containing solutions to attack glass is related to the presence in solution of the fluorine-containing species F^- , HF, and HF_2^- . The dissolution mechanism, in particular the role of the various fluorine-containing species, has been reviewed by Spierings.^{339,340} The HF_2^- ions are adsorbed on surface silanol groups, the HF molecules on vicinal silanol groups, and H^+ ions on surface bridging oxygens in siloxane units. Fluorine-containing adsorption complexes have been observed at hydrated SiO_2 surfaces in gaseous HF by infrared spectroscopy. These are transformed into surface groups such as $\equiv\text{Si}-\text{F}$ and $\equiv\text{Si}-\text{O}-\text{SiF}_3$. The adsorption of HF and HF_2^- increases the electronic density on the bridging oxygen in the siloxane unit. This in turn makes these oxygens more basic, so more H^+ ions are adsorbed, which leads to more siloxane bonds being broken per time unit, that is, a kind of catalytic effect. The rate-determining step is then the

breakage of the siloxane bond by the combined action of the adsorbed species.

Judge et al.³⁴¹ found that the etching rate depends on the concentration of HF molecules but does not depend on the concentration of the HF_2^- ion. This result showed that solutions with a pH of 7 and higher that contain essentially all fluorides in the deprotonated state exhibit essentially a zero rate of SiO_2 dissolution, which indicates that an HF_2^- or F^- ion in solution is quite benign and much less reactive than the HF molecule. Previous experimental studies showed that HF etching of SiO_2 films was enhanced by the addition of water. Consequently, H_2O may play a direct role in the etching mechanism itself.

Unlike many physical properties, no linear relations are observed between the composition of the glass and its dissolution rate. The dissolution rate of a multicomponent silicate glass is found to be largely determined by two factors: the degree of linkage or connectivity of the silicate network and the concentration of SiO_2 in the glass. It is proposed that glass dissolution is preceded by the leaching of alkali and alkaline earth components present in the glass, followed by the subsequent dissolution of the leached layer. Probably fluorine species will diffuse into the leached layer to enhance the dissolution rate. Analysis of the activation energy data indicates that in some corrosive glasses, the leaching itself becomes rate-determining.

Similarly to silicate glasses, silica-based skeletons of biological origin are also examples of multicomponent silica because of the presence of organic compounds as well as K^+ and Na^+ . By virtue of their embedded, mineralized skeletons, sponges are of great interest to both evolutionary biologists and materials scientists. As the most basal metazoans, they are the key to understanding the evolution of both calcium- and silicon-based biomineralization. The manifestation of this mineralization, a skeleton of spicules embedded in the body of the sponge, is a typically complex arrangement of calcite or silica. For example, the skeletal spicules of glass sponges (Hexactinellida, Porifera) are valuable model systems for the investigation of structure–function relationships in biomaterials, with the ultimate goal of identifying design strategies for new synthetic materials.

Demineralization of the siliceous spicules of sponges had already been described in the 19th century³⁴² based on the use of hydrofluoric acid. Kölliker was the first to describe the use of HF solution for the demineralization of *Hyalonema* spicules.³⁴³ In 1888, Sollas reported on sponge spicule desilicification methods based not only on HF but also on boiling solutions of KOH.³⁴⁴ A HF-etching procedure developed for microscopic investigations of the structure of sponge siliceous spicules was described by Vosmaer and Wijsmann,³⁴⁵ and this is still used today. A similar HF-based desilicification method was used by Schmidt in 1926 for a comparative study of organic and inorganic substances within the spicules of *Hyalonema* and *Monorhaphis* species.³⁴⁶ HF dissolution of silica was used more recently to visualize the sponges' axial filaments but was satisfactory only for determining their gross morphology; unfortunately, it also had the drawback of partially masking the filament fine detail.³⁴⁷ The removal of silica from the face of the block by soaking in HF circumvents some problems but results in the loss of the freed filaments, which are no longer supported by a surrounding matrix to hold them in the block.³⁴⁸ Also, cathepsin-like proteins called “silicateins” were isolated from siliceous spicules of *Tethya aurantia* by dissolving the silica

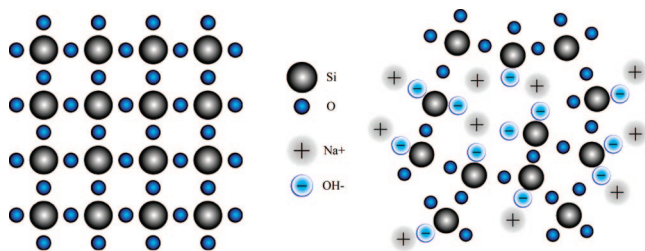


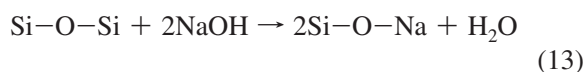
Figure 27. Principle schema of the alkali–silica reaction (left, crystalline; right, amorphous silica).

in HF/NH₄F solutions.³⁴⁹ However, a fibrillar organic matrix was described for *Euplectella* sp. spicules that had been desilicated using HF gas rather than solution.³⁵⁰

Even today, HF-based techniques are still in use.³⁵¹ As pointed out early by Bütschli,³⁵² this rapid technique may produce artifacts.^{353–355} “Collateral damages” due to the use of HF in biological objects are well-known. Hydrofluoric acid cleaves disulfide bonds, for example, in keratin,³⁵⁶ is a highly specific reagent for the cleavage of phosphate–oxygen bonds,³⁵⁷ dephosphorylates phospholipids,³⁵⁸ phosphoglycerides, and phosphoglycolipids,³⁵⁹ removes polysaccharides from peptidoglycan–polysaccharide complexes, and hydrolyzes oligosaccharides.³⁶⁰ In addition, fluoride binds to calcium and magnesium in hard tissues, modified cell membranes, organelles, and enzymes.³⁶¹ This problem becomes obvious, for example, during the analysis of the silaffins from diatoms as well as the silicateins from sponges. Both peptides were shown to become dephosphorylated by HF treatment.^{40,82,209} Therefore, NH₄F had to be used, which did not remove the phosphate groups. Another demineralization method³⁶² that is based on the use of Na₂CO₃ or 0.5 M NaOH with subsequent heating to 85 °C is also inapplicable for the isolation of native organic matrices because it leads to the denaturation of proteins. In order to overcome this obstacle, novel slow-etching methods that use solutions of 2.5 M NaOH (or at least 1% sodium dodecylsulfate, SDS, or 1% rhamnolipid biosurfactant) at 37 °C and take 14 days have been recently developed.³⁶³

The following mechanism can be put forth on the basis of the reaction of alkaline desilicification of organic–silicon materials (Figure 27). Hydroxyl ions primarily attack and subsequently break the stronger siloxane bonds (Si–O–Si) located on the surface of the silicone component.

The negative charge that appears as a result of this bond breakage is balanced by positively charged ions of the alkali element:



During the reaction of alkaline desilicification, the hydroxide ions penetrate into the SiO₂ particles, therefore weakening the structure of the latter. Such a pattern of disintegration of the lattice structure by alkaline hydroxide is virtually impossible in the case of highly crystallized silicates (quartz); however, and in contrast to amorphous silicates (opal A), this process proceeds very efficiently, due to the increased surface area and irregularly open structure of the particles.³⁶⁴

In the following sections, we describe recent reports on isolation of organic templates from silica-containing sponges obtained using HF- and alkali-based techniques.

6.2. Isolation of Protein-Based Templates

Silica deposition is a fundamental process in sponges. According to the modern point of view, two different mechanisms of silicification in sponges based on isolated and identified organic matrices are proposed: enzymatic (silicatein-based) and nonenzymatic or self-assembling (chitin- and collagen-based).

The group of Morse,^{349,365} using the HF-based dissolution method, discovered that the organic filaments in demersponge *Tethya aurantium* are composed of a cathepsin L related enzyme, termed silicatein. They cloned two of the proposed three isoforms of silicateins, the α - and β -forms, from this demersponge.³⁴⁹ In subsequent years, these molecules were cloned also from other sponges, among them *S. domuncula* and *Lubomirskia baicalensis*.^{349,366} The spicules are produced in special cells, the sclerocytes. Formation starts intracellularly around a silicatein filament and is completed extracellularly by apposition of silicatein onto the growing spicules.^{367,368} Cathepsin L is an endopeptidase that cleaves peptide bonds with hydrophobic amino acid residues in P2 and P3 positions and occurs in lysosomes as well as extracellularly as secreted enzymes. The silicateins are distinguished from the cathepsins by the replacement of the first amino acid residue in the catalytic triad, cysteine, by serine.³⁶⁵ It has been proposed that serine increases the nucleophilicity during the nucleophilic attack at the silicon atom. The polymerization-promoting activity of the silicateins has been shown to be catalytic and not stoichiometric. It is possible that the controlled punctuated secretion of low concentrations of monomeric silicateins, pulses in the transitory flux of silica-precursor molecules, oscillations in the pH, ionic or other conditions of the condensation environment, or a combination of these factors may be responsible for the annular patterning and continued deposition of silica in spicule biosynthesis *in vivo* once the axial filament has become completely covered during the early stages of silica deposition around this proteinaceous core. Alternatively, the continued growth of silica may be a result of dangling bonds at the growth surface of the newly deposited silica.³⁶⁹ More detailed information about the possible mechanisms for silicatein catalysis can be found in numerous recent papers.^{207,355,370–372}

Ehrlich and co-workers reported an example of *Hyalonema sieboldi* glass sponge in which its spicules are a biocomposite containing a silicified collagen matrix and in which high collagen content is the origin of the unique mechanical flexibility of the spicules.^{363,373} Glass sponges are largely restricted to deep, cold-water (between 0 and 4 °C) habitats.^{374–376} Therefore from an ecological point of view collagen-based (as well as chitin-based) silicification, which occurs in spicules and other skeletal formations of these sponges, is an example of unique cold-water biomineralization. There is no evidence in the literature about silicatein activities at this temperature level. Skeletal biomineralization requires energy and so imposes a metabolic cost on skeleton-forming organisms.³⁷⁷ A hypothesis was put forth that probably some phosphate moieties and ATPase-based mechanisms are in some way involved in biosilicification at temperatures near zero.⁴

Recently, two proteins, actin and hydroxylated collagen have also been identified for the first time in the *H. sieboldi* glass sponge basal spicules.⁴ The collagen peptides show the characteristic motif [Gly-Xaa-Yaa]_n with 33% of those proline residues in the Xaa position hydroxylated and 100%

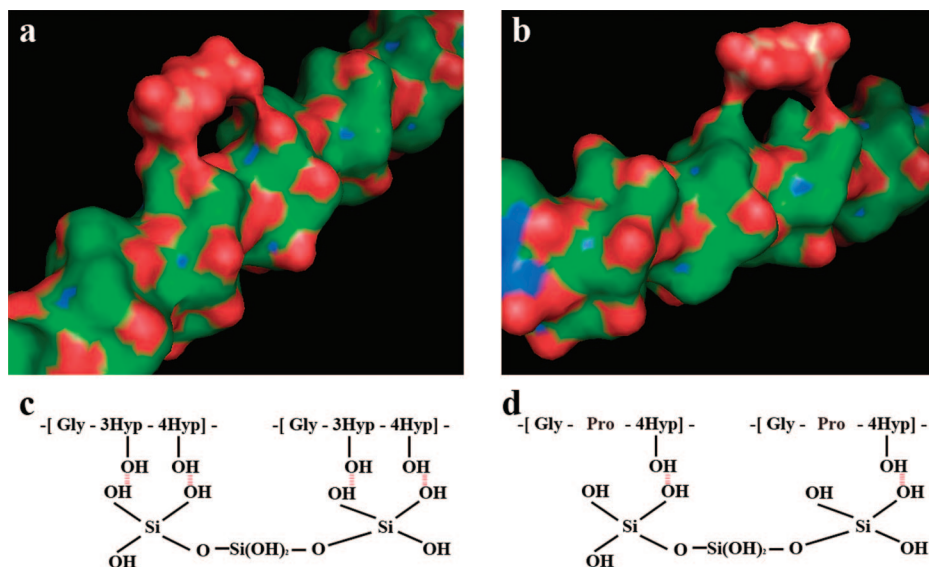


Figure 28. Model of interaction between polysilicic acid and Gly-3Hyp-4-Hyp polypeptide (a) or Gly-Pro-4-Hyp polypeptide (b) located in collagen triple helix (blue). In selected amino residues, carbon atoms are colored green, oxygen red, nitrogen blue, and silica orange. Mechanisms for these interactions are schematically represented in panels c and d. Figure reproduced with permission from ref 4, copyright 2011, Springer.

of proline residues in the Yaa position (as 3-hydroxyproline (Hyp) and 4-hydroxyproline, respectively, Figure 28) Hydroxylated collagen appears to form the basis for the extraordinary mechanical and optical properties of hexactinellid spicules. The self-assembly properties of collagen and its templating activity with respect to silicification are consistent with recent ideas on the development of hierarchical silica-based architectures. Macroscopic bundles of silica nanostructures result from the kinetic cross-coupling of two molecular processes: a dynamic supramolecular self-assembly and a stabilizing silica mineralization. The feedback interactions between template growth and inorganic deposition are driven nonenzymatically by means of hydrogen bonding. It may be suggested that the hydroxylated glass sponge collagen changes the nature of silica in aqueous solution by converting the distribution of oligomers to a more uniform and useful set of nanoparticle precursors for assembly into the growing solid.

The slow-etching alkali procedure provides the possibility to observe the forms of collagen fibrils located within silica layers of sponge spicules and their distribution. For example, the results obtained by SEM observations of the desilicified spicular layers of *Monorhaphis chuni* provide strong evidence that the collagen fibrils' orientation within spicules possesses a twisted plywood architecture.³⁷⁸ The partially desilicified nanofibrillar organic matrix observed on the surface of silica-based inner layers of the demineralized spicule provides strong evidence that silica nanoparticles of diameter about 35 nm are localized on the surface of corresponding nanofibrils.³⁷⁸ This kind of silica nanodistribution is very similar to the silica distribution on the surface of collagen fibrils in the form of nanoparticle necklets, first observed in the glass sponge *H. sieboldi*.^{363,373} It was suggested that the nanomorphology of silica on proteinaceous structures described above could be envisioned as an example of biodirected epitaxial nanodistribution of the amorphous silica phase on oriented collagenous fibrillar templates.³⁷⁹ From this point of view, basal spicules of *Monorhaphis* sponges could be also defined as natural plywood-like silica ceramics organized similarly to the crossed-lamellar layers of seashells. The authors also sug-

gested that the matrix of the *M. chuni* anchoring spicule is silicified fibrillar collagen rather than collagen-containing silica, which is the reason for their remarkable mechanical flexibility.

6.3. Isolation of Polysaccharide-Based Templates

The aminopolysaccharide chitin has a nanofibrous structure and the chain of pyranose ring arranges almost parallel to the (100) plane and extends along the fiber axis.³⁸⁰ The chitin molecule has C=O, O-H, and N-H groups, and oxygen atoms, which have affinity to the calcium, phosphate, carbonate, and hydroxyl ions of the corresponding calcium phases. However, the same functional groups possess affinity for silicate ions as well. Because there is a possibility that such an oriented organic matrix acts as a template or an ordered structural framework, the existence of naturally occurring silica-chitin composites was hypothesized.^{373,381} Moreover, silicon was found associated with glycosaminoglycans bound as an ether or ester-like silicate with C-O-Si or C-O-Si-O-Si-O-C bonds, in amounts of one Si atom per 130–280 repeating units of the organic.³⁸² At this point, it should be mentioned that the effect of a phosphonomethylated chitosan on silica formation *in vitro* has been also reported.^{383,384} The role of chitin in biosilicification is still not completely understood. Although chitin is one of the most important biopolymers in nature, proof of its interaction with silicon *in vivo* was absent up to now. Only recently, Ehrlich and co-workers isolated and identified chitin from skeletal formations of some marine glass sponges for the first time. The presence of chitin within the framework skeleton of *Farrea occa*³⁸⁵ and *Euplectella aspergillum*³⁸⁶ as well as separate spicules *Rossella fibulata*³⁷⁸ could also be revealed by the gentle, NaOH-based desilicification technique established by Ehrlich et al.^{363,386} The structure of the chitin extracted from these sponges turned out to be similar to α -chitin from invertebrates. It was suggested that silicate ions and silica oligomers preferentially interact with glycopyranose rings exposed at the chitin surface, presumably by polar and H-bonding interactions.³⁸⁶

It is well established that diatoms are characterized by a silica frustule, that surrounds their cell wall. Interestingly, however, chitin-based organic networks are an integral part of cell wall biosilica in the diatom *Thalassiosira pseudonana* as recently reported by Brunner and co-workers.³⁸⁷

Because chitin could play a crucial role also in biosilification in fungi,³¹ it was hypothesized³⁸⁵ that chitin molecules are probably part of a very old organic template system involved in the biosilicification phenomenon, which was established a long time before the origin of the first metazoan (e.g., glass sponges). From a chemical point of view, investigations on mono- and polysaccharide silica interactions both *in vivo* and *in vitro* are of high priority today. For example, having demonstrated that the Si–O–C linkage is stable toward hydrolysis in special diolato and alditolato ligands, Kluefers and co-workers showed recently³⁸⁸ the significance of specific patterns of stabilizing secondary interactions that have their origin in the unique polyfunctionality of the carbohydrates. The hydrogen bonds described counterbalance other destabilizing factors. Whether or not silicon complexation by carbohydrates is a potential transport or deposition mechanism of silica in organisms depends on the discovery of ligands that combine the principles outlined here: the stability range of complexes around neutral pH may be broadened by using ligands that are free of strain that give complexes that can be further stabilized by secondary interactions.³⁸⁸

7. Epilogue, Conclusions, and Outlook

Desilification of biocomposites is a complex process in which mineral dissolution proceeds through the strong interaction of the organic matrix with the inorganic material. The mechanism of silica dissolution from mineralized organisms is well described by models used for inorganic minerals in aqueous media taking into consideration surface speciation. These models explain satisfactorily not only the kinetics of dissolution but also the importance of functional groups (carboxylic or phosphate) involved in most types of the organic matrix. Bacteria and fungi, worms, and in general cells and tissues have a catalytic effect on dissolution of various forms of silica both amorphous and crystalline. The diversity of living matter on one hand and of the forms of silica on the other hand makes it necessary for further research to be done on the investigation of the relationship of the desilification mechanisms with respect to the microenvironment developed in the various forms of living organisms. In particular, with respect to the role of the organic matter, serving as template in the mineralization process specific attention should be given to the composition and structure of this supporting substance through the development of non aggressive methods like alkali treatment or enzymatic catalysis for the removal of silica from biocomposites.

The intricately complex mechanism of desilicification serves a plethora of purposes and functions, from organisms' survival to structural protection to "silicon" balance. Man's curiosity has been a significant driving force to delineate the mechanisms involved in either "natural" or "pathological" desilicification. Several important scientific and technical areas may benefit from Nature's desilicification pathways and mechanisms. For example, silica/silicate deposits are known to be significant problems in process water systems, because their chemical dissolution can be a safety and environmental burden.^{389–391} These can be desilicified or dissolved by the action of a variety of silicon-chelating

molecules.^{242,243} It is obvious that desilicification and silicification should be envisioned and studied as the "two sides of the same coin". It is often observed (and admired) that Nature uses these seemingly reverse processes in admirable synergy to achieve a multitude of purposes and functions. Continued advances in instrument technology, as well as biochemical methods, will make it possible to further tackle unresolved issues. There are many of opportunities for academic and applied research. In particular, applications geared toward health issues and nanoparticle research and technology may take the field of desilicification several steps forward.

8. Acknowledgments

K.D.D. thanks the General Secretariat of Science & Technology. H.E. thanks Prof. C. Skinner, Prof. E. Baeuerlein, Prof. E. Brunner, and Prof. H. Worch for their support and permanent interest in his research and V.V. Bazhenov for technical assistance.

9. References

- (1) Skinner, H. C. W. Minerals and Human Health. In *EMU Notes in Mineralogy. Environmental Mineralogy*; Varughan, D. J., Wogelius, R. A., Eds.; Eotvos University Press: Budapest, Hungary, 2000; Vol 2, p 434.
- (2) Ehrlich, H.; Koutsoukos, P. G.; Demadis, K. D.; Pokrovsky, O. S. *Micron* **2008**, *39*, 1062.
- (3) Mann, D. G.; Droop, S. J. M. *Hydrobiologia* **1996**, *336*, 19.
- (4) Ehrlich, H. in *Encyclopedia of Geobiology*; Reitner, J., Thiel, V., Kappler, A., Konhauser, K., Eds.; Encyclopedia of Earth Science Series; Springer: Heidelberg, 2011, in press.
- (5) Lakes, R. *Nature* **1993**, *361*, 511.
- (6) Mann, S. *J. Mater. Chem.* **1995**, *5*, 935.
- (7) Aizenberg, J.; Weaver, J. C.; Thanawala, M. S.; Sundar, V. C.; Morse, D. E.; Fratzl, P. *Science* **2005**, *309*, 275.
- (8) Meyers, M. A.; Lin, A. Y. M.; Seki, Y.; Chen, P.-Y.; Kad, B. K.; Bodde, S. *J. Miner.* **2006**, *58*, 34.
- (9) Fratzl, P. *J. R. Soc., Interface* **2007**, *4*, 637.
- (10) Pouget, E.; Dujardin, E.; Cavalier, A.; Moreac, A.; Valery, C.; Marchi- Artzner, V.; Weiss, T.; Renault, A.; Paternostre, M.; Artzner, F. *Nat. Mater.* **2007**, *6*, 434.
- (11) Mann, S.; Perry, C. C. In *Silicon Biochemistry*; Evered, D.; O' Connor, M., Eds.; CIBA Foundation Symposium 121; John Wiley & Sons: Sussex, U.K., 1986.
- (12) Policard, A.; Collet, A.; Daniel-Moussard, H.; Pregermain, S. *J. Phys. Biochem. Cytol.* **1961**, *9*, 236.
- (13) Green, D.; Howard, D.; Yang, X.; Kelly, M.; Oreffo, R. O. *Tissue Eng.* **2003**, *9*, 1159.
- (14) Phoenix, V. R.; Bennett, P. C.; Engel, A. S.; Tyler, S. W.; Ferris, F. G. *Geobiology* **2006**, *4*, 15.
- (15) Jones, B.; Rosen, M. R.; Renault, R. W. *J. Sediment. Res.* **2001**, *71*, 190.
- (16) Chafetz, H. S.; Guidry, S. A. *Sediment. Geol.* **1999**, *126*, 57.
- (17) McKenzie, E. J.; Brown, K. L.; Cady, S. L.; Campbell, K. A. *Geothermics* **2001**, *30*, 483.
- (18) Pancost, R. D.; Pressley, S.; Coleman, J. M.; Benning, L. G.; Mountain, B. W. *Environ. Microbiol.* **2005**, *7*, 66.
- (19) Jones, B.; Renaut, R. W.; Rosen, M. R. *Palaios* **1999**, *14*, 475.
- (20) Aubrecht, R.; Brewer-Carias, Ch.; Šmída, B.; Audy, M.; Kováčik, L. *Sediment. Geol.* **2008**, *203*, 181.
- (21) Handley, K. M.; Turner, S. J.; Campbell, K. A.; Mountain, B. W. *Astrobiology* **2008**, *8*, 747.
- (22) Fujino, Y.; Kawatsu, R.; Inagaki, A.; Umeda, Y. T.; Okaue, Y.; Iwai, S.; Ogata, S.; Oshima, T.; Doi, K. *J. Appl. Microb.* **2008**, *104*, 70.
- (23) Inagaki, F.; Yokoyama, T.; Doi, K.; Izawa, E.; Ogata, S. *Biosci., Biotechnol., Biochem.* **1998**, *62*, 1271.
- (24) Inagaki, F.; Motomura, Y.; Ogata, S. *Appl. Microbiol. Biotechnol.* **2003**, *60*, 605.
- (25) Jones, B.; Renaut, R. W.; Konhauser, K. O. *Sedimentology* **2005**, *52*, 1229.
- (26) Jones, B.; Renaut, R. W. *Palaios* **2006**, *21*, 406.
- (27) Asada, R.; Tazaki, K. *Can. Miner.* **2001**, *39*, 1.
- (28) Brasser, H. J.; Krijger, G. C.; van Meerten, T. G.; Wolterbeek, H. T. *Biol. Trace Elem. Res.* **2006**, *112*, 175.

- (29) Brasser, H. J.; Krijger, G. C.; Wolterbeek, H. T. *Biol. Trace Elem. Res.* **2008**, *125*, 81.
- (30) Jones, M. S.; Wakefield, R. D.; Forsyth, G. *Mater. Constr. (Madrid, Spain)* **1999**, *49*, 3.
- (31) Kolb, V. M.; Philip, A. I.; Perry, R. S. Testing the Role of Silicic Acid and Biochemical Materials in the Formation of Rock Coatings. In *Instruments, Methods, and Missions for Astrobiology VIII*; Hoover, R. B., Levin, G. V., Rozanov, A. Y., Eds.; SPIE: Bellingham, WA, 2004; p 312.
- (32) Anderson, O. R. *Protoplasma* **1994**, *181*, 61.
- (33) Patterson, D. J.; Dürrschmidt, M. J. *Cell Sci.* **1988**, *91*, 33.
- (34) Ogden, C. G. *Protoplasma* **1991**, *163*, 136.
- (35) Preisig-Mueller, R.; Günemann-Schäfer, K.; Kindl, H. *J. Biol. Chem.* **1994**, *269*, 20475.
- (36) Ludwig, M.; Lind, J. L.; Miller, E. A.; Wetherbee, R. *Planta* **1996**, *199*, 219.
- (37) Smol, J. P. *Pollution of Lakes and Rivers: A Paleoenvironmental Perspective*, 2nd ed.; Blackwell Publishing: Oxford, U.K., 2008; p 383.
- (38) Anderson, O. R. *Protoplasma* **1994**, *181*, 61.
- (39) Asano, K. *Pac. Sci.* **1950**, *4*, 158.
- (40) Kröger, N.; Deutzmann, R.; Sumper, M. *Science* **1999**, *286*, 1129.
- (41) Round, F. E.; Crawford, R. M.; Mann, D. G. *The Diatoms: Biology and Morphology of the Genera*; Cambridge University Press: Cambridge, U.K., 1990; p 757.
- (42) Hasle, G. R.; Sims, P. A. *Eur. J. Phycol.* **1985**, *20*, 219.
- (43) Mehard, C. W.; Sullivan, C. W.; Azam, F.; Volcani, B. E. *Physiol. Plant.* **1974**, *30*, 265.
- (44) Boury-Esnault, N.; Rützler, K. *Thesaurus of Sponge Morphology*; Smithsonian Contributions to Zoology, No. 596; Smithsonian Institution Press: Washington, DC, 1997; p 55.
- (45) Uriz, M.-J.; Turon, X.; Becerro, M. A.; Agel, G. *Microsc. Res. Tech.* **2003**, *62*, 279.
- (46) Uriz, M.-J. *Can. J. Zool.* **2006**, *84*, 322.
- (47) Lowenstam, H. A. *Science* **1971**, *171*, 487.
- (48) Labbé, A. *Notes C. R. Acad. Sci.* **1933**, *197*, 697.
- (49) Labbé, A. *C. R. Acad. Sci.* **1933**, *114*, 1002.
- (50) Labbé, A. *Ann. Inst. Oceanogr. (Monaco)* **1934**, *14*, 173.
- (51) Labbé, A. Opisthobranches et Silicodermés (Oncidiadés). In *Memoires du Musée royal d'histoire naturelle de Belgique. Hors série. Résultats scientifiques du voyage aux Indes Orientales Néerlandaises de LL. AA. RR. le Prince et la Princesse Léopold de Belgique, Vol. 2*; Musée Royal d' Histoire Naturelle de Belgique: Brussels, 1934.
- (52) Monniot, F.; Martoja, R.; Monniot, C. *Biochem. Syst. Ecol.* **1992**, *20*, 541.
- (53) Beklemishev, K. V. *Dokl. Akad. Nauk USSR* **1954**, *97*, 543.
- (54) Beklemishev, K. V. *Trudy Inst. Okeanol.* **1959**, *30*, 148.
- (55) Miller, C. B.; Nelson, D. M.; Guillard, R. L.; Woodward, B. L. *Biol. Bull. Mar. Biol. Lab.* **1980**, *159*, 349.
- (56) Miller, C. B.; Nelson, D. M.; Weiss, C.; Soeldner, A. H. *Mar. Biol.* **1990**, *106*, 91.
- (57) Williams, A.; Cusack, M.; Buckman, J. O.; Stachel, T. *Science* **1998**, *279*, 2094.
- (58) Prado Figueroa, M.; Barrera, F.; Cesaretti, N. N. Si⁴⁺ and Chalcedony Precipitation During Oxidative Stress in Rajidae Electrocyte: A Mineralogical Study. Presented at the 41st Annual Meeting. Argentine Society for Biochemistry and Molecular Biology Research, Pinamar, Argentina; 2005.
- (59) Prado Figueroa, M.; Sanchez, J.; Cesaretti, N. N. Chalcedony (incipient fossilization process) in Human Brain Cortex and Cerebellum from Aged Patients. Presented at the 42th Annual Meeting, Argentine Society for Biochemistry and Molecular Biology Research, Rosario, Santa Fe, Argentina, 2006.
- (60) Prado Figueroa, M.; Barrera, F.; Cesaretti, N. N. *Micron* **2007**, *39*, 1027.
- (61) Legendre, A. M. *J. Am. Vet. Med. Assoc.* **1976**, *168*, 418.
- (62) Baily, C. B. *Invest. Urol.* **1972**, *10*, 178.
- (63) Hidaka, S.; Okamoto, Y.; Oga, Y.; Hirose, T.; Abe, K. *Arch. Oral. Biol.* **1994**, *39*, 595.
- (64) Mehard, C. W.; Volcani, B. E. *Cell. Tiss. Res.* **1976**, *174*, 315.
- (65) Policard, A.; Collet, A.; Daniel-Moussard, H.; Pregermain, S. *J. Biophys. Biochem. Cytol.* **1961**, *9*, 236.
- (66) Prado Figueroa, M.; Flores, L.; Sanchez, J.; Cesaretti, N. N. *Micron* **2008**, *39*, 859.
- (67) Levison, D. A.; Crocker, P. R.; Banim, S.; Wallace, D. M. A. *Lancet* **1982**, *1* (8274), 704.
- (68) Jokes, A. M.; Rose, A. G.; Sutor, J. *Br. Med. J.* **1973**, *1*, 146.
- (69) Prado Figueroa, M.; Casavilca, S. Tumores Malignos de la Glia: Formación de Calcedonia (silice cristalina) y Posible Rol de la Anhidrasa Carbonica. VI Encuentro Científico Internacional de Invierno. ECI 2007i. <http://www.cienciaperu.org/eci2007i/Libroderesumen.es>. July 2007, Lima, Peru.
- (70) Rogerson, A.; DeFraitas, A. S. W.; McInnes, A. G. *J. Phycol.* **2008**, *22*, 56.
- (71) Bhatt, T. M.; Coombs, M.; O'Neil, C. *Int. J. Cancer.* **1984**, *34*, 519.
- (72) Hodson, M. J.; Sangster, A. G.; Parry, D. W. *Ann. Bot.* **1982**, *50*, 843.
- (73) Motomura, H.; Fujii, T.; Suzuki, M. *Ann. Bot.* **2006**, *97*, 513.
- (74) Sangster, A. G. *Ann. Bot.* **1970**, *34*, 557.
- (75) Judd, J. W. *Nature* **1887**, *35*, 396.
- (76) Sangster, A. G. *Am. J. Bot.* **1978**, *65*, 929.
- (77) Bovee, E. C. Distribution and Forms of Siliceous Structures Among Protozoa. In *Silicon and Siliceous Structures in Biological Systems*; Simpson, T., Volcani, B. E., Eds.; Springer-Verlag: New York, 1981.
- (78) Gooday, A. J.; Esteban, G. F.; Clarke, K. J. *J. Mar. Biol. Assoc. UK* **2006**, *86*, 679.
- (79) Esteban, G. F.; Gooday, A. J.; Clarke, K. J. *Polar Biol.* **2007**, *30*, 945.
- (80) Fourcade, E.; Mendez, J.; Azema, J.; Cros, P.; De Wever, P.; Duthou, J. L.; Romero, J. E.; Michaud, F. C. *R. Acad. Sci., Ser. IIA: Sci. Terre et des Planetes* **1994**, *318*, 527.
- (81) Kröger, N.; Deutzmann, R.; Bergsdorf, C.; Sumper, M. *Proc. Natl. Acad. Sci. U.S.A.* **2000**, *97*, 14133.
- (82) Kröger, N.; Lorenz, S.; Brunner, E.; Sumper, M. *Science* **2002**, *298*, 584.
- (83) Kröger, N.; Poulsen, N. *Annu. Rev. Genet.* **2008**, *42*, 83.
- (84) Sumper, M.; Brunner, E. *Adv. Funct. Mater.* **2006**, *16*, 17.
- (85) Sumper, M.; Brunner, E. *ChemBioChem* **2008**, *9*, 1187.
- (86) Anderson, O. R.; Perry, C. C.; Hughes, N. P. *Phil. Trans. R. Soc. London, Ser. B: Biol. Sci.* **1990**, *329*, 81.
- (87) Douglas, M. S. V.; Smol, J. P. *Hydrobiologia* **1987**, *154*, 13.
- (88) Douglas, M. S. V.; Smol, J. P. *Verh. Int. Ver. Limnol.* **1988**, *23*, 855.
- (89) Aoki, Y.; Hoshino, M.; Matsubara, T. *Geoderma* **2007**, *142*, 29.
- (90) Cavalier-Smith, T.; von der Heyden, S. *Mol. Phylogenet. Evol.* **2007**, *44*, 1186.
- (91) Gaponova, L. P.; Dovgal, I. P. *Vestn. Zool.* **2008**, *42*, e-79.
- (92) Leadbeater, B. S. C.; Henouil, M.; Berovic, N. *Protist* **2008**, *159*, 495.
- (93) Leadbeater, B. S. C. *Protoplasma* **1975**, *83*, 111.
- (94) Leadbeater, B. S. C. *Proc. R. Soc. London Biol.* **1979**, *204*, 57.
- (95) Leadbeater, B. S. C. *Eur. J. Protistol.* **1994**, *30*, 111.
- (96) Manton, I.; Bremer, G.; Oates, K. *Proc. R. Soc. London Biol.* **1981**, *213*, 15.
- (97) Leadbeater, B. S. C.; Morton, C. *Arch. Microbiol.* **1974**, *95*, 279.
- (98) Nichols, S.; Wörheide, G. *Integr. Comp. Biol.* **2005**, *45*, 333.
- (99) Hooper, J. A.; van Soest, R. W. M. *Systema Porifera: A guide to the classification of sponges*; Kluwer Academic/Plenum Publishers: New York, 2002; p 469.
- (100) Bergquist, P. R. *Sponges*; Hutchinson & Co.: London, 1978; p 268.
- (101) Tabachnick, K. R.; Reiswig, H. M. Dictionary of Hexactinellida. In *Systema Porifera: a guide to the classification of sponges*. Hooper, J. N. A., van Soest, R. W. M., Eds.; Kluwer Academic/Plenum: New York, 2002; p 1224.
- (102) Maldonado, M.; Carmona, M.; Velásquez, Z.; Puig, A.; Cruzado, A.; López, A.; Young, C. M. *Limnol. Oceanogr.* **2005**, *50*, 799.
- (103) Dayton, P. K.; Robilliard, G. A.; Paine, R. T.; Dayton, L. B. *Ecol. Monogr.* **1974**, *44*, 105.
- (104) Dayton, P. K. Observations of growth, dispersal and population dynamics of some sponges in McMurdo Sound, Antarctica. In *Colloques internationaux du C.N.R.S. 291. Biologie des spongiaires*; Lévi, C., Boury-Esnault, N., Eds.; Centre National de la Recherche Scientifique: Paris, 1979; p 271.
- (105) Gatti, S. *Bollettino Musei Inst. Biol., Univ. Genoa* **2002**, *66–67*, 76.
- (106) Koltun, V. M. *Symp. Zool. Soc. London* **1970**, *25*, 285.
- (107) Ehrlich, H.; Koutsoukos, P. G.; Demadis, K. D.; Pokrovsky, O. *Micron* **2008**, *39*, 1062.
- (108) Krautter, M.; Conway, K. W.; Barrie, J. V.; Neuweiler, M. *Facies* **2001**, *44*, 265.
- (109) Conway, K. W.; Barrie, J. V.; Krautter, M. *Neues Jahrb. Geol. Palaeontol., Monatsch.* **2004**, *6*, 335.
- (110) Conway, K. W.; Krautter, M.; Barrie, J. V.; Whitney, F.; Thomson, R. E.; Reiswig, H.; Lehnert, H.; Mungov, G.; Bertram, M. Sponge reefs in the Queen Charlotte Basin, Canada: controls on distribution, growth and development. In *Cold water Corals and Ecosystems*; Freiwald, A., Roberts, J. M., Eds.; Springer-Verlag: Berlin, 2005; p 601.
- (111) Krautter, M.; Conway, K. W.; Barrie, J. V. *J. Paleontol.* **2006**, *80*, 38.
- (112) Conway, K. W.; Krautter, M.; Barrie, J. V.; Neuweiler, M. *Geosci. Can.* **2001**, *28*, 71.
- (113) Lehnert, H.; Conway, K. W.; Barrie, J. V.; Krautter, M. *Contrib. Zool.* **2005**, *74*, 265.
- (114) Carlisle, E. M. *Nutr. Rev.* **1982**, *40*, 193.

- (115) Lipworth, E.; Bloomberg, B. M.; Reid, F. P. *S. Afr. Med. J.* **1964**, *52*, 50.
- (116) Medina, J. A.; Sanchidrian, J. R.; Delatte, L. C. Silica in urinary calculi. In *Urolithiasis, Clinical and Basic Research*; Smith, L. L., Robertson, W. G., Finlayson, B., Eds; Plenum Press: New York, 1981; p 923.
- (117) Keeler, R. F. *Ann. N.Y. Acad. Sci.* **1963**, *104*, 592.
- (118) Herman, J. R.; Goldberg, A. S. *J. Am. Med. Assoc.* **1960**, *174*, 1206.
- (119) Haddad, F. S.; Kouyoumdjian, A. *Urol. Int.* **1986**, *41*, 70.
- (120) Daudon, M.; Hennequin, C.; Lacour, B.; Le Moel, G.; Donsimoni, R.; Fellahi, S.; Paris, M.; Troupel, S. *Urol. Res.* **1995**, *23*, 319.
- (121) Kim, K. M.; David, R.; Johnson, F. B. *Urol. Res.* **1983**, *11*, 155.
- (122) Lagergren, C. *J. Urol.* **1962**, *87*, 994.
- (123) Farrer, J. H.; Rajfer, J. *J. Urol.* **1984**, *132*, 739.
- (124) Lee, M. H.; Lee, Y. H.; Hsu, T. H.; Chen, M. T.; Chang, L. S. *Scand. J. Urol. Nephrol.* **1993**, *27*, 267.
- (125) Ichiyanagi, O.; Sasagawa, I.; Adachi, Y.; Suzuki, H.; Kubota, Y.; Nakada, T. *Urol. Int.* **1998**, *61*, 39.
- (126) Page, R. C.; Heffner, R. R.; Frey, A. *Am. J. Dig. Dis.* **1941**, *8*, 13.
- (127) Takemoto, M.; Itatani, I.; Kinoshita, K.; Yachiku, S. *Jpn. Urol. Assoc. J.* **1978**, *69*, 664.
- (128) Osborne, C. A.; Hammer, R. F.; Klausner, J. S. *Am. J. Vet. Med. Assoc.* **1981**, *178*, 809.
- (129) Bailey, C. B. *Biochem. Cell Biol.* **1972**, *50*, 305.
- (130) Gadd, G. M. *Mycologist* **2004**, *18*, 60.
- (131) Leopold, L. B.; Wolman, M. G.; Miller, G. P. *Fluvial Processes in Geomorphology*; W.H. Freeman & Co.: San Francisco, CA, 1964.
- (132) Siever, R. *Am. Mineral.* **1957**, *42*, 821.
- (133) Sauer, D.; Saccone, L.; Conley, D. J.; Herrmann, L.; Sommer, M. *Biogeochemistry* **2006**, *80*, 89.
- (134) Ehrlich, H. L. Geomicrobiology of Iron. In *Geomicrobiology*, 2nd ed.; Ehrlich, H. L., Ed.; Marcel Dekker: New York, 1990; p 283.
- (135) Bennett, P. C.; Rogers, J. R.; Choi, W. J.; Hiebert, F. K. *Geomicrobiol. J.* **2001**, *18*, 3.
- (136) Bonneville, S.; Smits, M. M.; Brown, A.; Harrington, J.; Leake, J. R.; Brydson, R.; Benning, L. G. *Geology* **2009**, *37*, 615.
- (137) Friedrich, S.; Platonova, N. P.; Karavaiko, G. I.; Glombitza, F. *Acta Biotechnol.* **1991**, *11*, 187.
- (138) Lauwers, A. M.; Heinen, W. *Arch. Microbiol.* **1974**, *95*, 67.
- (139) Clarke, J. *Earth-Sci. Rev.* **2003**, *60*, 175.
- (140) Sommer, M.; Kaczorek, D.; Kuzyakov, Y.; Breuer, J. *J. Plant Nutr. Soil Sci.* **2006**, *169*, 310.
- (141) Alexandre, A.; Meunier, J. D.; Colin, F.; Koud, J. M. *Geochim. Cosmochim. Acta* **1997**, *61*, 677.
- (142) Bansal, V.; Achmad, A.; Sastry, M. *J. Am. Chem. Soc.* **2006**, *128*, 14059.
- (143) Bidle, K. D.; Azam, F. *Limnol. Oceanogr.* **2001**, *46*, 1606.
- (144) Patrick, S.; Holding, A. J. *J. Appl. Bacteriol.* **1985**, *59*, 7.
- (145) Tréguer, P.; Nelson, D. M.; Bennekom, A. J. V.; Demaster, D. J.; Laynaert, A.; Quéguiner, B. *Science* **1995**, *268*, 375.
- (146) Wainwright, M.; Al-Wajeeh, K.; Wickramasinghe, N. C.; Narlikar, J. V. *Int. J. Astrobiol.* **2003**, *2*, 227.
- (147) Tajima, M. *Nippon Jibiinkoka Gakkai Kaiho* **1992**, *95*, 630.
- (148) Chakraborty, A. N.; Das, S.; Mukherjee, K.; Dastidar, S. G.; Sen, D. K. *Indian J. Exp. Biol.* **1988**, *26*, 839.
- (149) Das, S.; Chattopadhyay, U. K. *Indian J. Tuberc.* **2000**, *47*, 87.
- (150) Ehrlich, H. L. *Chem. Geol.* **1996**, *132*, 5.
- (151) Savostin, P. Z. *Pflanz. Boden.* **1972**, *1*, 37.
- (152) Vernadsky, V. I. *Essays on Geochemistry*; Selected Works, Vol. 1 (Izd. AN SSSR); Publishing House of the Academy of Sciences of the USSR: Moscow, 1954 (in Russian).
- (153) Brussoff, A. *Arch. Mikrob.* **1933**, *4*, 1.
- (154) Fessenden, R. J.; Fessenden, J. S. *Adv. Drug. Res.* **1967**, *4*, 95.
- (155) Webley, D. M.; Duff, R. B.; Mitchell, W. A. *Nature* **1960**, *188*, 766.
- (156) Dopson, M.; Halinen, A. K.; Rahunen, N.; Boström, D.; Sundkvist, J. E.; Riekkola-Vanhanen, M.; Kaksonen, A. H.; Puhakka, J. A. *Biotechnol. Bioeng.* **2008**, *99*, 811.
- (157) Dopson, M.; Lövgren, L.; Boström, D. *Hydrometallurgy* **2009**, *96*, 288.
- (158) Heinen, W. *Arch. Mikrob.* **1960**, *37*, 199.
- (159) Heinen, W. *Arch. Mikrob.* **1965**, *52*, 49.
- (160) Oberlies, F.; Pohlmann, G. *Naturwissenschaften* **1958**, *45*, 487.
- (161) Duff, R. B.; Webley, D. M.; Scott, R. O. *Soil Sci.* **1963**, *95*, 105.
- (162) Malinovskaya, I. M.; Kosenko, L. V.; Votselko, S. K.; Podgorskii, V. S. *Mikrobiologiya (Engl. Transl.)* **1990**, *59*, 49.
- (163) Brehm, U.; Gorbushina, A.; Mottershead, D. *Palaeogeogr., Palaeoclimatol., Palaeoecol.* **2005**, *219*, 117.
- (164) Groudev, S. N. *Acta. Biotechnol.* **1987**, *7*, 299.
- (165) Cvetcovic, O.; Vrvic, M. M.; Dragutinovic, V.; Vitorovic, D. *Mikrobiologija (Beograd)* **2006**, *43*, 41.
- (166) Vrvic, M. M.; Matic, V.; Vucetic, J.; Vitorovic, D. *Adv. Org. Geochem.* **1989**, *16*, 1203.
- (167) Pokrovsky, O. S.; Shirokova, L. S.; Bénézeth, P.; Schott, J.; Golubev, S. V. *Am. J. Sci.* **2009**, *309*, 731.
- (168) Heinen, W.; Lauwers, A. M. *Microbiol. Ecol.* **1988**, *15*, 135.
- (169) Mohanty, B. K.; Ghosh, S.; Mishra, A. K. *J. Appl. Bacteriol.* **1990**, *68*, 55.
- (170) Singh, S.; Bhatta, U. M.; Satyam, P. V.; Dhawan, A.; Sastry, M.; Prasad, B. L. V. *J. Mater. Chem.* **2008**, *18*, 2601.
- (171) Gadd, G. M. *Mycol. Res.* **2007**, *111*, 3.
- (172) DREWELLO, R.; WEISSSMANN, R. *Appl. Microbiol. Biotechnol.* **1997**, *47*, 337.
- (173) Krumbein, W. E.; Gorbushina, A. A.; Rudolph, C.; Urzi, C. Biological investigations on the question of organic and inorganic eutrophication induced biocorrosions and biogenic deposits on late medieval church windows of the cathedral of Tours and St. Katharina in Oppenheim. In *Gemeinsames Erbe gemeinsam erhalten. 1. Statuskolloquium des deutsch-französischen Forschungsprogramms zur Erhaltung von Baudenkmälern*; Welk, S., Ed.; Secretariat General Champs-sur-Marne: Karlsruhe, Germany, p 269.
- (174) Bansal, V.; Sanyal, A.; Rautaray, D.; Ahmad, A.; Sastry, M. *Adv. Mater.* **2005**, *17*, 889.
- (175) Bennett, P. C. *Geochim. Cosmochim. Acta* **1991**, *55*, 1781.
- (176) Greenwood, J. E.; Truesdale, V. W.; Rendell, A. R. *Aquat. Geochem.* **2005**, *11*, 1.
- (177) Kidder, D. L.; Erwin, D. H. *J. Geol.* **2001**, *109*, 509.
- (178) Penna, A.; Magnani, M.; Fenoglio, I.; Fubini, B.; Cerrano, C.; Giovine, M.; Bavestrello, G. *Aquat. Microb. Ecol.* **2003**, *32*, 299.
- (179) Jorgensen, C. B. *Det. Kgl. Dan. Vidensk. Selsk., Biol. Medd.* **1944**, *7*, 1.
- (180) Cattaneo-Vietti, R.; Bavestrello, G.; Cerrano, C.; Chiantore, M. C.; Cortesogno, L.; Gaggero, L. *Period. Mineral.* **2004**, *73*, 141.
- (181) Bavestrello, G.; Arillo, A.; Banatti, U.; Cerrano, C.; Cattaneo-Vietti, R.; Cortesogno, L.; Gaggero, L.; Giovine, M.; Tonetti, M.; Sara, M. *Nature* **1995**, *378*, 374.
- (182) Fenoglio, I.; Martra, G.; Coluccia, S.; Fubini, B. *Chem. Res. Toxicol.* **2000**, *27*, 971.
- (183) Bavestrello, G.; Benatti, U.; Cattaneo-Vietti, R.; Cerrano, C.; Giovine, M. *Microsc. Res. Tech.* **2003**, *62*, 327.
- (184) Bavestrello, G.; Bonito, M.; Sara, M. *Sci. Mar.* **1993**, *57*, 421.
- (185) Estevez, M.; Vargas, S.; Castañó, V. M.; Rodríguez, R. *J. Non-Cryst. Solids* **2009**, *355*, 844.
- (186) Thomas, M. V.; Puleo, D. A.; Al-Sabbagh, M. J. *Long-Term Eff. Med. Implants* **2005**, *15*, 585.
- (187) Vigliani, E. C.; Pernis, B. *Adv. Tuberc. Res.* **1963**, *12*, 230.
- (188) Skinner, H. C.; Berger, A. R. *Geology and Health: Closing the Gap*; Oxford University Press: Oxford, U.K., 2003; p 179.
- (189) Saffiotti, U. *Acta Biomed.* **2005**, *2*, 30.
- (190) Green, F. H. Y.; Vallyathan, V.; Fletcher, F.; Hahn, F. F. *Toxicol. Pathol.* **2007**, *35*, 136.
- (191) Gilberti, R. M.; Joshi, G. N.; Knecht, D. A. *Am. J. Respir. Cell Mol. Biol.* **2008**, *39*, 619.
- (192) International Agency for Research on Cancer Evaluation of Carcinogenic Risks to Humans. *Silica, some silicates, coal dust, and para-aramid fibrils*; IARC Publications: Lyon, France, 1997; Vol. 68.
- (193) Pernis, B. *Acta Biomed.* **2005**, *2*, 38.
- (194) Mills, R. *Am. J. Hyg.* **1931**, *XIII*, 224.
- (195) Reffitt, D. M.; Ogston, M.; Powel, J. J.; Hampson, G. N. *Bone* **2003**, *32*, 127.
- (196) Hamilton, R. F., Jr.; Thakur, S. A.; Holian, A. *Free Radical Biol. Med.* **2008**, *44*, 1246.
- (197) Fubini, B.; Otero Arean, C. *Chem. Soc. Rev.* **1999**, *28*, 373.
- (198) Saffiotti, U.; Daniel, L. N.; Mao, Y.; Williams, A. O.; Kaighn, M. E.; Ahmed, N.; Knapton, A. D. *Rev. Mineral.* **1993**, *28*, 523.
- (199) Saffiotti, U.; Shubik, P. *Natl. Cancer Inst. Monogr.* **1963**, *14*, 489.
- (200) Stayton, I.; Winiarz, J.; Shannon, K.; Ma, Y. *Anal. Bioanal. Chem.* **2009**, *394*, 1595.
- (201) Conrad, C. F.; Yasuhara, H.; Bandstra, J. Z.; Icopini, G. A.; Brantley, S. L.; Heaney, P. J. *Geochim. Cosmochim. Acta* **2007**, *71*, 531.
- (202) Berridge, M. J. *Nature* **1993**, *361*, 315.
- (203) Prado Figueroa, M.; Barrera, F.; Cesaretti, N. N. *Micron* **2008**, *39*, 1027.
- (204) Schröder, H. C.; Krasko, A.; Le Pennec, G.; Adell, T.; Wiens, M.; Hassanein, H.; Müller, I. M.; Müller, W. E. G. *Prog. Mol. Subcell. Biol.* **2003**, *33*, 250.
- (205) Krasko, A.; Batel, R.; Schöder, H. C.; Müller, I. M.; Müller, W. E. G. *Eur. J. Biochem.* **2000**, *267*, 4878.
- (206) Schröder, H. C.; Krasko, A.; Batel, R.; Skorokhod, A.; Pähler, S.; Kruse, M.; Müller, I. M.; Müller, W. E. G. *FASEB J.* **2000**, *14*, 2022.
- (207) Müller, W. E. G.; Boreiko, A.; Wang, X.; Belikov, S. I.; Wiens, M.; Grebenjuk, V. A.; Schloßmacher, U.; Schröder, H. C. *Gene* **2007**, *395*, 62.
- (208) Hazelaar, S. J.; van der Strate, H. J.; Gieskes, W. W. C.; Vrieling, E. G.; Hildebrand, M. *Thalassiosira pseudonana's* ferredoxin-NADP reductase: a homologue of carbonic anhydrase and sponge silicase

- lacking action on solid silica. In Hazelaar, S. Nanoscale architecture; the role of proteins in diatom silicon biomineralization. PhD Thesis, University of Groningen, The Netherlands, 2006.
- (209) Xiao, Y.; Lasaga, A. C. *Geochim. Cosmochim. Acta* **1996**, *60*, 2283.
- (210) Nangia, S.; Garrison, B. J. *J. Phys. Chem. A* **2008**, *112*, 2027.
- (211) Hiemstra, T.; Van Riemsdijk, W. H. J. *Colloid Interface Sci.* **1990**, *136*, 132.
- (212) Cadore, E. Mécanismes de dissolution du quartz dans les solutions naturelles. Etude expérimentale et modélisation. PhD Dissertation; Université Paul Sabatier, Toulouse, France, 1995.
- (213) Pokrovsky, O. S.; Golubev, S. V.; Mielczarski, J. A. *J. Colloid Interface Sci.* **2006**, *296*, 189.
- (214) Mielczarski, J. A.; Pokrovsky, O. S. In: *Surface Complexation Modelling*; Lutzenkirchen, J., Ed.; Interface Science and Technology, Vol. 11; Academic Press: London, 2006; p 397.
- (215) Schott, J.; Pokrovsky, O. S.; Oelkers, E. H. The Link Between Mineral Dissolution/Precipitation Kinetics and Solution Chemistry. In *Reviews in Mineralogy & Geochemistry, Thermodynamics and Kinetics of Water-Rock Interaction*; Oelkers, E. H., Schott, J., Eds; Mineralogical Society of America: St. Louis, MO, 2009; Vol. 70, p 207.
- (216) Dove, P.-M. *Rev. Mineral.* **1996**, *31*, 235.
- (217) Duval, Y.; Mielczarski, J. A.; Pokrovsky, O. S.; Mielczarski, E.; Ehrhardt, J. J. *J. Phys. Chem. B* **2002**, *106*, 2937.
- (218) Nangia, S.; Garrison, B. J. *J. Am. Chem. Soc.* **2009**, *131*, 9538–9546.
- (219) Okunev, A. G.; Shaurman, S. A.; Danilyuk, A. F.; Aristov, Y. I.; Bergeret, G.; Renouprez, A. *J. Non-Cryst. Solids* **1999**, *260*, 21.
- (220) Okunev, A. G.; Shmakov, A. N.; Danilyuk, A. F.; Aristov, Y. I. *Nucl. Instrum. Methods Phys. Res. A* **2000**, *448*, 261.
- (221) Niibori, Y.; Kunita, M.; Tochiyama, O.; Chida, T. *J. Nucl. Sci. Technol.* **2000**, *37*, 349.
- (222) Jendoubi, F.; Mgaidi, A.; El Maaoui, M. *Can. J. Chem. Eng.* **1998**, *76*, 233.
- (223) Bickmore, B. R.; Nagy, K. L.; Gray, A. K.; Brinkerhoff, A. R. *Geochim. Cosmochim. Acta* **2006**, *70*, 290.
- (224) Icenhower, P. M.; Dove, C. *Geochim. Cosmochim. Acta* **2000**, *64*, 4193.
- (225) Dove, P. M.; Han, N.; Wallace, A. F.; De Yoreo, J. J. *Proc. Natl. Acad. Sci. U.S.A.* **2008**, *105*, 9903.
- (226) Van Cappellen, P.; Qiu, L. *Deep-Sea Res. II* **1997**, *44*, 1109.
- (227) Van Cappellen, P.; Qiu, L. *Deep-Sea Res. II* **1997**, *44*, 1129.
- (228) Grambow, B. *Mater. Res. Soc. Symp. Proc.* **1985**, *44*, 15.
- (229) Vernaz, E. Y.; Dussossoy, J. L. *Appl. Geochem.* **1992**, *7* (suppl.1), 13.
- (230) Blesa, M. A.; Weisz, A. D.; Morando, P. J.; Salfity, J. A.; Magaz, G. E.; Regazzoni, A. E. *Coord. Chem. Rev.* **2000**, *196*, 31.
- (231) Rimer, J. D.; Trofymuk, O.; Navrotsky, A.; Lobo, R. F.; Vlachos, D. G. *Chem. Mater.* **2007**, *19*, 4189.
- (232) Goworek, J.; Borówka, A.; Kusak, R. *Colloids Surf. A* **1999**, *157*, 127.
- (233) Evans, D. F.; Parr, J.; Wong, C. Y. *Polyhedron* **1992**, *11*, 567.
- (234) Marley, N. A.; Bennett, P.; Janecky, D. R.; Gaffney, J. S. *Org. Geochem.* **1989**, *14*, 525.
- (235) Mizutani, T.; Takahashi, K.; Kato, T.; Yammamoto, J.; Ueda, N.; Nakashima, R. *Bull. Chem. Soc. Jpn.* **1993**, *66*, 3802.
- (236) Swanson, K. A. The Effect of Dissolved Catechol on the Dissolution of Amorphous Silica in Seawater. PhD Thesis, Pennsylvania State University, 1988.
- (237) Demadis, K. D. *Chem. Process.* **2003**, *66*, 29.
- (238) Demadis, K. D.; Katarachia, S. D. *Phosphorus, Sulfur Silicon* **2004**, *179*, 627.
- (239) Demadis, K. D. Combating Heat Exchanger Fouling and Corrosion Phenomena in Process Waters. In *Compact Heat Exchangers and Enhancement Technology for the Process Industries*; Shah, R. K., Ed.; Begell House Inc.: New York, 2003; p 483.
- (240) Frenier, W. *Technology for Chemical Cleaning of Industrial Equipment*; NACE: Houston, TX, 2000.
- (241) Jendoubi, F.; Mgaidi, A.; El Maaoui, M. *Can. J. Chem. Eng.* **1997**, *75*, 721.
- (242) Demadis, K. D.; Mavredaki, E. *Environ. Chem. Lett.* **2005**, *3*, 127.
- (243) Mavredaki, E.; Neofotistou, E.; Demadis, K. D. *Ind. Eng. Chem. Res.* **2005**, *44*, 7019.
- (244) Coradin, T.; Lopez, P. J.; Gautier, C.; Livage, J. C. *R. Palevol.* **2004**, *3*, 443.
- (245) Xiao, Y.; Lasaga, A. *Geochim. Cosmochim. Acta* **1994**, *58*, 5379.
- (246) Patwardhan, S. V.; Clarkson, S. J. *Silicon Chem.* **2002**, *1*, 207.
- (247) Patwardhan, S. V.; Clarkson, S. J. *Mater. Sci. Eng., C* **2003**, *23*, 495.
- (248) Ranganathan, S.; Rao, C. C.; Vudayagiri, S. D.; Rajesh, Y. B. R. D.; Jagadeesh, B. *J. Chem. Sci.* **2004**, *116*, 169.
- (249) Golubev, S. V.; Bauer, A.; Pokrovsky, O. S. *Geochim. Cosmochim. Acta* **2006**, *70*, 4436.
- (250) Golubev, S. V.; Pokrovsky, O. S. *Chem. Geol.* **2006**, *235*, 377.
- (251) Pokrovsky, O. S.; Schott, J.; Castillo, A. *Geochim. Cosmochim. Acta* **2005**, *69*, 905.
- (252) Pokrovsky, O. S.; Schott, J. *Am. J. Sci.* **2001**, *301*, 597.
- (253) Pokrovsky, G. S.; Schott, J. *Geochim. Cosmochim. Acta* **1998**, *62*, 3413.
- (254) Simkiss, K.; Wilbur, K. M. *Biomineralization. Cell Biology and Mineral Deposition*; Academic Press: San Diego, CA, 1989.
- (255) Smetacek, V. *Protist* **1999**, *150*, 25.
- (256) Harper, H. E., Jr.; Knoll, A. H. *Geology* **1975**, *3*, 175.
- (257) Raven, J. A.; Waite, A. M. *New Phytol.* **2004**, *162*, 45.
- (258) Simpson, T. L.; Volcani, B. E., *Silicon and Siliceous Structures in Biology Systems*; Springer-Verlag: New York, 1981.
- (259) Siever, R. Silica in the Oceans: Biological-Geochemical Interplay. In *Scientists on Gaia*; Schneider, S. H., Boston, P. J., Eds.; MIT Press: Cambridge, MA, 1991; p 287.
- (260) Milligan, A. J.; Morel, F. M. M. *Science* **2002**, *297*, 1848.
- (261) Pondaven, P.; Gallinari, M.; Chollet, S.; Bucciarelli, E.; Sarthou, G.; Schultes, S.; Jean, F. *Protist* **2007**, *158*, 21.
- (262) Volcani, B. E. Cell Wall Formation in Diatoms. In *Silicon and siliceous structures in biological systems*; Simpson, T. L., Volcani, B. E., Eds.; Springer-Verlag: New York, 1981; p 157.
- (263) Perry, C. C.; Keeling-Tucker, T. J. *Biol. Inorg. Chem.* **2000**, *5*, 537.
- (264) Hecky, R. E.; Mopper, K.; Kilham, P.; Degens, E. T. *Mar. Biol.* **1973**, *19*, 323.
- (265) Lobel, K. D.; West, J. K.; Hench, L. L. *Mar. Biol.* **1996**, *126*, 353.
- (266) Frigeri, L. G.; Radabaugh, T. R.; Haynes, P. A.; Hildebrand, M. *Mol. Cell. Proteomics* **2006**, *5*, 182.
- (267) Vrieling, E. G.; Beelen, T. P. M.; Gieskes, W. W. J. *Phycol.* **1999**, *35*, 548.
- (268) Vrieling, E. G.; Poort, L.; Beelen, T. P. M.; Gieskes, W. W. C. *Eur. J. Phycol.* **1999**, *34*, 307.
- (269) Sumper, M. *Science* **2002**, *295*, 2430.
- (270) Pohnert, G. *Angew. Chem., Int. Ed.* **2002**, *41*, 3167.
- (271) Sumper, M.; Kröger, N. *J. Mater. Chem.* **2004**, *14*, 2059.
- (272) Sumper, M. *Science* **2007**, *295*, 2430.
- (273) Armbrust, E. V. *Nature* **2009**, *459*, 185.
- (274) Zurzolo, C. C.; Bowler, C. C. *Plant Physiol.* **2001**, *127*, 1339.
- (275) Bertermann, R.; Kröger, N.; Tacke, R. *Anal. Bioanal. Chem.* **2003**, *375*, 630.
- (276) Gendron-Badou, A.; Coradin, T.; Maquet, J.; Fröhlich, F.; Livage, J. J. *Non-Cryst. Solids* **2003**, *316*, 331.
- (277) Freitas, J. C. C.; Emmerich, F. G.; Bonagamba, T. J. *Chem. Mater.* **2000**, *12*, 711.
- (278) Kinrade, S. D.; Del Nin, J. W.; Schach, A. S.; Sloan, T. A.; Wilson, K. L.; Knight, C. T. G. *Science* **1999**, *285*, 1542.
- (279) Kinrade, S. D.; Hamilton, R. J.; Schach, A. S.; Knight, C. T. G. *J. Chem. Soc., Dalton Trans.* **2001**, 961.
- (280) Kinrade, S. D.; Gillson, A. M. E.; Knight, C. T. G. *J. Chem. Soc., Dalton Trans.* **2002**, 307.
- (281) Kubicki, J. D.; Heaney, P. J. *Geochim. Cosmochim. Acta* **2003**, *67*, 4113.
- (282) Sahai, N. *Geochim. Cosmochim. Acta* **2004**, *68*, 227.
- (283) Conley, D. J.; Kilham, S. S.; Theriot, E. *Limnol. Oceanogr.* **1989**, *34*, 205.
- (284) Gélabert, A.; Pokrovsky, O. S.; Schott, J.; Boudou, A.; Feurtet-Mazel, A.; Mielczarski, J.; Mielczarski, E.; Mesmer-Dudons, N.; Spalla, O. *Geochim. Cosmochim. Acta* **2004**, *68*, 4039.
- (285) Noll, F.; Sumper, M.; Hampp, N. *Nano Lett.* **2002**, *2*, 91.
- (286) Vrieling, E. G.; Beelen, T. P. M.; van Santen, R. A.; Gieskes, W. W. C. *J. Phycol.* **2000**, *36*, 146.
- (287) Kates, M.; Volcani, B. E. Z. *Pflanzenphysiol.* **1968**, *60*, 19.
- (288) Swift, D. M.; Wheeler, A. P. *J. Phycol.* **1992**, *28*, 202.
- (289) Kröger, N.; Bergsdorf, C.; Sumper, M. *EMBO J.* **1994**, *13*, 4676.
- (290) Dufrière, Y. F.; Rouxhet, P. G. *Colloids Surf. B* **1996**, *7*, 271.
- (291) Dufrière, Y.; van der Wal, A.; Rouxhet, P. G. *J. Bacteriol.* **1997**, *179*, 1.
- (292) Ragueneau, O.; Tréguer, P.; Leynaert, A.; Anderson, R. F.; Brzezinski, M. A. *Global Planet. Change* **2000**, *26*, 317.
- (293) Kamatani, A. *Mar. Biol.* **1982**, *68*, 91.
- (294) Kamatani, A.; Riley, J. P. *Mar. Biol.* **1979**, *55*, 29.
- (295) Kamatani, A.; Riley, J. P.; Skirrow, G. *J. Jpn. Oceanogr. Soc.* **1980**, *36*, 201.
- (296) Kamatani, A.; Ejiri, N.; Tréguer, P. *Deep-Sea Res.* **1988**, *35*, 1195.
- (297) Rickert, D.; Schlüter, M.; Wallmann, K. *Geochim. Cosmochim. Acta* **2002**, *66*, 439.
- (298) Shemesh, A.; Mortlock, R. A.; Smith, R. J.; Froelich, P. N. *Mar. Chem.* **1988**, *25*, 305.
- (299) Ellwood, M. J.; Hunter, K. A. *Mar. Chem.* **1999**, *66*, 149.
- (300) Singh, R.; Singh, R.; Thakar, M. K. *Indian Internet J. Forensic Med. Toxicol.* **2006**, *4*, 2.
- (301) Lewin, J. C. *Geochim. Cosmochim. Acta* **1961**, *21*, 182.
- (302) Dove, P. M. Kinetic and Thermodynamic Controls on Silica Reactivity in Weathering Environments. In *Chemical Weathering Rates of Silicate Minerals*; White, A. F., Brantley, S. L., Eds.;

- Reviews in Mineralogy, Vol. 31; Mineralogical Society of America: Washington, DC, 1995; p 235.
- (303) Van Cappellen, P.; Qiu, L. *Deep-Sea Res. II* **1997**, *44*, 1129.
- (304) Dixit, S.; Van Cappellen, P.; Van Bennekom, J. A. *Mar. Chem.* **2001**, *73*, 333.
- (305) Dixit, S.; Van Cappellen, P. *Geochim. Cosmochim. Acta* **2002**, *66*, 2559.
- (306) Gehlen, M.; Beck, L.; Calas, G.; Flank, A.-M.; Van Bennekom, A. J.; Van Beusekom, J. E. E. *Geochim. Cosmochim. Acta* **2002**, *66*, 1601.
- (307) Van Bennekom, A. J.; Jansen, F.; Van Der Gaast, S.; Van Iperen, J.; Pieters, J. *Deep-Sea Res.* **1989**, *36*, 173.
- (308) Van Bennekom, A. J.; Buma, A. G. J.; Nolting, R. F. *Mar. Chem.* **1991**, *35*, 423.
- (309) Van Cappellen, P.; Dixit, S.; van Beusekom, J. *Global Biogeochem. Cycles* **2002**, *16*, 1075.
- (310) McManus, J.; Hammond, D. E.; Berelson, W. M.; Kilgore, T. E.; Demaster, D. J.; Ragueneau, O. G.; Collier, R. W. *Deep-Sea Res.* **1995**, *42*, 871.
- (311) Lewin, J.; Reimann, B. E. F. *Annu. Rev. Plant Physiol.* **1969**, *20*, 289.
- (312) Epstein, E. *Proc. Natl. Acad. Sci. U.S.A.* **1994**, *91*, 11.
- (313) Bartoli, F. Le cycle biogéochimique du silicium sur roches acides. Application à deux systèmes forestiers tempérés. Thèse de Doctorat, Université de Nancy I, 1981.
- (314) Piperno, D. R. *Phytolith. An archaeological and geological perspective*; Academic Press: San Diego, CA, 1988.
- (315) Neethirajan, S.; Gordon, R.; Wang, L. *Trends Biotechnol.* **2009**, *27*, 461.
- (316) Richmond, K. E.; Sussman, M. *Curr. Opin. Plant Biol.* **2003**, *6*, 268.
- (317) Epstein, E. *Annu. Rev. Plant Physiol. Plant Mol. Biol.* **1999**, *50*, 641.
- (318) Exley, C. J. *Inorg. Biochem.* **1998**, *69*, 139.
- (319) Motomura, H.; Hikosaka, K.; Suzuki, M. *Ann. Bot.* **2008**, *101*, 463.
- (320) Hodson, M. J.; Parker, A. G.; Leng, M. G.; Sloane, H. J. J. *Q. Sci.* **2008**, *23*, 331.
- (321) Stromberg, C. A. E. *Palaeogeog. Paleoclimatol. Palaeoecol.* **2004**, *207*, 239.
- (322) Bartoli, F.; Wilding, W. P. *Soil Sci. Soc. Am. J.* **1980**, *44*, 873.
- (323) Frayse, F.; Pokrovsky, O. S.; Schott, J.; Meunier, J.-D. *Geochim. Cosmochim. Acta* **2006**, *70*, 1939.
- (324) Stumm, W. *Chemistry of the Solid-Water Interface*; Wiley-Interscience: New York, 1992.
- (325) Guy, C.; Schott, J. *Chem. Geol.* **1989**, *78*, 181.
- (326) Brady, P. V.; Walther, J. V. *Chem. Geol.* **1990**, *82*, 253.
- (327) Schott, J. Modelling of the Dissolution of Strained and Unstrained Multiple Oxides: The Surface Speciation Approach. In *Aquatic chemical kinetics: Reaction rates of processes in natural waters*; Stumm, W., Ed.; John Wiley & Sons: New York, 1990; p 337.
- (328) Frayse, F.; Cantais, F.; Pokrovsky, O. S.; Schott, J.; Meunier, J. D. *J. Explorat. Geochem.* **2006**, *88*, 202.
- (329) Wirth, G. S.; Gieskes, J. M. J. *Colloid Interface Sci.* **1979**, *68*, 492.
- (330) Bartoli, F. *J. Soil Sci.* **1985**, *36*, 335.
- (331) Frayse, F.; Pokrovsky, O. S.; Schott, J.; Meunier, J.-D. *Chem. Geol.* **2009**, *258*, 197.
- (332) Inanaga, S.; Okasaka, A. *Soil Sci. Plant Nutr.* **1995**, *41*, 103.
- (333) Watteau, F.; Villedon, G. *Eur. J. Soil Sci.* **2001**, *52*, 385.
- (334) Watteau, F.; Villedon, G.; Jaafar Ghanbaja, J.; Genet, P.; Pargney, J.-C. *Biol. Cell* **2002**, *94*, 55.
- (335) Coradin, T.; Coupé, A.; Livage, J. *Colloids Surf. B.* **2003**, *29*, 189.
- (336) Frayse, F.; Shirokova, L. S.; Pokrovsky, O. S.; Meunier, J.-D. Release of Organic Carbon, Silica, Major and Trace Elements from Degrading Plant Litter under Microbial Activity in Laboratory Experiments. In *Conference Programme and Abstracts of the 6th International Symposium on Ecosystem Behaviour, BIOGEOMON 2009*; Ukonmaanaho, L.; Nieminen, T. M.; Starr, M., Eds.; Finnish Forest Research Institute: Vantaa, Finland, 2009; p 375.
- (337) Frayse, F.; Pokrovsky, O. S.; Meunier, J.-D. *Geochim. Cosmochim. Acta* **2010**, *74*, 70.
- (338) Scheele, C. W. *Sämtliche physische und chemische Werke. Nach dem Tode des Verfassers gesammelt und in deutscher Sprache herausgegeben von Sigismund Friedrich Hermbstädt*, 2 Vols., Unchanged reprint of the 1793 ed., Niederwalluf: Wiesbaden, Germany, 1971; Vol. 2, pp 3–31 (first publ. 1771).
- (339) Spierings, G. A. C. M. *J. Mater. Sci.* **1991**, *26*, 3329.
- (340) Spierings, G. A. C. M. *J. Mater. Sci.* **1993**, *28*, 6261.
- (341) Judge, J. S. *J. Electrochem. Soc.* **1971**, *118*, 1771.
- (342) Schultze, M. *Die Hyalonemen. Ein Beitrag zur Naturgeschichte der Spongiae*; Adolph Marcus: Bonn, 1860.
- (343) Kölliker, A. *Der Feinere Bau der Protozoen*; Wilhelm Engelmann: Leipzig, 1864.
- (344) Sollas, W. J. In Report on the Scientific Results of the Voyage of H.M.S. Challenger During the Years 1873–76; Published by order of Her Majesty's Government: XLVII-L.; Thomson, W. J., Murray, J., Eds.; London, 1888.
- (345) Vosmajer, G. S. J.; Wijsman, H. P. K. *Akad. Wet.* **1902**, *13*, 15.
- (346) Schmidt, W. J. *Zool. Jahrb., Abt. Anat. Ontog. Tiere* **1926**, *48*, 311.
- (347) Simpson, T. L.; Langenbruch, P. F.; Scalera-Liaci, L. *Zoomorphology* **1985**, *105*, 375.
- (348) Willenz, P. Aspects cinétiques quantitatifs et ultrastructuraux de l'endocytose, la digestion, et l'exocytose chez les sponges, Ph.D. Thesis, Université Libre de Bruxelles, Bruxelles, 1983.
- (349) Cha, J. N.; Shimizu, K.; Zhou, Y.; Christiansen, S. C.; Chmelka, B. F.; Stucky, G. D.; Morse, D. E. *Proc. Natl. Acad. Sci. U.S.A.* **1999**, *96*, 361.
- (350) Travis, D. F.; Francois, C. J.; Bonar, L. C.; Glimcher, M. J. *J. Ultrastruct. Res.* **1967**, *18*, 519.
- (351) Weaver, J. C.; Morse, D. E. *Microsc. Res. Tech.* **2003**, *62*, 356.
- (352) Bütschli, O. Z. *Wiss. Zool.* **1901**, *59*, 235.
- (353) Kono, K.; Yoshida, Y.; Watanabe, M.; Tanioka, Y.; Dote, T.; Orita, Y.; Bescho, Y.; Yoshida, J.; Sumi, Y.; Umehayashi, K. *Arch. Environ. Contam. Toxicol.* **1992**, *22*, 414.
- (354) Croce, G.; Frache, A.; Milanesio, M.; Marchese, L.; Causa, M.; Viterbo, D.; Barbaglia, A.; Bolis, V.; Bavestrello, G.; Cerrano, C.; Benfatti, U.; Pazzolini, M.; Giovine, M.; Armenischi, M. *Biophys. J.* **2004**, *86*, 526.
- (355) Schröder, H. C.; Boreiko, A.; Korzhev, M.; Tahir, M. N.; Tremel, W.; Eckert, C.; Ushijima, H.; Drozdov, A.; Müller, I. M.; Müller, W. E. G. *J. Biol. Chem.* **2006**, *281*, 12001.
- (356) Schiettecatte, D.; Mullie, G.; Depoorter, M. *Acta Chir. Belg.* **2003**, *103*, 375.
- (357) Fuchs, E.; Gilvarg, C. *Anal. Biochem.* **1978**, *90*, 465.
- (358) Shaw, N.; Stead, A. *Biochem. J.* **1974**, *143*, 461.
- (359) Reddy, P. V.; Natarajan, V.; Sastry, P. S. *Chem. Phys. Lipids* **1976**, *17*, 373.
- (360) Jürgens, U. J.; Weckesser, J. *J. Bacteriol.* **1986**, *168*, 568.
- (361) Gubbay, A. D.; Fitzpatrick, R. I. *Aust. N. Z. J. Surg.* **1997**, *67*, 304.
- (362) Conley, D. J. *Mar. Chem.* **1998**, *63*, 39.
- (363) Ehrlich, H.; Ereskovsky, A.; Drozdov, A.; Krylova, D.; Hanke, T.; Meissner, H.; Heinemann, S.; Worch, H. *Russ. J. Mar. Biol.* **2006**, *32*, 186.
- (364) Ferraris, C. F. Alkali-Silica Reaction and High Performance Concrete, NIST Internal Report No. 5742, National Institute of Standards and Technology; USA, 1995.
- (365) Shimizu, K.; Cha, J. N.; Stucky, G. D.; Morse, D. E. *Proc. Natl. Acad. Sci. U.S.A.* **1998**, *95*, 6234.
- (366) Müller, W. E. G. *Silicon Biomineralization: Biology-Biochemistry-Molecular Biology-Biotechnology*; Springer-Verlag: Berlin, 2003.
- (367) Müller, W. E. G.; Rothenberger, M.; Boreiko, A.; Tremel, W.; Reiber, A.; Schröder, H. *Cell Tissue Res.* **2005**, *321*, 285.
- (368) Müller, W. E. G.; Belikov, S. I.; Tremel, W.; Perry, C. C.; Gieskes, W. W. C.; Boreiko, A.; Schröder, H. C. *Micron* **2006**, *37*, 107.
- (369) Saito, Y.; Isobe, T.; Senna, M. *J. Solid State Chem.* **1995**, *120*, 96.
- (370) Leys, S. P.; Mackie, G. O.; Reising, H. M. *Adv. Mar. Biol.* **2007**, *52*, 1.
- (371) Fairhead, M.; Johnson, K. A.; Kowatz, T.; McMahon, S. A.; Carter, L. G.; Oke, M.; Liu, H.; Naismith, J. H.; van der Walle, C. F. *Chem. Commun.* **2008**, 1765.
- (372) Brutchey, R. L.; Morse, D. E. *Chem. Rev.* **2008**, *108*, 4915.
- (373) Ehrlich, H.; Worch, H. Sponges as Natural Composites: From Biomimetic Potential to Development of New Biomaterials. In *Porifera Research: Biodiversity, Innovation & Sustainability*; Custodio, M. R.; Lobo-Hajdu, G.; Hajdu, E.; Muricy, G., Eds.; Museu Nacional: Rio de Janeiro, 2007.
- (374) Tabachnick, K. R. Adaptation of the Hexactinellid Sponges to Deep-sea Life. In *Fossil and Recent Sponges*; Reitner, J., Keupp, H., Eds.; Springer-Verlag: Berlin, 1991.
- (375) Janussen, D.; Tabachnick, K. R.; Tendal, O. S. *Deep-Sea Res. II* **2004**, *51*, 1857.
- (376) Dohrmann, M.; Janussen, D.; Reitner, J.; Collins, A. G.; Wörheide, G. *Syst. Biol.* **2008**, *57*, 388.
- (377) Knoll, A. *Rev. Mineral. Geochem.* **2003**, *54*, 329.
- (378) Ehrlich, H.; Heinemann, S.; Heinemann, C.; Simon, P.; Bazhenov, V.; Shapkin, N.; Born, R.; Tabachnick, K.; Hanke, T.; Worch, H. *J. Nanomater.* **2008**; 623838.
- (379) Ehrlich, H.; Janussen, D.; Simon, P.; Heinemann, S.; Bazhenov, V. V.; Shapkin, N. P.; Mertig, M.; Erler, C.; Born, R.; Worch, H.; Hanke, T. *J. Nanomater.* **2008**; 670235.
- (380) Iijima, M.; Moriwaki, Y. *Calcif. Tissue Int.* **1990**, *47*, 237.
- (381) Ogasawara, W.; Shenton, W.; Davis, S. A.; Mann, S. *Chem. Mater.* **2000**, *12*, 2835.
- (382) Schwartz, K. *Proc. Natl. Acad. Sci. U.S.A.* **1973**, *70*, 1608.
- (383) Demadis, K. D.; Ketsetzi, A.; Pachis, K.; Ramos, V. M. *Biomacromolecules* **2008**, *9*, 3288.
- (384) Demadis, K. D.; Ketsetzi, A.; Pachis, K.; Stathoulopoulou, A. *Adv. Colloid Interface Sci.* **2009**, *151*, 33.
- (385) Ehrlich, H.; Krautter, M.; Hanke, T.; Simon, P.; Knieb, C.; Heinemann, S.; Worch, H. *J. Exp. Zool.* **2007**, *B308*, 473.

- (386) Ehrlich, H.; Worch, H. Collagen, a Huge Matrix in Glass-Sponge Flexible Spicules of the Meter-Long *Hyalonema Sieboldi*. In *The Biology of Biominerals Structure Formation*, Baurlein, E., Ed.; Handbook of Biomineralization. Vol. 1; Wiley VCH: Weinheim, Germany, 2007; Chapter 2, p 23.
- (387) Brunner, E.; Richthammer, P.; Ehrlich, H.; Paasch, S.; Simon, P.; Ueberlein, S.; van Pee, K.-H. *Angew. Chem., Int. Ed.* **2009**, *48*, 9724.
- (388) Benner, K.; Klüfers, P.; Vogt, M. *Angew. Chem., Int. Ed.* **2003**, *42*, 1058.
- (389) Demadis, K. D.; Neofotistou, E.; Mavredaki, E.; Tsiknakis, M.; Sarigiannidou, E.-M.; Katarachia, S. D. *Desalination* **2005**, *179*, 281.
- (390) Demadis, K. D.; Mavredaki, E.; Stathouloupoulou, A.; Neofotistou, E.; Mantzaridis, C. *Desalination* **2007**, *213*, 38.
- (391) Mavredaki, E.; Stathouloupoulou, A.; Neofotistou, E.; Demadis, K. D. *Desalination* **2007**, *210*, 257.

CR900334Y